HAMILTONIAN METHODS IN $\mathcal{PT}$-SYMMETRIC SYSTEMS

HAMILTONIAN METHODS IN $\mathcal{PT}$-SYMMETRIC SYSTEMS

By ALEXANDER CHERNYAVSKY, M.Sc., B.Sc.

A Thesis Submitted to the Department of Mathematics and Statistics and the School of Graduate Studies in Partial Fulfilment of the Requirements for the Degree
Doctor of Philosophy

DOCTOR OF PHILOSOPHY (2018) (Mathematics)	McMaster University Hamilton, Ontario, Canada

TITLE:	Hamiltonian Methods in $\mathcal{PT}$-symmetric Systems
AUTHOR:	Alexander Chernyavsky M.Sc. (MIET) B.Sc. (MIET)
SUPERVISOR:	Dr. Dmitry Pelinovsky
NUMBER OF PAGES:	xii, 127

Abstract

This dissertation is concerned with analysis of spectral and orbital stability of solitary wave solutions to discrete and continuous $\mathcal{PT}$-symmetric nonlinear Schrödinger equations. The main tools of this analysis are inspired by Hamiltonian systems, where conserved quantities can be used for proving orbital stability and Krein signature can be computed for prediction of instabilities in the spectrum of linearization. The main results are obtained for the chain of coupled pendula represented by a discrete NLS model, and for the trapped atomic gas represented by a continuous NLS model. Analytical results are illustrated with various numerical examples.

Acknowledgements

First of all, I would like to express my deepest gratitude to my advisor, Dr. Dmitry Pelinovsky. His guidance and patience with me were priceless throughout my studies at McMaster, and weekly meetings kept me on my toes at all times. I also want to thank his family for hosting me and other graduate students for annual dinners at Dr. Pelinovsky's house. These evenings gave me a taste of home and made me feel a part of the family. I have also enjoyed our joint cross-country skiing activies and traveling together.

I would like to thank McMaster University for providing financial support during my stay in Canada. A combination of scholarships and teaching duties gave me an opportunity to do research and work part-time to deepen my knowledge of undergraduate material by conveying it to others. I enjoyed working as a Teaching Assistant for various courses and even got to teach one as an instructor. This teaching experience is invaluable for me and would give a great advantage in the future.

My journey will not be the same without all the good people I met here. I cannot list them all, but I must mention Adrien Thierry, Karsten Hempel, Tyler Meadows, Yusuke Shimabukuro, Lee van Brussel, Niky Hristov, Aaron Saalmann, Zelalem Negeri, and many, many others. But the list does not end with the graduate students. I enjoyed taking courses and engaging in conversations with Dr. Stanley Alama, Dr. Lia Bronsard, Dr. Gail Wolkowicz, Dr. Eric Sawyer, and Dr. Rachel Rensink-Hoff. They gave me numerous life advices and shared their experiences of being a graduate student. I also came to know various staff members within and outside the department: Pam, Shirley, TJ, Dragan, Kenneth, Brian, Paula, Sheree. They cheered and supported me even when I was not confident in myself, and I did my best to return the favor.

Last but not least, I would like to thank my family and friends from home for calling me regularly and making sure of my well-being. They provided a link to home and made me proud to be who I am.

To my wife, Lorena

Contents

List of Figures

List of Tables

Declaration of Academic Achievement

My supervisor, Dr. Dmitry Pelinovsky, and myself, conducted the research presented in this dissertation. In recognition of this fact, I have chosen to use the personal pronoun "we" where applicable throughout the text. Original results based on published work joint with my supervisor are presented in Chapters 2, 3 and 5. There, I was responsible for analyzing the problem, programming numerical simulations and interpreting data, as well as writing the manuscript with the editorial advice and supervision of Dr. Pelinovsky. Chapter 4 is based on published work developed in collaboration with Dr. Panayotis Kevrekidis, who provided invaluable insight on physical applications. In that Chapter, I was responsible for numerical simulations, analytical computations and writing the manuscript, and Dr. Pelinovsky provided guidance on the analysis involved.

Chapter 1

Introduction

This thesis focuses on studies of the stability of nonlinear waves in discrete and continuous models based on the nonlinear Schrödinger equation. The key feature of the models is the presence of $\mathcal{PT}$-symmetry which relaxes the condition of Hermiticity, yet retains surprisingly many properties of Hamiltonian systems. On the other hand, the interplay between nonlinearity, $\mathcal{PT}$ symmetry, and dispersion gives birth to numerous new phenomena unseen in the realm of Hamiltonian systems. These phenomena motivate the choice of the subject.

From nonlinear optics to condensed matter, the nonlinear Schrödinger equation (NLS) enjoys many applications in physics. For example, it provides a canonical description for the envelope dynamics of a quasi-monochromatic plane wave (the carrying wave) propagating in a weakly nonlinear dispersive medium when dissipative processes are negligible. On short times and small propagation distances, the dynamics are linear, but cumulative nonlinear interactions result in a significant modulation of the wave amplitude on large spatial and temporal scales. In optics, NLS can also be viewed as the extension of the paraxial approximation to nonlinear media. In the context of quantum mechanics, a nonlinear potential arises in the 'mean field' description of interacting particles. In the wave context of electromagnetic theory, the second-order linear operator describes the dispersion and diffraction of the wave-packet, and the nonlinearity arises from the sensitivity of the refractive index to the medium on the wave amplitude [134].

One of the first important questions related to the NLS is concerned with linear stability of a constant-wave solution that is uniform in space and oscillatory in time. It corresponds to the effect of slow temporal modulation on a monochromatic wave whose frequency is slightly shifted by the nonlinearity. When the constant-wave solution is modulationally unstable, the spatial modulation leads to the formation of solitonic structures resulting from an exact balance between the dispersive and nonlinear effects.

The discrete nonlinear Schrödinger equation (dNLS) is one of the most fundamental lattice models. On one hand, it is a prototypical discretization of the nonlinear Schrödinger equation, on the other hand, it has many physical applications in its own right. One of the relevant areas for dNLS is the field of optically induced lattices in photorefractive media, where the dNLS model can yield

accurate predictions about existence and stability of nonlinear localized modes. Since the numerical prediction in [48] and experimental realization in [55], there has been an tremendous number of studies in the area of nonlinear waves and solitons in such structures. A number of them has been predicted and experimentally demonstrated in lattices with induced self-focusing nonlinearity: dipoles, quadrupoles, necklaces, etc. Such structures have a potential to be used as carriers for data transmission in all-optical communication schemes [72].

As we have seen, both continuous and discrete NLS models have a variety of physical applications. The incorporation of $\mathcal{PT}$ symmetry into these models enriches this variety and introduces fascinating phenomena: existence of continuous families of nonlinear modes, $\mathcal{PT}$ symmetry breaking and stabilization above phase transition. The study of these phenomena and prediction of instabilities is an important step towards understanding intrinsic nonlinear processes. This thesis develops the tools for such analysis and paves the way for the future work relevant to many branches of modern physics.

This introduction is structured as follows. Section 1.1 gives a brief overview of Hamiltonian systems and the stability problem. Section 1.2 introduces $\mathcal{PT}$-symmetric systems and their important features. In Section 1.3 we talk about stability analysis in discrete systems, and introduce the model studied in Chapters 2 and 3. Section 1.4 gives the outline of stability analysis in continuous system, and presents the material of Chapters 4 and 5. Section 1.5 introduces spaces and properties of operators that will be used throughout the thesis.

1.1 Hamiltonian Systems

Hamiltonian systems arise in applications where the damping can be neglected. Hamiltonian view of mechanics becomes important for approximate methods of perturbation theory, e.g. celestial mechanics; for understanding the general character of motion in complicated mechanical systems, e.g. ergodic theory, statistical mechanics; and in connection with other areas of physics, e.g. optics, quantum mechanics, etc. [8]. The rich structure of Hamiltonian systems stems from the conservation of the underlying energy, the Hamiltonian, as well as other quantities such as mass and momentum.

Linear and nonlinear stability of wave solutions to Hamiltonian systems is an old field. In 1872 Boussinesq [26], studying water waves, suggested that the constraint due to symmetry could be used to understand the stability of the critical points of the energy, represented by the Hamiltonian. General framework of this theory was developed by Grillakis, Shatah, and Strauss [59, 60] in the infinite-dimensional Hamiltonian systems in the presence of symmetries. Their approach characterizes the critical points of systems with symmetry and conserved quantities via the analysis of a constraint operator. We will review the finite-dimensional theory [69], and show that minimizers of the Hamiltonian are nonlinearly stable [57, 94].

1.1.1 Finite-Dimensional Hamiltonian Systems

Consider a state vector $\vec{u} \in \mathbb{R}^{2d}$ for some dimension $d \geq 1$, and a Hamiltonian $H \colon \mathbb{R}^{2d} \mapsto \mathbb{R}$, which depends smoothly upon $\vec{u}$ and corresponds to the conserved energy of the system. The Hamiltonian

system describing time evolution of the state vector $\vec{u}$ in time t takes the form

$$\frac{d\vec{u}}{dt} = J\nabla_u H(\vec{u}). \tag{1.1}$$

Here J is a $2d \times 2d$ nonsingular matrix skew-symmetric with respect to the usual Euclidean inner product: $J^T = -J$, where superscript T stands for matrix transpose. Such matrices map a vector into its perpendicular subspace:

$$\langle J\vec{x}, \vec{x}\rangle = \langle \vec{x}, J^T\vec{x}\rangle = -\langle \vec{x}, J\vec{x}\rangle,$$

and thus $\langle J\vec{x}, \vec{x}\rangle = 0$. Using this property, we can prove the following:

Lemma 1. *Let $\vec{u}$ be the solution of (1.1) with initial data $\vec{u}(0) = \vec{u}_0$. Then $H(\vec{u}(t)) = H(\vec{u}_0)$ for all nonzero t.*

Proof. Let us take the time derivative of $H(\vec{u}(t))$:

$$\frac{dH(\vec{u})}{dt} = \langle \nabla_u H(\vec{u}), \frac{d\vec{u}}{dt}\rangle = \langle \nabla_u H(\vec{u}), J\nabla_u H(\vec{u})\rangle = 0.$$

Thus the functional H is constant. □

The canonical Hamiltonian system is derived from the Newton's second law. The skew-symmetric matrix J then takes the form

$$J = \begin{bmatrix} 0_d & I_d \\ -I_d & 0_d \end{bmatrix},$$

where $I_d \in \mathbb{R}^{d\times d}$ is the identity matrix, and $0_d \in \mathbb{R}^{d\times d}$ is the zero matrix. The state vector is written as $\vec{u} = [\vec{p}, \vec{q}]^T$ for $\vec{p}, \vec{q} \in \mathbb{R}^d$, and the Hamiltonian system becomes

$$\frac{dp_j}{dt} = \frac{\partial H}{\partial q_j}, \quad \frac{dq_j}{dt} = -\frac{\partial H}{\partial p_j}.$$

where $j = 1, \ldots, d$. The vectors $\vec{p} = (p_1, \ldots, p_d)$ and $\vec{q} = (q_1, \ldots, q_d)$ are traditionally called the momentum and position vectors, respectively. In the context of molecular physics, Hamiltonian describes the total energy as a combination of kinetic and potential energy due to interactions between the molecules.

Consider a critical point $\vec{\phi}$ of the Hamiltonian energy functional: $\nabla_u(H(\vec{\phi})) = 0$. Obviously, $\vec{\phi}$ is also an equilibrium of the Hamiltonian system (1.1). Our interest lies in dynamics of solutions with initial data $\vec{u}_0$ that lies close to $\vec{\phi}$. Asymptotic stability is generally ruled out in finite-dimensional Hamiltonian systems, since if $H(\vec{u}_0) \neq H(\vec{\phi})$, then $\vec{u}(t)$ cannot converge to $\vec{\phi}$. If it did, we would have $H(\vec{u}_0) = H(\vec{u}(t)) \to H(\vec{\phi})$ as $t \to \infty$, which gives us a contradiction. So at most we can have $\vec{u}(t)$ staying close to $\vec{\phi}$.

Let us study the structure of the Hamiltonian about $\vec{\phi}$. Taking $\vec{v} = \vec{u} - \vec{\phi}$ to be a perturbation of $\vec{\phi}$, a Taylor expansion about ϕ yields

$$H(\vec{u}) = H(\vec{\phi}) + \langle \nabla_u H(\vec{\phi}), \vec{v} \rangle + \frac{1}{2}\langle \vec{v}, L\vec{v} \rangle + \mathcal{O}(|\vec{v}|^3), \tag{1.2}$$

where $L \in \mathbb{R}^{2d \times 2d}$ is a Hessian matrix which has the following entries:

$$L_{ij} = \frac{\partial H}{\partial u_i \partial u_j}(\vec{\phi}).$$

It is important to note that the Hessian operator is symmetric (or Hermitian). Since $\vec{\phi}$ is a critical point of H, $\nabla_u H(\vec{\phi}) = 0$, and Hamiltonian can be written as

$$H(\vec{u}) - H(\vec{\phi}) = \frac{1}{2}\langle \vec{v}, L\vec{v} \rangle + \mathcal{O}(|\vec{v}|^3). \tag{1.3}$$

Taking ∇_v of both sides, we can rewrite Hamiltonian system (1.1) as

$$\frac{d\vec{v}}{dt} = JL\vec{v} + N(\vec{v}),$$

where $N(\vec{v}) = \mathcal{O}(|\vec{v}|^2)$ denotes nonlinear terms in v, and JL denotes the linearization about $\vec{\phi}$. Such linearizations typically have the structure outlined in the following lemma.

Lemma 2. *Let $L \in M^{2d \times 2d}$ be a linear symmetric operator: $L^T = L$. The spectrum $\sigma(JL)$ is symmetric with respect to the real and imaginary axes of the complex plane, so that the eigenvalues of JL come in quartets: $\{\pm\lambda, \pm\bar{\lambda}\}$. In particular, either $\sigma(JL) \subset i\mathbb{R}$, or the critical point $\vec{\phi}$ is linearly exponentially unstable.*

Proof. Suppose that $\lambda \in \sigma(JL)$ with the associated eigenvector $\vec{w}$. Since JL has real-valued entries,

$$JL\vec{w} = \lambda\vec{w} \quad \Leftrightarrow \quad JL\overline{\vec{w}} = \bar{\lambda}\overline{\vec{w}}.$$

In other words, $\bar{\lambda}$ also belongs to the spectrum of JL, with an eigenvector $\overline{\vec{w}}$. Moreover, due to $(JL)^T = -LJ$

$$JL\vec{w} = \lambda\vec{w} \quad \Leftrightarrow \quad -LJ(J^{-1}\vec{w}) = (-\lambda)J^{-1}\vec{w} \quad \Leftrightarrow \quad (JL)^T(J^{-1}\vec{w}) = -\lambda(J^{-1}\vec{w})$$

we can see that $-\lambda \in \sigma((JL)^T)$ with the eigenvector $J^{-1}\vec{w}$. On the other hand, knowing $\sigma(JL) = \overline{\sigma((JL)^T)}$, we can deduce that $-\bar{\lambda} \in \sigma(JL)$, as well. By taking complex conjugation, we also have $-\lambda \in \sigma(JL)$. The spectral stability statement follows from the spectral symmetry, since the existence of an eigenvalue with negative real part implies the existence of an eigenvalue with positive real part. □

If $\vec{\phi}$ is a nondegenerate minima of H, then it is stable in finite-dimensional Hamiltonian systems as per the following lemma.

Lemma 3. *Suppose that $\vec{\phi}$ is a critical point for the Hamiltonian system* (1.1)*. If $\vec{\phi}$ is a strict local minimum, i.e. L is a positive-definite matrix, then $\vec{\phi}$ is stable. Specifically, there exist $C, \delta > 0$ such that for $|\vec{u}_0 - \vec{\phi}| \leq \delta$, the solution $\vec{u}$ of* (1.1) *satisfies*

$$|\vec{u}(t) - \vec{\phi}| \leq C|\vec{u}_0 - \vec{\phi}|, \quad t \geq 0.$$

Proof. Set $\vec{v} = \vec{u} - \vec{\phi}$, and recall the Taylor expansion of H about $\vec{\phi}$:

$$H(\vec{u}) - H(\vec{\phi}) = \frac{1}{2}\langle \vec{v}, L\vec{v}\rangle + \mathcal{O}(|\vec{v}|^3).$$

Since L is symmetric, all of its eigenvalues are real-valued: $\mu_j \in \mathbb{R}, j = 1, 2, \ldots, 2d$. Positive-definite property implies that all eigenvalues are positive: $\mu^- := \min_j\{\mu_j\} > 0$. Moreover, $\mu^+ := \max_j\{\mu_j\} \geq \mu^-$, and

$$\mu^-|\vec{v}|^2 \leq \langle \vec{v}, L\vec{v}\rangle \leq \mu^+|\vec{v}|^2,$$

where the inequality is attained at corresponding eigenvectors. The Taylor expansion implies that there exists a $\delta > 0$ such that for every $\vec{v} \in \mathbb{R}^{2d}$ satisfying $|\vec{v}| \leq \delta$ there exist constants $0 < C_- < C_+ < \infty$ such that

$$C_-|\vec{v}|^2 \leq H(\vec{u}) - H(\vec{\phi}) \leq C_+|\vec{v}|^2.$$

The lower bound implies that the initial data $\vec{u}_0$ controls the norm of the perturbation:

$$|\vec{v}(t)|^2 \leq \frac{1}{C_-}(H(\vec{u}) - H(\vec{\phi})) = \frac{1}{C_-}(H(\vec{u}_0) - H(\vec{\phi})),$$

where we have used the conservation of Hamiltonian. The upper bound allows us to rewrite the latter estimate as

$$|\vec{u}(t) - \vec{\phi}|^2 \leq \frac{C_+}{C_-}|\vec{u}_0 - \vec{\phi}|^2,$$

where the conclusion of the lemma is achieved with $C = \sqrt{C_+/C_-}$. □

In practice, Hamiltonian systems often possess symmetries. In that case, the image of the critical point under these symmetries will generate a manifold of critical points, and the set of derivatives of this manifold with respect to parameter will lie in the kernel of the linearization JL about $\vec{\phi}$. Thus L will have a null space and at best can be semi-definite. This obstacle can be overcome through the notion of orbital stability, see, e.g., Definition 10 in Chapter 2.

Each symmetry generates a conserved quantity due to Noether's Theorem [97]. Even when L has eigenvalues of negative real part, the critical point may still be stable: the conserved quantities can be used to perform a search for a constrained minimizer. This is realized in the approach of Grillakis-Shatah-Strauss [59, 60], which we do not review here.

1.1.2 Infinite-Dimensional Hamiltonian Systems

Let X be an infinite-dimensional Hilbert space X with inner product $\langle \cdot, \cdot \rangle_X$, $\| \cdot \|$ be the induced norm, and X^* be the dual of X with respect to the inner product in X. A Hamiltonian on X is a

nonlinear functional $\mathcal{H}\colon X \mapsto \mathbb{R}$, which we assume to be C^2 on all of X. The associated Hamiltonian system then takes the form

$$\frac{du}{dt} = \mathcal{J}\frac{\delta \mathcal{H}}{\delta u}(u), \quad u\colon \mathbb{R} \to X, \tag{1.4}$$

where $\mathcal{J}\colon X^* \mapsto X$ is a linear closed operator with dense domain $\mathrm{D}(J) \subset X^*$, and skew-symmetric respect to $\langle \cdot, \cdot \rangle_X$:

$$\langle \mathcal{J}u, v\rangle_X = -\langle u, \mathcal{J}v\rangle_X$$

for all $u, v \in \mathrm{D}(J) \subset X^*$. Moreover, we assume that $\mathcal{J}$ is one-to-one and onto. The first variation with respect to the X-inner product, denoted $\delta\mathcal{H}/\delta u\colon X \to X^*$, is defined as

$$\lim_{\epsilon \to 0} \frac{\mathcal{H}(u + \epsilon v) - \mathcal{H}(u)}{\epsilon} = \left\langle \frac{\delta \mathcal{H}}{\delta u}(u), v \right\rangle_X$$

for all u, v in X. Using the chain rule, we see that smooth solutions of (1.4) conserve the Hamiltonian:

$$\frac{d\mathcal{H}(u(t))}{dt} = \left\langle \frac{\delta \mathcal{H}}{\delta u}(u), \frac{du}{dt} \right\rangle_X = \left\langle \frac{\delta \mathcal{H}}{\delta u}(u), \mathcal{J}\frac{\delta \mathcal{H}}{\delta u}(u) \right\rangle_X = 0.$$

Let us generalize the finite-dimensional expansion (1.2). Fix $\phi \in X$. For $u = \phi + Iv$ with $v \in X$ the Hamiltonian admits a formal Taylor expansion

$$\mathcal{H}(u + \epsilon v) - \mathcal{H}(\phi) = \left\langle \frac{\delta \mathcal{H}}{\delta u}(\phi), v \right\rangle_X + \frac{1}{2}\langle \mathcal{L}v, v\rangle_X + \mathcal{O}(\|v\|^3),$$

where the quadratic form $\langle \mathcal{L}v, v\rangle_X$ is called the second variation of $\mathcal{H}$, and the self-adjoint linear operator $\mathcal{L}$ is called the Hessian operator:

$$\mathcal{L} := \frac{\delta^2 \mathcal{H}}{\delta u^2}(\phi)\colon\ \mathrm{D}(\mathcal{L}) \subset X \mapsto X^*.$$

If ϕ is a critical point of $\mathcal{H}$, in other words

$$\frac{\delta \mathcal{H}}{\delta u}(\phi) = 0,$$

then the Taylor expansion reduces to an infinite-dimensional version of (1.3):

$$\mathcal{H}(u) - \mathcal{H}(\phi) = \frac{1}{2}\langle \mathcal{L}v, v\rangle + \mathcal{O}(\|v\|^3).$$

Compared to the symmetric matrix L in (1.3), the self-adjoint operator $\mathcal{L}$ is generally unbounded and has a nontrivial kernel.

The approach outlined previously for studying stability of wave solutions in finite-dimensional systems can be readily extended to infinite-dimensional ones.

1.2 $\mathcal{PT}$-Symmetric Systems

In classical quantum mechanics, one usually considers observables as Hermitian operators in the Hilbert space L^2. Bender and Boettcher [21] suggested that Hermitian operators can be replaced by the so-called $\mathcal{PT}$-symmetric operators for an alternative formulation of quantum mechanics. They have shown that a non-Hermitian operator might still possess real spectrum if it is symmetric with respect to combined parity $\mathcal{P}$ and time-reversal $\mathcal{T}$ symmetries. Their idea was later extended in the works of Mostafazadeh [101, 102] who considered a more general class of pseudo-Hermitian operators with purely real spectrum. A number of reviews emerged on the topic [18, 84, 133].

Starting in quantum mechanics, the concept of $\mathcal{PT}$ symmetry found applications in many areas of physics [19, 123, 128]. In particular, there is a lot of interest in optics due to experimental realizations of paraxial $\mathcal{PT}$ symmetric optics [93, 103]. Recent applications include single-mode $\mathcal{PT}$ lasers [52, 64] and unidirectional reflectionless $\mathcal{PT}$-symmetric metamaterials at optical frequencies [53]. $\mathcal{PT}$ symmetric systems demonstrate many nontrivial non-conservative wave interactions and phase transitions, which can be employed for signal filtering and switching, opening new prospects for active control of light [133].

Discovered by John Scott Russell in 1834, solitons have attracted a lot of attention in many nonlinear physical systems, ranging from optics to BECs [54, 81]. Conservative solitons requiring balance of nonlinear response and medium dispersion usually form families with different amplitudes. Nonlinear dissipative systems, however, require an additional balance between gain and loss to support soliton solutions [4, 122]. This requirement is usually satisfied only for selected soliton amplitudes and shapes, and no continuous families can generally be found. On the other hand, $\mathcal{PT}$-symmetric systems, being a subclass of dissipative systems, can commonly support continuous families of solitons due to symmetry property [141]. Thus $\mathcal{PT}$-symmetric systems, being dissipative systems, possess features of conservative ones [133].

Let us review the main concepts in the theory of $\mathcal{PT}$-symmetric (or, more generally, non-Hermitian) linear systems.

1.2.1 $\mathcal{PT}$-Symmetric Linear Operators

Let $\psi(\vec{x},t)$ be a complex valued wave function of a quantum particle, where $\vec{x}$ is a space variable, and t represents time. Evolution of $\psi(\vec{x},t)$ is governed by the Schrödinger equation

$$i\frac{\partial\psi}{\partial t} = H\psi(\vec{x},t),$$

where the linear operator H acts in a Hilbert space $L^2(\mathbb{R}^d)$ equipped with an inner product

$$\langle\phi,\psi\rangle = \int_{\mathbb{R}^d} \phi(\vec{x},t)\overline{\psi(\vec{x},t)}d\vec{x},$$

d is the space dimension, and we consider units where $\hbar = m = 1$ with m being the mass of the particle.

Recall that for Hermitian operator $H^* = H$, and

$$\langle H\phi, \psi\rangle = \langle \phi, H\psi\rangle,$$

for any $\phi, \psi \in \mathrm{D}(H)$. The spectrum of any Hermitian operator is purely real, while the opposite is not true: Hermiticity is a sufficient but not necessary condition for reality of the spectrum.

The two fundamental discrete symmetries in physics [139] are given by the parity operator $\mathcal{P}$ defined as $\mathcal{P}\psi(\vec{x}, t) = \psi(-\vec{x}, t)$, and by the time reversal operator $\mathcal{T}$ defined as $\mathcal{T}\psi(\vec{x}, t) = \overline{\psi(\vec{x}, -t)}$. The operator $\mathcal{T}$ is antilinear:

$$\mathcal{T}(\alpha\phi) = \overline{\alpha}\mathcal{T}\phi, \quad \mathcal{T}(\phi + \psi) = \mathcal{T}\phi + \mathcal{T}\psi \tag{1.5}$$

for any two vectors ψ, ϕ and a complex number α. Moreover,

$$\mathcal{P}^2 = \mathcal{T}^2 = I, \quad [\mathcal{P}, \mathcal{T}] = 0, \tag{1.6}$$

where I is the identity operator.

Definition 1 ($\mathcal{PT}$-symmetric operator)**.** *An operator H is said to be* $\mathcal{PT}$-symmetric *if*

$$[\mathcal{PT}, H] = 0, \tag{1.7}$$

or, using (1.6)*, $H = \mathcal{PT}H\mathcal{PT}$.*

In the work of Bender and Boettcher [21], where a connection between $\mathcal{PT}$ symmetry and reality of the spectrum was pointed out, they also introduced the notion of *unbroken $\mathcal{PT}$ symmetry.*

Definition 2 (Broken and unbroken $\mathcal{PT}$ symmetry)**.** *$\mathcal{PT}$ symmetry of a $\mathcal{PT}$-symmetric operator is said to be* unbroken *if any eigenfunction of H is at the same time an eigenfunction of the $\mathcal{PT}$ operator. If the unbroken $\mathcal{PT}$ symmetry does not hold, then the $\mathcal{PT}$ symmetry is called* broken*.*

The broken $\mathcal{PT}$ symmetry is typically associated with the presence of complex eigenvalues in the spectrum of H. Since H and $\mathcal{PT}$ commute, $H\psi = E\psi$ implies the existence of λ such that $\mathcal{PT}\psi = \lambda\psi$. From (1.5) and (1.6) it follows that there exists a real constant β such that $\lambda = e^{i\beta}$. In other words, any eigenvalue of the $\mathcal{PT}$ operator is a pure phase [22].

Unlike Hermiticity, $\mathcal{PT}$ symmetry is not sufficient for the eigenvalues of H to be purely real. It becomes sufficient when combined with the requirement for the $\mathcal{PT}$ symmetry to be unbroken. Indeed, let E be an eigenvalue of H with the eigenfunction ψ, $H\psi = E\psi$. Applying $\mathcal{PT}$ operator to both sides and using (1.6), we obtain $H(\mathcal{PT}\psi) = \bar{E}(\mathcal{PT}\psi)$. Then, if the $\mathcal{PT}$ symmetry of H is unbroken, $H\psi = \bar{E}\psi$, and hence the eigenvalue E is real. This procedure is applied to every eigenvalue of H, therefore the eigenvalues of H are entirely real.

Interestingly, in the case of unbroken $\mathcal{PT}$ symmetry it is possible to construct a similarity transformation that maps a non-Hermitian $\mathcal{PT}$-symmetric Hamiltonian to an equivalent Hermitian Hamiltonian. The equivalence is understood in the sense that both Hamiltonians have the same eigenvalues [47, 140]. Unfortunately, in practice this transformation is too complicated to be constructed

except at the perturbative level [18]. Another problem is that the transformation is a *similarity* but not a *unitary* transformation. That is, orthogonal pairs of vectors are mapped into pairs of vectors that are not orthogonal.

Let us give an example illustrating basic concepts outlined above.

1.2.2 Example

Consider a Hamiltonian defined by a 2 x 2 matrix [20]:

$$H = \begin{bmatrix} i\gamma & \kappa \\ \kappa & -i\gamma \end{bmatrix} = k\sigma_1 + i\gamma\sigma_3, \tag{1.8}$$

where $\gamma \geq 0$ and $\kappa \geq 0$ are real parameters and we use the conventional notations for Pauli matrices:

$$\sigma_1 = \begin{bmatrix} 0 & 1 \\ 1 & 0 \end{bmatrix}, \quad \sigma_2 = \begin{bmatrix} 0 & -i \\ i & 0 \end{bmatrix}, \quad \sigma_3 = \begin{bmatrix} 1 & 0 \\ 0 & -1 \end{bmatrix}.$$

The Hamiltonian (1.8) acts in a Hilbert space of two-component column vectors $\psi = (\psi_1, \psi_2)^T$, with complex entries ψ_1, ψ_2, and the inner product is defined as

$$\langle \phi, \psi \rangle = \phi_1 \overline{\psi_1} + \phi_2 \overline{\psi_2}.$$

The Hamiltonian (1.8) is $\mathcal{PT}$ symmetric with $\mathcal{P} = \sigma_1$ and $\mathcal{T}$ being complex conjugation. The eigenvalues and eigenvectors of H are given by

$$E_{1,2} = \pm\sqrt{\kappa^2 - \gamma^2}, \quad \psi^{(1,2)} = \begin{bmatrix} i\gamma/\kappa \pm \sqrt{1 - \gamma^2/\kappa^2} \\ 1 \end{bmatrix}.$$

Thus $\mathcal{PT}$ symmetry is unbroken (all eigenvalues are real) if $\gamma < \kappa$ and is broken (both eigenvalues are imaginary) if $\gamma > \kappa$. At $\gamma = \kappa$, $\mathcal{PT}$ symmetry breaking occurs. At this point, two eigenvalues collide, and eigenvectors become linearly dependent, thus Hamiltonian has a nondiagonal Jordan block. Algebraic multiplicity of the eigenvalue is two and is larger than its geometric multiplicity one. Such points in the parameter space (γ, κ) are called *exceptional points* [71] or *branch points* [100].

1.2.3 Pseudo-Hermiticity

A necessary and sufficient condition for the spectrum of a non-Hermitian Hamiltonian to be purely real can be formulated in terms of a more general property called *pseudo-Hermiticity* [88, 101].

Definition 3 (Pseudo-Hermitian operator)**.** *A Hamiltonian H is said to be* η-pseudo-Hermitian *if there exists a Hermitian invertible linear operator η such that*

$$H^* = \eta H \eta^{-1}.$$

Obviously, if η is the identity operator, this definition is equivalent to Hermiticity. In many cases, pseudo-Hermiticity can be considered as a generalization of $\mathcal{PT}$ symmetry. For example, if H is a symmetric matrix Hamiltonian, then $\mathcal{PT}$ symmetry implies $H\mathcal{P} - \mathcal{P}\bar{H} = 0$, and then $H^* = \bar{H} = \mathcal{P}H\mathcal{P}$, i.e. a pseudo-Hermiticity of H.

The notion of pseudo-Hermiticity allows one to formulate necessary and sufficient condition for a Hamiltonian to possess a purely real spectrum. Let us consider the case of the discrete spectrum, and let a Hamiltonian have a complete set of biorthonormal eigenvectors $\{(\psi_n, \phi_n)\}$ defined by

$$H\psi_n = E_n\psi_n, \quad H^*\phi_n = \bar{E}_n\phi_n, \quad \langle\phi_n, \psi_n\rangle = \delta_{n,m}.$$

Then the following theorem holds.

Theorem 1 (Mostafazadeh [102]). *Let H be a Hamiltonian that acts in a Hilbert space, has a discrete spectrum, and admits a complete set of biorthonormal eigenvectors $\{(\psi_n, \phi_n)\}$. Then the spectrum of H is real if and only if there is an invertible linear operator O such that H is OO^*-pseudo-Hermitian: $H = (OO^*)H^*(OO^*)^{-1}$.*

As an example of application of Theorem 1, consider the $\mathcal{PT}$-symmetric Hamiltonian (1.8). It possesses a complete set of biorthonormal eigenvectors unless $\epsilon = \gamma/\kappa = 1$. Since the spectrum is real if $\epsilon \in (0, 1)$, Theorem 1 guarantees that for $\epsilon \in (0, 1)$ there exists the operator O such that H is η-pseudo-Hermitian with $\eta = OO^*$. Although H is also P-pseudo-Hermitian, this cannot be used in Theorem 1, since the parity operator $\mathcal{P} = \sigma_1$ does not admit the representation $\mathcal{P} = OO^*$. Therefore there must exist another operator $\eta \neq \mathcal{P}$ such that $\eta = OO^*$. By straightforward calculation one finds that

$$\eta = \frac{1}{\epsilon^2}\begin{bmatrix} 1 & i\epsilon \\ -i\epsilon & 1 \end{bmatrix}, \quad O = \frac{1}{\epsilon}\begin{bmatrix} 0 & i \\ \sqrt{1-\epsilon^2} & \epsilon \end{bmatrix}, \quad \epsilon \in (0, 1).$$

Theorem 1 also indicates that no such operators exist in the broken $\mathcal{PT}$ symmetry case $\epsilon > 1$.

Although $\mathcal{PT}$ symmetry is not sufficient to guarantee the reality of the spectrum of a Hamiltonian H, it ensures that complex eigenvalues (if any) always exist in complex-conjugate pairs: if E is a complex eigenvalue with nonzero imaginary part and ψ is corresponding eigenvector, then $\bar{E}$ is also an eigenvalue with eigenvector $\mathcal{PT}\psi$. Thus one can expect that if $\mathcal{PT}$ symmetry is unbroken and the real eigenvalues are simple and isolated from each other, then the reality of the spectrum is "robust" against relatively small perturbations. For example, it happens when perturbed $\mathcal{PT}$-symmetric operator is "close" to a self-adjoint operator with simple eigenvalues [30, 29]. Consider a Hermitian operator H_0 perturbed as $H(\epsilon) = H_0 + \epsilon H_1$, where ϵ is a small parameter, and H_0, H_1 are $\mathcal{PT}$-symmetric. Then the spectrum of $H(\epsilon)$ is real provided ϵ is small enough. More precisely, the following theorem holds.

Theorem 2 (Caliceti, Graffi, and Sjöstandt [30]). *Let H_0 be a self-adjoint positive operator in a Hilbert space. Let H_0 have only discrete spectrum $\{0 \leq \lambda_0 < \lambda_1 < \ldots < \lambda_n < \ldots\}$, where each eigenvalue λ_j is simple, and $\delta = \inf_{j\geq 0}\{\lambda_{j+1} - \lambda_j\}/2 > 0$. Let also H_0 and H_1 be $\mathcal{PT}$-symmetric in the sense of (1.7), and assume that H_1 is relatively compact perturbation of H_0. Then the spectrum of $H(\epsilon)$ is real if $\epsilon \in \mathbb{R}$ and $|\epsilon| < \delta/\|H_1\|$.*

Theorem 2 guarantees the existence of a large class of pseudo-Hermitian operators with real spectra constructed as perturbations of a Hermitian operator, provided the spectrum of the latter is bounded below and its eigenvalues are well separated. As a simple example, we can consider a Schrödinger operator with a harmonic potential $H_0 = -\partial_x^2 + x^2$ and $\mathcal{PT}$-symmetric perturbation $H_1 = iW(x)$ with $W(x) = -W(-x)$ and $W(x) \in L^\infty(\mathbb{R})$. Then the spectrum of H_0 can be given explicitly:

$$\sigma(H_0) = \{2n + 1, \text{ where } n = 0, 1, 2, \ldots\}.$$

From here we deduce that $\delta = 2$, and the spectrum of $H_0 + \epsilon H_1$ is real at least for $|\epsilon| < 1/\|W\|_\infty$.

1.3 Stability in Discrete Systems

$\mathcal{PT}$-symmetric multi-site systems (oligomers) have recently attracted a lot of attention, motivated by possibilities of their experimental realization [120, 125]. Many studies address the question of existence and stability of nonlinear states in $\mathcal{PT}$-symmetric oligomers, which may drastically differ from the corresponding linear systems. The nonlinear effects in $\mathcal{PT}$-symmetric systems can be utilized for an efficient control of light including all-optical low-threshold switching and unidirectional invisibility [86, 91, 120]. The possibility to build nonlinear $\mathcal{PT}$-symmetric oligomers gave an uprise to numerous studies of both few-site systems and $\mathcal{PT}$-symmetric lattices. The former ones include one-dimensional $\mathcal{PT}$-symmetric dimer [6, 98], trimer [44, 89], quadrimer [89, 144]; the latter ones include two-dimensional plaquettes [90, 144], finite and infinite chains [23, 96, 115, 146], necklaces [14], ladders [5] and multicore fibers [95].

The most basic multi-site system having $\mathcal{PT}$ symmetry is a dimer, which represents a system of two coupled oscillators, one of which has losses due to damping and the other one gains some energy from external sources. This configuration was studied in numerous laboratory experiments involving electric circuits [127], superconductivity [123], optics [14, 125] and microwave cavities [24].

On the analytical side, dimer equations were found to be completely integrable [13, 117]. Integrability of dimers is obtained by using Stokes variables and it is lost when more coupled nonlinear oscillators are added into a $\mathcal{PT}$-symmetric system. Nevertheless, it was understood recently [15, 16] that there is a remarkable class of $\mathcal{PT}$-symmetric dimers with cross-gradient Hamiltonian structure, where the real-valued Hamiltonians exist both in finite and infinite chains of coupled nonlinear oscillators. Analysis of synchronization in the infinite chains of coupled oscillators in such class of models is a subject of Chapters 2 and 3. The results of this analysis were published in papers [34, 36].

In Chapter 2, we reduce Newton's equation of motion for coupled pendula shown on Figure 1.1 under a resonant periodic force to the following system of $\mathcal{PT}$-symmetric dNLS equations:

$$\begin{cases} 2i\dot{u}_n = \epsilon\left(v_{n+1} - 2v_n + v_{n-1}\right) + \Omega v_n + i\gamma u_n + 2\left[\left(2|u_n|^2 + |v_n|^2\right)v_n + u_n^2\bar{v}_n\right], \\ 2i\dot{v}_n = \epsilon\left(u_{n+1} - 2u_n + u_{n-1}\right) + \Omega u_n - i\gamma v_n + 2\left[\left(|u_n|^2 + 2|v_n|^2\right)u_n + \bar{u}_n v_n^2\right], \end{cases}$$

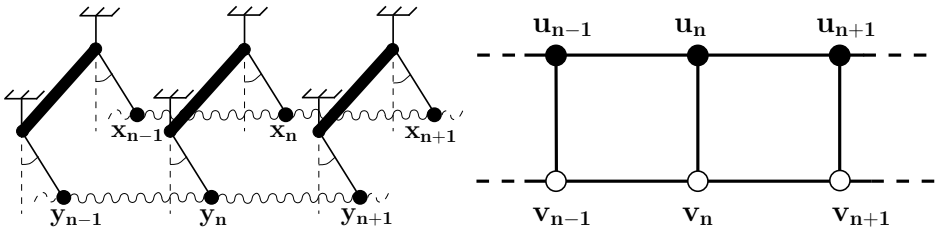

Figure 1.1: Left: A schematic picture for the chain of coupled pendula connected by torsional springs, where each pair is hung on a common string. Right: The chain of $\mathcal{PT}$-symmetric dimers representing coupled pendula. Filled (empty) circles correspond to sites with gain (loss).

where Ω, γ, ϵ are real-valued parameters, $n \in \mathbb{Z}$, and overdot denotes the derivative in time t. We show that this system is Hamiltonian with conserved energy

$$H_{u,v} = \sum_{n\in\mathbb{Z}} (|u_n|^2 + |v_n|^2)^2 + (u_n\bar{v}_n + \bar{u}_n v_n)^2 + \Omega(|u_n|^2 + |v_n|^2) - \epsilon|u_{n+1} - u_n|^2 - \epsilon|v_{n+1} - v_n|^2 + i\gamma(u_n\bar{v}_n - \bar{u}_n v_n),$$

and an additional constant of motion

$$Q_{u,v} = \sum_{n\in\mathbb{Z}} (u_n\bar{v}_n + \bar{u}_n v_n).$$

We study breather solutions of this model, which generalize symmetric synchronized oscillations of coupled pendula. We show existence of three branches of breathers. We also investigate their spectral stability analytically and numerically. For one of these branches, we are also able to prove orbital stability and instability from the energy method.

Chapter 3 is dedicated to the proof of nonlinear stability. It turns out that one of the branches of breathers is an infinite-dimensional saddle point of the extended energy functional, and the standard energy methods [69] cannot be applied to the proof of nonlinear stability of this branch. However, by modifying the energy functional we achieve long-time nonlinear stability of the breathers on a long but finite time interval. Such long-time stability is usually referred to as *metastability*.

1.4 Stability in Continuous Systems

Consider the following nonlinear Schrödinger's equation (NLSE) with a complex potential $U(x)$:

$$i\partial_t\psi + \partial_x^2\psi - U(x)\psi + g|\psi|^2\psi = 0, \tag{1.9}$$

where $U(x) = V(x) + i\gamma W(x)$ with $V(x) = V(-x)$ and $W(x) = -W(-x)$, $\gamma \in \mathbb{R}$ is a gain-loss parameter, $g = +1$ ($g = -1$) defines focusing (defocusing) nonlinearity, and $U(x)$ is $\mathcal{PT}$-symmetric:

$$U(x) = \mathcal{PT}U(x) = \overline{U(-x)}. \tag{1.10}$$

We will focus on potentials that are either localized ($U(x) \to 0$ as $x \to \pm\infty$) or unbounded ($U(x) \to \infty$ as $x \to \pm\infty$). Stationary nonlinear modes in (1.9) have the form $\psi(x,t) = \Phi(x)e^{-i\mu t}$, where $\mu \in \mathbb{R}$ is a real propagation parameter, and $\Phi(x)$ solves

$$\Phi_{xx} - U(x)\Phi + g|\Phi|^2\Phi = \mu\Phi \tag{1.11}$$

subject to the zero boundary condition: $\Phi(x) \to 0$ as $x \pm \infty$. Analysis of stability of these nonlinear modes is the subject of Chapters 4 and 5. The results of this analysis were published in [33, 35].

The NLSE (1.9) with a $\mathcal{PT}$-symmetric potential is used in the paraxial nonlinear optics. In that context, time and space have a meaning of longitudinal and transverse coordinates, and complex potential models the complex refractive index [124]. Another possible application of the NLSE (1.9) with complex potential $V + i\gamma W$ is Bose-Einstein condensate, where it models the dynamics of the self-gravitating boson gas trapped in a confining potential V. Intervals, where W is positive and negative, allow one to compensate atom injection and particle leakage, correspondingly [32]. The NLSE (1.9) is $\mathcal{PT}$-symmetric under the condition (1.10) in the sense that if $\psi(x,t)$ is a solution to (1.9), then

$$\widetilde{\psi}(x,t) = \mathcal{PT}\psi(x,t) = \overline{\psi(-x,-t)}$$

is also a solution to (1.9).

In Hamiltonian systems, instabilities arising due to coalescence of purely imaginary eigenvalues can be predicted by computing the *Krein signature* for each eigenvalue, which is defined as the sign of the quadratic part of Hamiltonian restricted to the associated eigenspace of the linearized problem. When two purely imaginary eigenvalues coalesce, they bifurcate off to the complex plane only if they have opposite Krein signatures prior to collision [69]. The concept of Krein signature was introduced by MacKay [92] in the case of finite-dimensional Hamiltonian systems, although the idea dates back to the works of Weierstrass [138]. An overview of Krein signature in Hamiltonian systems is given in Chapter 4.

There have been several attempts to extend the concept of Krein signature to the non-Hamiltonian $\mathcal{PT}$-symmetric systems. Nixon and Yang [105] considered the linear Schrödinger equation with a complex-valued $\mathcal{PT}$-symmetric potential and introduced the indefinite $\mathcal{PT}$-inner product with the induced $\mathcal{PT}$-Krein signature, in the exact correspondence with the Hamiltonian-Krein signature. In the recent works [5, 7, 131], a coupled non-Hamiltonian $\mathcal{PT}$-symmetric system was considered and the linearized system was shown to be block-diagonalizable to the form where Krein signature of eigenvalues can be introduced. All these cases were too special, the corresponding Krein signatures cannot be extended to a general $\mathcal{PT}$-symmetric system.

In Chapter 5 we deal with the stationary states in the $\mathcal{PT}$-symmetric NLSE (1.9) and introduce Krein signature of isolated eigenvalues in the spectrum of their linearization. We prove that the necessary condition for the onset of instability of the stationary states from a defective eigenvalue of algebraic multiplicity two is the *opposite* Krein signature of the two simple isolated eigenvalues prior to their coalescence. Compared to the Hamiltonian systems, or the linear Schrödinger equation in [105], the Krein signature of eigenvalues cannot be computed from the eigenvectors in the linearized problem. This is also shown in Appendix A, where perturbation theory failed to yield a simple

relationship between eigenvectors and their adjoint counterparts. As a result, the adjoint eigenvectors need to be computed separately and the sign of the adjoint eigenvector needs to be chosen by a continuity argument.

We show how to compute Krein signature numerically for several examples of the $\mathcal{PT}$-symmetric potentials. In the focusing case $g = 1$, we consider the Scarf II potential studied in [3, 17, 75, 105] with

$$U(x) = -V_0 \operatorname{sech}^2(x) + iV_1 \operatorname{sech}(x) \tanh(x), \tag{1.12}$$

where $V_0 > 0$ is a parameter. This potential is a complexification of the real Scarf potential [11], which bears the name from the pioneer work in [126]. The spectrum of this potential was found analytically by Ahmed [3] through a transformation of the corresponding linear Schrödinger equation to the Gauss hypergeometric equation, and by Bagchi and Quesne [9, 10] via complex Lie algebras. In Appendix B, we explain the former method and correct an error in [3], where the author omitted some admissible eigenvalues. When $|V_1| < V_{cr} = -V_0 + \frac{1}{4}$, the discrete spectrum consists of the sequence of real eigenvalues. At $|V_1| = V_{cr}$, a pair of real eigenvalues coalesce, and for $|V_1| > V_{cr}$ the double eigenvalue splits into the complex conjugate pairs in the complex plane. In other words, $\mathcal{PT}$ symmetry becomes broken.

The nonlinear model (1.11) for the Scarf II potential has an exact particular solution [103, 129] for $\mu = 1$:

$$\Phi = \sqrt{\frac{-V_0 - (V_1/3)^2 - 2}{g}} \frac{\exp(iV_1/3) \arctan(\sinh(x))}{\cosh(x)},$$

where V_0, V_1 and g are chosen so that the argument of the radical is positive. In Appendix C, we derive another exact solution for the nonlinear model using the method developed in [17].

In the defocusing case $g = -1$, we consider the confining potential studied in [1] with

$$U(x) = \Omega^2 x^2 + i\gamma x e^{-\frac{x^2}{2}}, \tag{1.13}$$

where Ω is a parameter. When $\gamma = 0$ and $U(x)$ is real, the eigenvalues are given by $E_n = -(2n+1)$, $n = 0, 1, 2, \ldots$ whereas the eigenfunctions can be expressed in terms of Hermite polynomials. A numerical study of the linear spectrum for the $\mathcal{PT}$-symmetric Gaussian potential with $\Omega = 0$ was performed by Ahmed [3], and nonlinear modes were recently computed numerically [65, 67]. We will focus on the more general case with $\Omega > 0$.

In agreement with the theory, we show for both examples (1.12) and (1.13) that the coalescence of two isolated imaginary eigenvalues in the linearized problem associated with the stationary states in the NLSE (1.9) leads to instability only if the Krein signatures of the two eigenvalues are opposite to each other.

1.5 Preliminaries

Before proceeding to technical details presented in the thesis, let us give a few basic definitions. For further details see classical texts [2, 50, 61, 63, 68, 71, 87, 142].

1.5.1 Sobolev Spaces

Given a function $u\colon \mathbb{R} \mapsto \mathbb{C}$, we define the L^p norm for any $1 \leq p < \infty$ as

$$\|u\|_p := \left(\int_{\mathbb{R}} |u(x)|^p dx \right)^{1/p},$$

and the L^∞ norm as

$$\|u\|_\infty := \sup_{x \in \mathbb{R}} |u(x)|.$$

For any $p \geq 1$ the associated Lebesgue space $L^p(\mathbb{R})$ is given by

$$L^p(\mathbb{R}) := \{u\colon \|u\|_p < \infty\},$$

and it is known to be a complete metric space (called Banach space). For differentiable functions we define the $W^{k,p}$ norm with $1 \leq p < \infty$ and $k \in \mathbb{N}$:

$$\|u\|_{W^{k,p}} := \left(\sum_{i=0}^{k} \left\| \frac{\partial^i u}{\partial x^i} \right\|_p^p \right)^{1/p},$$

and the associated Sobolev space

$$W^{k,p} := \{u\colon \|u\|_{W^{k,p}} < \infty\}.$$

The L^2-based Sobolev spaces $H^k := W^{k,2}$ is used frequently. Note that $H^0(\mathbb{R}) = L^2(\mathbb{R})$.

Let us introduce the inner product

$$\langle f, g \rangle = \int_{\mathbb{R}} f(x) \overline{g(x)} dx,$$

with complex conjugation in the second component. The Sobolev spaces $H^k(\mathbb{R})$ with $k \in \mathbb{N}$ are Hilbert spaces, since their norm is induced by the inner product

$$\|u\|_{H^k}^2 = \sum_{i=0}^{k} \left\langle \frac{\partial^i u}{\partial x^i}, \frac{\partial^i u}{\partial x^i} \right\rangle.$$

Moreover, $H^k(\mathbb{R})$ is a Banach algebra with respect to pointwise multiplication for any $k \geq 1$: there exists a constant $C \geq 1$ such that for all $u \in H^k(\mathbb{R})$

$$\|u^m\|_{H^k} \leq C \|u\|_{H^k}^m, \quad m \in \mathbb{N}.$$

This property makes the map $u \mapsto u^m$ continuous in the $H^k(\mathbb{R})$ norm. The spaces $H^m(\mathbb{R}) \subset H^k(\mathbb{R})$ are dense for $m > k$, i.e., for each $u \in H^k(\mathbb{R})$ there is a sequence $\{u_n\}_{n \in \mathbb{N}} \subset H^m(\mathbb{R})$ such that $\|u_n - u\|_{H^k} \to 0$ as $n \to \infty$.

1.5.2 Sequence Spaces

Consider a linear space of all bi-infinite sequences with complex-valued entries:

$$x = \{x_n\}_{n\in\mathbb{Z}}, \quad x_n \in \mathbb{C} \quad \forall n \in \mathbb{Z}.$$

For an element of this space, we define $l^p(\mathbb{Z})$ norm for any $1 \le p < \infty$ as

$$\|x\|_{l^p} = \left(\sum_{n\in\mathbb{Z}} |x_n|^p\right)^{1/p}.$$

The space $l^p(\mathbb{Z})$ equipped with this norm can be defined as

$$l^p(\mathbb{Z}) := \{x\colon \|x\|_{l^p} < \infty\}.$$

$l^p(\mathbb{Z})$ is a Banach space for any $p \ge 1$. The space of all bounded bi-infinite sequences, $l^\infty(\mathbb{Z})$, is also a Banach space:

$$l^\infty(\mathbb{Z}) := \{x\colon \|x\|_{l^\infty} < \infty\},$$

where the corresponding norm $\|\cdot\|_{l^\infty}$ is given by

$$\|x\|_{l^\infty} = \sup_{n\in\mathbb{Z}} |x_n|.$$

We are going to use embedding of l^p spaces: $l^p(\mathbb{Z}) \subset l^q(\mathbb{Z})$ with $p < q$, such that

$$\|x\|_{l^q} \le \|x\|_{l^p}.$$

An element from the space $l^q(\mathbb{Z})$ can be approximated by a sequence of elements from the space $l^p(\mathbb{Z})$. In other words, $l^p(\mathbb{Z})$ is dense in $l^q(\mathbb{Z})$ for $p < q$.

The sequence space $l^2(\mathbb{Z})$ is Hilbert space with the inner product:

$$\langle x, y\rangle = \sum_{n\in\mathbb{Z}} x_n \bar{y}_n,$$

where $x = \{x_n\}_{n\in\mathbb{Z}}$ and $y = \{y_n\}_{n\in\mathbb{Z}}$.

The space $l^p(\mathbb{Z})$ is a Banach algebra with respect to multiplication:

$$\|w\|_{l^p} \le \|x\|_{l^p}\|y\|_{l^p},$$

where $x, y \in l^p(\mathbb{Z})$, and $w = \{x_n y_n\}_{n\in\mathbb{Z}}$.

1.5.3 Bounded and Closed Operators

Let X and Y be two Banach spaces, with norms $\|\cdot\|_X$ and $\|\cdot\|_Y$, respectively. Assume that $Y \subset X$ is dense, for example $X = L^2(\mathbb{R})$ and $Y = H^k(\mathbb{R})$ for any $k \ge 1$. Consider linear operator

$\mathcal{L}\colon Y \subset X \to X$, where Y is the maximal domain of operator $\mathcal{L}$ denoted by $\mathrm{D}(\mathcal{L})$. The kernel of $\mathcal{L}$ is given by

$$\ker(\mathcal{L}) := \{u \in Y \colon \mathcal{L}u = 0\},$$

and the range of $\mathcal{L}$ is

$$\mathrm{range}(\mathcal{L}) := \{\mathcal{L}u \in X \colon u \in Y\} \subset X.$$

A linear operator $\mathcal{L}$ is said to be closed if for any sequence $\{u_n\} \subset Y$ with

$$\lim_{n\to\infty} \|u_n - u\|_X = 0 \quad \text{and} \quad \lim_{n\to\infty} \|\mathcal{L}u_n - v\|_X = 0,$$

we have $u \in Y$ and $\mathcal{L}u = v$. The operator is bounded from Y to X if

$$\sup\{\|\mathcal{L}u\|_X \colon \quad u \in Y, \quad \|u\|_Y = 1\} < \infty.$$

From here we can define a norm associated with the space of bounded linear operators $\mathcal{B}(Y, X)$:

$$\|\mathcal{L}\|_{\mathcal{B}(Y,X)} := \sup_{\|u\|_Y = 1} \|\mathcal{L}u\|_X.$$

If $X = Y$, then the induced norm of $\mathcal{L}$ is denoted by $\|\mathcal{L}\|$. If $\mathcal{L}$ is a closed operator with $X = Y$, then $\mathcal{L}$ is a bounded operator. If for each bounded sequence $\{u_n\} \subset Y$ the sequence $\{\mathcal{L}u_n\} \subset X$ has a convergent subsequence, then the operator $\mathcal{L}$ is said to be *compact*.

1.5.4 Resolvent and Spectrum

Definition 4 (Resolvent set)**.** *The* resolvent set *of $\mathcal{L}$, $\rho(\mathcal{L})$, is the set of complex numbers $\lambda \in \mathbb{C}$ such that*

- *$\lambda I - \mathcal{L}$ is invertible*
- *$(\lambda I - \mathcal{L})^{-1}$ is defined on a dense set*
- *$(\lambda I - \mathcal{L})^{-1}$ is a bounded linear operator.*

Here $I\colon X \mapsto X$ is the identity operator: $Iu = u$. For $\lambda \in \rho(\mathcal{L})$ the operator $(\lambda I - \mathcal{L})^{-1}$ is called the resolvent of $\mathcal{L}$. The spectrum of $\mathcal{L}$ is the complement of the resolvent set, i.e.

$$\sigma(\mathcal{L}) = \mathbb{C}\backslash\rho(\mathcal{L}).$$

A complex number $\lambda \in \sigma(\mathcal{L})$ is called an eigenvalue if $\ker(\lambda I - \mathcal{L}) \neq \{0\}$. The kernel $\ker(\lambda I - \mathcal{L})$ is called the eigenspace associated with the eigenvalue λ, and any element $u \in \ker(\lambda I - \mathcal{L})\backslash\{0\}$ is called an eigenvector associated with the eigenvalue λ. If $\mathcal{L}$ is a closed operator, then $\sigma(\mathcal{L})$ is a closed set. If $\mathcal{L}$ is a bounded operator, then $\sigma(\mathcal{L})$ is a closed, bounded, and nonempty set.

Suppose that $\lambda \in \sigma(\mathcal{L})$ is an eigenvalue. The dimension of $\ker(\lambda I - \mathcal{L})$ is called the *geometric multiplicity* of the eigenvalue. An eigenvalue with geometric multiplicity one is called geometrically simple. If the eigenvalue is isolated, then the *algebraic multiplicity* of the eigenvalue is the dimension of the largest subspace $Y_\lambda \subset Y$, which

- is invariant under the action of $\mathcal{L}$: if $u_\lambda \in Y_\lambda$, then $\mathcal{L}u_\lambda \in Y_\lambda$,
- satisfies the property $\sigma(\mathcal{L}|_{Y_\lambda}) = \{\lambda\}$.

Note that algebraic multiplicity is always greater or equal to geometric multiplicity. An eigenvalue is called *semi-simple* if algebraic and geometric multiplicities coincide and *defective* if algebraic multiplicity exceeds geometric multiplicity. An eigenvalue is *simple* if it is algebraically (and geometrically) simple.

1.5.5 Adjoint and Fredholm Operators

Assume that X is a Hilbert space equipped with the inner product $\langle\cdot,\cdot\rangle_X$, and that $\mathcal{L}$ is a closed operator with a dense domain $\mathrm{D}(\mathcal{L}) \subset X$. Let $\mathcal{L}^*$ be the adjoint operator, then its domain is the set of all $v \in X$ for which the linear functional

$$u \to \langle \mathcal{L}u, v\rangle$$

is continuous in the Hilbert norm on X. From Riesz representation theorem we know that there exists a unique $w \in X$ for which

$$\langle \mathcal{L}u, v\rangle = \langle u, w\rangle.$$

For such $v \in \mathrm{D}(\mathcal{L}^*)$ the adjoint operator $\mathcal{L}^*$ is uniquely defined by the map $\mathcal{L}^*v = w$. The adjoint operator is closed, and its domain is also dense in X. The spectrum of an operator and its adjoint are related as

$$\sigma(\mathcal{L}^*) = \overline{\sigma(\mathcal{L})}.$$

Definition 5 (Self-adjoint operator)**.** *A linear operator* $\mathcal{L}\colon \mathrm{D}(\mathcal{L}) \subset X \mapsto X$ *in a Hilbert space* X*, with dense domain* $\mathrm{D}(\mathcal{L})$*, is called* self-adjoint *if its adjoint* $\mathcal{L}^*\colon D(\mathcal{L}^*) \subset X \mapsto X$ *satisfies* $\mathrm{D}(\mathcal{L}) = \mathrm{D}(\mathcal{L}^*)$ *and* $\mathcal{L}u = \mathcal{L}^*u$ *for all* $u \in \mathrm{D}(\mathcal{L})$*.*

The spectrum of a self-adjoint operator is real. The algebraic and geometric multiplicities of an isolated eigenvalue $\lambda \in \sigma(\mathcal{L})$ of a self-adjoint operator are the same, i.e., every isolated eigenvalue is semi-simple.

Definition 6 (Positive operator)**.** *Let* X *be a Hilbert space. A linear operator* $\mathcal{L}\colon X \to X$ *is called* positive *if* $\langle \mathcal{L}u, u\rangle \geq 0$ *for all* $u \in X$*.*

Definition 7 (Fredholm operator)**.** *The operator* $\mathcal{L}$ *is a* Fredholm operator *if*

- $\ker(\mathcal{L})$ *is finite-dimensional,*
- $\mathrm{range}(\mathcal{L})$ *is closed with finite codimension.*

The integer

$$\mathrm{ind}(\mathcal{L}) = \dim(\ker(\mathcal{L})) - \mathrm{codim}(\mathrm{range}(\mathcal{L})).$$

is called the Fredholm index.

The operator $\mathcal{L}$ is Fredholm if and only if $\mathcal{L}^*$ is, and their indices are related as

$$\operatorname{ind}(\mathcal{L}) = -\operatorname{ind}(\mathcal{L}^*).$$

If $\lambda \in \sigma(\mathcal{L})$ is an isolated eigenvalue with finite algebraic multiplicity, then $\lambda I - \mathcal{L}$ is a Fredholm operator with index zero. If $\mathcal{L}u = f$, then for every $v \in \ker(\mathcal{L}^*)$

$$\langle f, v\rangle = \langle \mathcal{L}u, v\rangle = \langle u, \mathcal{L}^* v\rangle = 0.$$

In other words, the range of $\mathcal{L}$ is orthogonal to the kernel of $\mathcal{L}^*$. It turns out that the orthogonality $\langle f, v\rangle = 0$ for every $v \in \ker(\mathcal{L}^*)$ is a necessary condition for solvability of equation $\mathcal{L}u = f$. It becomes also a sufficient condition if $\mathcal{L}$ is a Fredholm operator. More precisely, the following theorem holds.

Theorem 3 (Fredholm Alternative)**.** *Suppose that X is a Hilbert space with inner product $\langle\cdot,\cdot\rangle_X$, and $\mathcal{L}\colon \mathrm{D}(\mathcal{L}) \subset X \mapsto X$ is a closed Fredholm operator with dense domain $\mathrm{D}(\mathcal{L}) \subset X$. For $f \in X$ the nonhomogeneous problem $\mathcal{L}u = f$ has a solution $u \in \mathrm{D}(\mathcal{L})$ if and only if $f \in \ker(\mathcal{L}^*)^\perp$:*

$$\operatorname{range}(\mathcal{L}) = \ker(\mathcal{L}^*)^\perp.$$

Moreover, the Fredholm index counts the dimensional mismatch between the kernels of $\mathcal{L}$ and $\mathcal{L}^*$:

$$\dim(\ker(\mathcal{L})) - \dim(\ker(\mathcal{L}^*)) = \operatorname{ind}(\mathcal{L}).$$

For any Fredholm operator the space X can be decomposed as

$$X = \operatorname{range}(\mathcal{L}) \oplus \ker(\mathcal{L}^*).$$

Definition 8. *Let X be a Banach space and let $\mathcal{L}\colon \mathrm{D}(\mathcal{L}) \subset X \to X$ be a closed linear operator with dense domain $\mathrm{D}(\mathcal{L})$ in X. The spectrum of $\mathcal{L}$ is decomposed into the following three sets:*

- *The* point spectrum *or* discrete spectrum *$\sigma_p(\mathcal{L})$ is a set of $\lambda \in \sigma(\mathcal{L})$ such that the operator $\lambda I - \mathcal{L}$ is not invertible.*
- *The* residual spectrum *$\sigma_r(\mathcal{L})$ is a set of $\lambda \in \sigma(\mathcal{L})$ such that operator $(\lambda I - \mathcal{L})^{-1}$ is not defined on a dense set.*
- *The* continuous spectrum *$\sigma_c(\mathcal{L})$ is a set of $\lambda \in \sigma(\mathcal{L})$ such that $(\lambda I - \mathcal{L})^{-1}$ is defined on a dense set, but $(\lambda I - \mathcal{L})^{-1}$ is an unbounded operator.*

The following spectral properties hold for self-adjoint operators:

Theorem 4. *Let $\mathcal{L}$ be a self-adjoint operator on a Hilbert space X. Then*

- *$\mathcal{L}$ has no residual spectrum: $\sigma_r(\mathcal{L}) = \emptyset$.*
- *The spectrum is real: $\sigma(\mathcal{L}) \subset \mathbb{R}$.*
- *Eigenvectors corresponding to distinct eigenvalues of $\sigma_p(\mathcal{L})$ are orthogonal.*

To locate continuous spectrum, one needs to compute the Fredholm index of an operator. One of the techniques is to perturb a Fredholm operator.

Definition 9. *Let $\mathcal{L}_0$ be a closed operator with $\rho(\mathcal{L}_0) \neq \emptyset$. The operator $\mathcal{L}$ is called a* relatively compact perturbation *of $\mathcal{L}_0$ (or relatively $\mathcal{L}_0$-compact) if*

- $\mathrm{D}(\mathcal{L}) \subset \mathrm{D}(\mathcal{L} - \mathcal{L}_0)$
- $(\mathcal{L}_0 - \mathcal{L})(\lambda I - \mathcal{L}_0)^{-1}$ *is compact for some (and hence, for all) $\lambda \in \rho(\mathcal{L}_0)$.*

A number of stability theorems for relatively compact perturbations of Fredholm operators exist. They are usually referred to as the Weyl Spectrum Theorem:

Theorem 5 (Weyl Spectrum Theorem)**.** *Let $\mathcal{L}$ and $\mathcal{L}_0$ be closed linear operators on a Hilbert space X. If $\mathcal{L}$ is a relatively compact perturbation of $\mathcal{L}_0$, then the following properties hold:*

- *The operator $\lambda I - \mathcal{L}$ is Fredholm if and only if $\lambda I - \mathcal{L}_0$ is Fredholm.*
- $\mathrm{ind}(\lambda I - \mathcal{L}) = \mathrm{ind}(\lambda I - \mathcal{L}_0)$.
- *The operators $\mathcal{L}$ and $\mathcal{L}_0$ have the same continuous spectra: $\sigma_c(\mathcal{L}) = \sigma_c(\mathcal{L}_0)$.*

1.5.6 Useful results

Here we list individual results which will be used in this thesis.

Implicit Function Theorem. (Theorem 4.E in [142]) *Let X, Y and Z be Banach spaces and let $F(x, y)\colon X \times Y \to Z$ be a C^1 map on an open neighborhood of the point $(x_0, y_0) \in X \times Y$. Assume that*

$$F(x_0, y_0) = 0$$

and that

$$D_x F(x_0, y_0)\colon X \to Z \text{ is one-to-one and onto.}$$

There are $r > 0$ and $\sigma > 0$ such that for each y with $\|y - y_0\|_Y \leq \sigma$ there exists a unique solution $x \in X$ of the nonlinear equation $F(x, y) = 0$ with $\|x - x_0\|_X \leq r$. Moreover, the map $Y \ni y \mapsto x(y) \in X$ is C^1 near $y = y_0$.

Perturbation Theory for Linear Operators. (Theorem VII.1.7 in [71]) *Let $T(\epsilon)$ be a family of operators from Banach space X to itself, which depends analytically on the small parameter ϵ. If the spectrum of $T(0)$ is separated into two parts, the subspaces of X corresponding to the separated parts also depend on ϵ analytically. In particular, the spectrum of $T(\epsilon)$ is separated into two parts for any $\epsilon \neq 0$ sufficiently small.*

Lyapunov's Stability Theorem. [87] *Consider the following evolution problem on a Hilbert space X,*

$$\frac{d\vec{x}}{dt} = \vec{f}(\vec{x}), \quad \vec{x} \in X, \tag{1.14}$$

where $\vec{f}: X \to X$ satisfies $\vec{f}(\vec{0}) = \vec{0}$. Let $V: X \to \mathbb{R}$ satisfy the following properties:

1. *$V \in C^2(X)$ with $V(\vec{0}) = 0$;*
2. *There exists $C > 0$ such that $V(\vec{x}) \geq C\|\vec{x}\|_X^2$ for every $\vec{x} \in X$;*
3. *$\frac{d}{dt}V(\vec{x}) \leq 0$ for every solution of (1.14).*

Then the zero equilibrium of the evolution system (1.14) *is nonlinearly stable in the sense: for every $\nu > 0$ there is $\delta > 0$ such that if $\vec{x}_0 \in X$ satisfies $\|\vec{x}_0\|_X \leq \delta$, then the unique solution $\vec{x}(t)$ of the evolution system (1.14) such that $\vec{x}(0) = \vec{x}_0$ satisfies $\|\vec{x}(t)\|_X \leq \epsilon$ for every $t \in \mathbb{R}^+$.*

Hamilton–Krein Index Theorem (Theorem 3.3 in [68]). *Let L be a self-adjoint operator in a Hilbert space X with finitely many negative eigenvalues $n(L)$, a simple zero eigenvalue with eigenfunction v_0, and the rest of its spectrum is bounded from below by a positive number. Let J be a bounded invertible skew-symmetric operator in X. Let k_r be a number of positive real eigenvalues of JL, k_c be a number of quadruplets $\{\pm\lambda, \pm\bar{\lambda}\}$ that are neither in $\mathbb{R}$ nor in $i\mathbb{R}$, and k_i^- be a number of purely imaginary pairs of eigenvalues of JL whose invariant subspaces lie in the negative subspace of L. Let $D = \langle L^{-1}J^{-1}v_0, J^{-1}v_0\rangle_X$ be finite and nonzero. Then,*

$$K_{HAM} = k_r + 2k_c + 2k_i^- = \begin{cases} n(L) - 1, & D < 0, \\ n(L), & D > 0. \end{cases} \tag{1.15}$$

Chapter 2

Breathers in Discrete Systems

2.1 Model

A simple yet universal model widely used to study coupled nonlinear oscillators is the Frenkel-Kontorova (FK) model [85]. It describes a chain of classical particles coupled to their neighbors and subjected to a periodic on-site potential. In the continuum approximation, the FK model reduces to the sine-Gordon equation, which is exactly integrable. The FK model is known to describe a rich variety of important nonlinear phenomena, which find applications in solid-state physics and nonlinear science [27].

We consider here a two-array system of coupled pendula, where each pendulum is connected to the nearest neighbors by linear couplings. Figure 2.1 shows schematically that each array of pendula is connected in the longitudinal direction by the torsional springs, whereas each pair of pendula is connected in the transverse direction by a common string. Newton's equations of motion are given by

$$\begin{cases} \ddot{x}_n + \sin(x_n) = C\left(x_{n+1} - 2x_n + x_{n-1}\right) + Dy_n, \\ \ddot{y}_n + \sin(y_n) = C\left(y_{n+1} - 2y_n + y_{n-1}\right) + Dx_n, \end{cases} \qquad n \in \mathbb{Z}, \quad t \in \mathbb{R}, \tag{2.1}$$

where (x_n, y_n) correspond to the angles of two arrays of pendula, dots denote derivatives of angles with respect to time t, and the positive parameters C and D describe couplings between the two arrays in the longitudinal and transverse directions, respectively. The type of coupling between the two pendula with the angles x_n and y_n is referred to as the *direct coupling* between nonlinear oscillators (see Section 8.2 in [118]).

We consider oscillatory dynamics of coupled pendula under the following assumptions.

(A1) The coupling parameters C and D are small. Therefore, we can introduce a small parameter μ such that both C and D are proportional to μ^2.

(A2) A resonant periodic force is applied to the common strings for each pair of coupled pendula. Therefore, D is considered to be proportional to $\cos(2\omega t)$, where ω is selected near the unit

frequency of linear pendula indicating the $1:2$ parametric resonance between the force and the pendula.

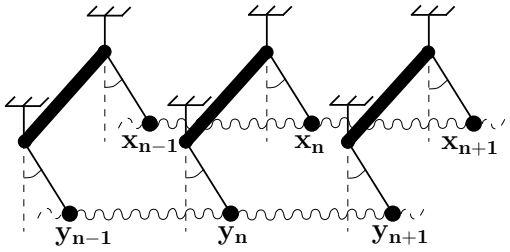

Figure 2.1: A schematic picture for the chain of coupled pendula connected by torsional springs, where each pair is hung on a common string.

Mathematically, we impose the following representation for parameters C and $D(t)$:

$$C = \epsilon\mu^2, \quad D(t) = 2\gamma\mu^2\cos(2\omega t), \quad \omega^2 = 1 + \mu^2\Omega, \tag{2.2}$$

where γ, ϵ, Ω are μ-independent parameters, whereas μ is the formal small parameter to characterize the two assumptions (A1) and (A2).

In the formal limit $\mu \to 0$, the pendula are uncoupled, and their small-amplitude oscillations can be studied with the asymptotic multi-scale expansion

$$\begin{cases} x_n(t) = \mu\left[A_n(\mu^2 t)e^{i\omega t} + \bar{A}_n(\mu^2 t)e^{-i\omega t}\right] + \mu^3 X_n(t;\mu), \\ y_n(t) = \mu\left[B_n(\mu^2 t)e^{i\omega t} + \bar{B}_n(\mu^2 t)e^{-i\omega t}\right] + \mu^3 Y_n(t;\mu), \end{cases} \tag{2.3}$$

where (A_n, B_n) are amplitudes for nearly harmonic oscillations and (X_n, Y_n) are remainder terms. In a similar context of single-array coupled nonlinear oscillators, it is shown in [110] how the asymptotic expansions like (2.3) can be justified. From the conditions that the remainder terms (X_n, Y_n) remain bounded as the system evolves, the amplitudes (A_n, B_n) are shown to satisfy the discrete nonlinear Schrödinger (dNLS) equations, which bring together all the phenomena affecting the nearly harmonic oscillations (such as cubic nonlinear terms, the detuning frequency, the coupling between the oscillators, and the amplitude of the parametric driving force). A similar derivation for a single pair of coupled pendula is reported in [16].

Using the algorithm in [110] and restricting the scopes of this derivation to the formal level, we write the truncated system of equations for the remainder terms:

$$\begin{cases} \ddot{X}_n + X_n = F_n^{(1)}e^{i\omega t} + \overline{F_n^{(1)}}e^{-i\omega t} + F_n^{(3)}e^{3i\omega t} + \overline{F_n^{(3)}}e^{-3i\omega t}, \\ \ddot{Y}_n + Y_n = G_n^{(1)}e^{i\omega t} + \overline{G_n^{(1)}}e^{-i\omega t} + G_n^{(3)}e^{3i\omega t} + \overline{G_n^{(3)}}e^{-3i\omega t}, \end{cases} \quad n \in \mathbb{Z}, \quad t \in \mathbb{R}, \tag{2.4}$$

where $F_n^{(1,3)}$ and $G_n^{(1,3)}$ are uniquely defined. Bounded solutions to the linear inhomogeneous equations (2.4) exist if and only if $F_n^{(1)} = G_n^{(1)} = 0$ for every $n \in \mathbb{Z}$. Straightforward computations show that the conditions $F_n^{(1)} = G_n^{(1)} = 0$ are equivalent to the following evolution equations for slowly

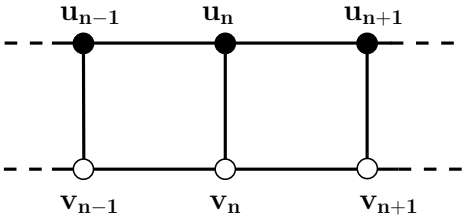

Figure 2.2: The chain of $\mathcal{PT}$-symmetric dimers representing coupled pendula. Filled (empty) circles correspond to sites with gain (loss).

varying amplitudes (A_n, B_n):

$$\begin{cases} 2i\dot{A}_n = \epsilon\left(A_{n+1} - 2A_n + A_{n-1}\right) + \Omega A_n + \gamma\bar{B}_n + \frac{1}{2}|A_n|^2 A_n, \\ 2i\dot{B}_n = \epsilon\left(B_{n+1} - 2B_n + B_{n-1}\right) + \Omega B_n + \gamma\bar{A}_n + \frac{1}{2}|B_n|^2 B_n, \end{cases} \quad n \in \mathbb{Z},\ t \in \mathbb{R}. \tag{2.5}$$

The system (2.5) takes the form of coupled parametrically forced dNLS equations. There exists an invariant reduction of system (2.5) given by

$$A_n = B_n, \quad n \in \mathbb{Z} \tag{2.6}$$

to the scalar parametrically forced dNLS equation. Existence and stability of breathers in such scalar dNLS equations was considered numerically by Susanto *et al.* in [135, 136].

The reduction (2.6) corresponds to the symmetric synchronized oscillations of coupled pendula of the model (2.1) with

$$x_n = y_n, \quad n \in \mathbb{Z}. \tag{2.7}$$

In what follows, we consider a more general class of synchronized oscillations of coupled pendula of the model (2.1). The solutions we consider also generalize the breather solutions of the coupled parametrically forced dNLS equations (2.5).

It turns out that the model (2.5) can be cast to the form of the parity–time reversal ($\mathcal{PT}$) dNLS equations [16]. Using the variables

$$u_n := \frac{1}{4}\left(A_n - i\bar{B}_n\right), \quad v_n := \frac{1}{4}\left(A_n + i\bar{B}_n\right), \tag{2.8}$$

the system of coupled dNLS equations (2.5) is rewritten in the equivalent form

$$\begin{cases} 2i\dot{u}_n = \epsilon\left(v_{n+1} - 2v_n + v_{n-1}\right) + \Omega v_n + i\gamma u_n + 2\left[\left(2|u_n|^2 + |v_n|^2\right)v_n + u_n^2\bar{v}_n\right], \\ 2i\dot{v}_n = \epsilon\left(u_{n+1} - 2u_n + u_{n-1}\right) + \Omega u_n - i\gamma v_n + 2\left[\left(|u_n|^2 + 2|v_n|^2\right)u_n + \bar{u}_n v_n^2\right], \end{cases} \tag{2.9}$$

which is the starting point for our analytical and numerical work. Figure 2.2 depicts schematically the chain of coupled pendula represented by (2.9). The invariant reduction (2.6) for system (2.5) becomes

$$\mathrm{Im}(e^{\frac{i\pi}{4}}u_n) = 0, \quad \mathrm{Im}(e^{-\frac{i\pi}{4}}v_n) = 0, \quad n \in \mathbb{Z}. \tag{2.10}$$

In the context of hard nonlinear oscillators (e.g. in the framework of the ϕ^4 theory), the cubic nonlinearity may have the opposite sign compared to the one in the system (2.9). However, given the applied context of the system of coupled pendula, we will stick to the specific form (2.9) in further analysis.

2.2 Symmetries and conserved quantities

The system of coupled dNLS equations (2.9) is referred to as the $\mathcal{PT}$-symmetric dNLS equation because the solutions remain invariant with respect to the action of the parity $\mathcal{P}$ and time-reversal $\mathcal{T}$ operators given by

$$\mathcal{P}\begin{bmatrix} u \\ v \end{bmatrix} = \begin{bmatrix} v \\ u \end{bmatrix}, \qquad \mathcal{T}\begin{bmatrix} u(t) \\ v(t) \end{bmatrix} = \begin{bmatrix} \bar{u}(-t) \\ \bar{v}(-t) \end{bmatrix}. \tag{2.11}$$

The parameter γ introduces the gain–loss coefficient in each pair of coupled oscillators due to the resonant periodic force. In the absence of all other effects, the γ-term of the first equation of system (2.9) induces the exponential growth of amplitude u_n, whereas the γ-term of the second equation induces the exponential decay of amplitude v_n, if $\gamma > 0$.

The system (2.9) truncated at a single site (say $n = 0$) is called the $\mathcal{PT}$-symmetric dimer. In the work of Barashenkov *et al.* [16], it was shown that all $\mathcal{PT}$-symmetric dimers with physically relevant cubic nonlinearities represent Hamiltonian systems in appropriately introduced canonical variables. However, the $\mathcal{PT}$-symmetric dNLS equation on a lattice does not typically have a Hamiltonian form if $\gamma \neq 0$.

Nevertheless, the particular nonlinear functions arising in the system (2.9) correspond to the $\mathcal{PT}$-symmetric dimers with a cross–gradient Hamiltonian structure [16], where variables $(u_n, \bar{v}_n)$ are canonically conjugate. As a result, the system (2.9) on the chain $\mathbb{Z}$ has additional conserved quantities. This fact looked like a mystery in the recent works [15, 16].

Here we clarify the mystery in the context of the derivation of the $\mathcal{PT}$-symmetric dNLS equation (2.9) from the original system (2.1). Indeed, the system (2.1) of classical Newton particles has a standard Hamiltonian structure with the energy function

$$\begin{aligned} H_{x,y}(t) &= \sum_{n\in\mathbb{Z}} \frac{1}{2}(\dot{x}_n^2 + \dot{y}_n^2) + 2 - \cos(x_n) - \cos(y_n) \\ &\quad + \frac{1}{2}C(x_{n+1} - x_n)^2 + \frac{1}{2}C(y_{n+1} - y_n)^2 - D(t)x_n y_n. \end{aligned} \tag{2.12}$$

Since the periodic movement of common strings for each pair of pendula result in the time-periodic coefficient $D(t)$, the energy $H_{x,y}(t)$ is a periodic function of time t. In addition, no other conserved quantities such as momenta exist typically in lattice differential systems such as the system (2.1) due to broken continuous translational symmetry.

After the system (2.1) is reduced to the coupled dNLS equations (2.5) with the asymptotic expansion (2.3), we can write the evolution problem (2.5) in the Hamiltonian form with the standard straight-gradient symplectic structure

$$2i\frac{dA_n}{dt} = \frac{\partial H_{A,B}}{\partial \bar{A}_n}, \quad 2i\frac{dB_n}{dt} = \frac{\partial H_{A,B}}{\partial \bar{B}_n}, \quad n \in \mathbb{Z}, \tag{2.13}$$

where the time variable t stands now for the slow time $\mu^2 t$ and the energy function is

$$\begin{aligned} H_{A,B} &= \sum_{n\in\mathbb{Z}} \frac{1}{4}(|A_n|^4 + |B_n|^4) + \Omega(|A_n|^2 + |B_n|^2) + \gamma(A_n B_n + \bar{A}_n \bar{B}_n) \\ &\quad -\epsilon|A_{n+1} - A_n|^2 - \epsilon|B_{n+1} - B_n|^2. \end{aligned} \tag{2.14}$$

The energy function $H_{A,B}$ is conserved in the time evolution of the Hamiltonian system (2.13). In addition, there exists another conserved quantity

$$Q_{A,B} = \sum_{n\in\mathbb{Z}} (|A_n|^2 - |B_n|^2), \tag{2.15}$$

which is related to the gauge symmetry $(A, B) \to (Ae^{i\alpha}, Be^{i\alpha})$ with $\alpha \in \mathbb{R}$ for solutions to the system (2.5).

When the transformation of variables (2.8) is used, the $\mathcal{PT}$-symmetric dNLS equation (2.9) is cast to the Hamiltonian form with the cross-gradient symplectic structure

$$2i\frac{du_n}{dt} = \frac{\partial H_{u,v}}{\partial \bar{v}_n}, \quad 2i\frac{dv_n}{dt} = \frac{\partial H_{u,v}}{\partial \bar{u}_n}, \quad n \in \mathbb{Z}, \tag{2.16}$$

where the energy function is

$$\begin{aligned} H_{u,v} &= \sum_{n\in\mathbb{Z}} (|u_n|^2 + |v_n|^2)^2 + (u_n\bar{v}_n + \bar{u}_n v_n)^2 + \Omega(|u_n|^2 + |v_n|^2) \\ &\quad -\epsilon|u_{n+1} - u_n|^2 - \epsilon|v_{n+1} - v_n|^2 + i\gamma(u_n\bar{v}_n - \bar{u}_n v_n). \end{aligned} \tag{2.17}$$

The gauge-related function is written in the form

$$Q_{u,v} = \sum_{n\in\mathbb{Z}} (u_n\bar{v}_n + \bar{u}_n v_n). \tag{2.18}$$

The functions $H_{u,v}$ and $Q_{u,v}$ are conserved in the time evolution of the system (2.9). These functions follow from (2.14) and (2.15) after the transformation (2.8) is used. Thus, the cross-gradient Hamiltonian structure of the $\mathcal{PT}$-symmetric dNLS equation (2.9) is inherited from the Hamiltonian structure of the coupled oscillator model (2.1).

2.3 Breathers (time-periodic solutions)

We characterize the existence of breathers supported by the $\mathcal{PT}$-symmetric dNLS equation (2.9). In particular, breather solutions are continued for small values of coupling constant ϵ from solutions of the dimer equation arising at a single site, say the central site at $n = 0$. We shall work in a sequence space $\ell^2(\mathbb{Z})$ of square integrable complex-valued sequences.

Time-periodic solutions to the $\mathcal{PT}$-symmetric dNLS equation (2.9) are given in the form [80, 115]:

$$u(t) = Ue^{-\frac{1}{2}iEt}, \quad v(t) = Ve^{-\frac{1}{2}iEt}, \tag{2.19}$$

where the frequency parameter E is considered to be real, the factor $1/2$ is introduced for convenience, and the sequence (U, V) is time-independent. The breather (2.19) is a localized mode if $(U, V) \in \ell^2(\mathbb{Z})$, which implies that $|U_n|, |V_n| \to 0$ as $|n| \to \infty$. The breather (2.19) is considered to be $\mathcal{PT}$-symmetric with respect to the operators in (2.11) if $V = \bar{U}$.

The reduction (2.10) for symmetric synchronized oscillations is satisfied if

$$E = 0: \quad \text{Im}(e^{\frac{i\pi}{4}}U_n) = 0, \quad \text{Im}(e^{-\frac{i\pi}{4}}V_n) = 0, \quad n \in \mathbb{Z}. \tag{2.20}$$

The time-periodic breathers (2.19) with $E \neq 0$ generalize the class of symmetric synchronized oscillations (2.20).

The time-independent sequence $(U, V) \in \ell^2(\mathbb{Z})$ can be found from the stationary $\mathcal{PT}$-symmetric dNLS equation:

$$\begin{cases} EU_n = \epsilon\left(V_{n+1} - 2V_n + V_{n-1}\right) + \Omega V_n + i\gamma U_n + 2\left[\left(2|U_n|^2 + |V_n|^2\right)V_n + U_n^2\bar{V}_n\right], \\ EV_n = \epsilon\left(U_{n+1} - 2U_n + U_{n-1}\right) + \Omega U_n - i\gamma V_n + 2\left[\left(|U_n|^2 + 2|V_n|^2\right)U_n + \bar{U}_n V_n^2\right]. \end{cases} \tag{2.21}$$

The $\mathcal{PT}$-symmetric breathers with $V = \bar{U}$ satisfy the following scalar difference equation

$$EU_n = \epsilon\left(\bar{U}_{n+1} - 2\bar{U}_n + \bar{U}_{n-1}\right) + \Omega\bar{U}_n + i\gamma U_n + 6|U_n|^2\bar{U}_n + 2U_n^3. \tag{2.22}$$

Note that the reduction (2.20) is compatible with equation (2.22) in the sense that if $E = 0$ and $U_n = R_n e^{-i\pi/4}$, then R satisfies a real-valued difference equation.

Let us set $\epsilon = 0$ for now and consider solutions to the dimer equation at the central site $n = 0$:

$$(E - i\gamma)U_0 - \Omega\bar{U}_0 = 6|U_0|^2\bar{U}_0 + 2U_0^3. \tag{2.23}$$

The parameters γ and Ω are considered to be fixed, and the breather parameter E is thought to parameterize continuous branches of solutions to the nonlinear algebraic equation (2.23). The solution branches depicted on Figure 2.3 are given in the following lemma.

Lemma 4. *Assume $\gamma \neq 0$. The algebraic equation (2.23) admits the following solutions depending on γ and Ω:*

(a) $\Omega > |\gamma|$ - two symmetric unbounded branches exist for $\pm E > E_0$,

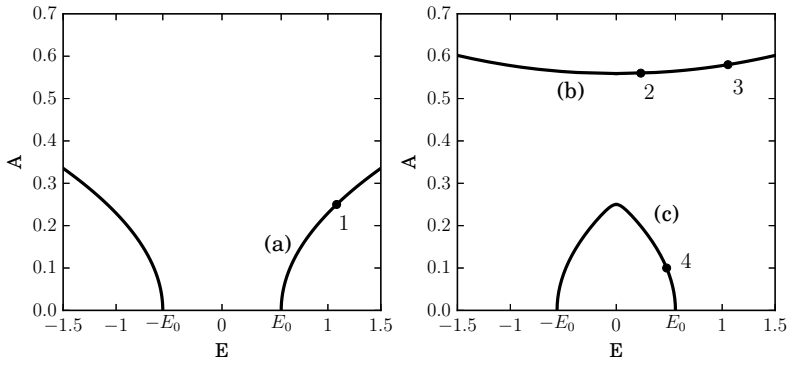

Figure 2.3: Solution branches for the dimer equation (2.23).

(b) $\Omega < |\gamma|$ *- an unbounded branch exists for every* $E \in \mathbb{R}$*,*

(c) $\Omega < -|\gamma|$ *- a bounded branch exists for* $-E_0 < E < E_0$*,*

where $E_0 := \sqrt{\Omega^2 - \gamma^2}$*.*

Proof. Substituting the decomposition $U_0 = Ae^{i\theta}$ with $A > 0$ and $\theta \in [-\pi, \pi)$ into the algebraic equation (2.23), we obtain

$$\sin(2\theta) = \frac{\gamma}{4A^2 + \Omega}, \quad \cos(2\theta) = \frac{E}{8A^2 + \Omega}. \tag{2.24}$$

Excluding θ by using the fundamental trigonometric identity, we obtain the explicit parametrization of the solutions to the algebraic equation (2.23) by the amplitude parameter A:

$$E^2 = (8A^2 + \Omega)^2 \left[1 - \frac{\gamma^2}{(4A^2 + \Omega)^2}\right]. \tag{2.25}$$

The zero-amplitude limit $A = 0$ is reached if $|\Omega| > |\gamma|$, in which case $E = \pm E_0$, where $E_0 := \sqrt{\Omega^2 - \gamma^2}$. If $|\Omega| < |\gamma|$, the solution branches (if they exist) are bounded away from the zero solution.

Now we analyze the three cases of parameters γ and Ω formulated in the lemma.

(a) If $\Omega > |\gamma|$, then the parametrization (2.25) yields a monotonically increasing map $\mathbb{R}^+ \ni A^2 \mapsto E^2 \in (E_0^2, \infty)$ because

$$\frac{dE^2}{dA^2} = \frac{8(8A^2 + \Omega)}{(4A^2 + \Omega)^3} \left[2(4A^2 + \Omega)^3 - \gamma^2\Omega\right] > 0. \tag{2.26}$$

In the two asymptotic limits, we obtain from (2.25):

$$E^2 = E_0^2 + \mathcal{O}(A^2) \quad \text{as} \quad A \to 0 \quad \text{and} \quad E^2 = 64A^4 + \mathcal{O}(A^2) \quad \text{as} \quad A \to \infty.$$

See Figure 2.3(a).

(b) If $\Omega < |\gamma|$, the parametrization (2.25) yields a monotonically increasing map $(A_+^2, \infty) \ni A^2 \mapsto E^2 \in \mathbb{R}^+$, where

$$A_+^2 := \frac{|\gamma| - \Omega}{4}. \tag{2.27}$$

Indeed, we note that $4A^2 + \Omega \geq 4A_+^2 + \Omega = |\gamma| > 0$ and

$$2(4A^2 + \Omega)^3 - \gamma^2\Omega \geq \gamma^2(2|\gamma| - \Omega) > 0,$$

so that the derivative in (2.26) is positive for every $A^2 \geq A_+^2$. We have

$$E^2 \to 0 \quad \text{as} \quad A^2 \to A_+^2 \quad \text{and} \quad E^2 = 64A^4 + \mathcal{O}(A^2) \quad \text{as} \quad A \to \infty.$$

See Figure 2.3(b).

(c) If $\Omega < -|\gamma|$, then the parametrization (2.25) yields a monotonically decreasing map $(0, A_-^2) \ni A^2 \mapsto E^2 \in (0, E_0^2)$, where

$$A_-^2 := \min\left\{\frac{|\Omega| - |\gamma|}{4}, \frac{|\Omega|}{8}\right\}. \tag{2.28}$$

In (2.28), the first choice is made if $|\Omega| \in (|\gamma|, 2|\gamma|)$ and the second choice is made if $|\Omega| \in (2|\gamma|, \infty)$. Both choices are the same if $|\Omega| = 2|\gamma|$. We note that $8A^2 \leq |\Omega|$, therefore, the derivative (2.26) needs to be rewritten in the form

$$\frac{dE^2}{dA^2} = -\frac{8(|\Omega| - 8A^2)}{(|\Omega| - 4A^2)^3}\left[2(|\Omega| - 4A^2)^3 - \gamma^2|\Omega|\right] < 0, \tag{2.29}$$

where $2(|\Omega| - 4A^2)^3 - \gamma^2|\Omega| > 0$ for both $|\Omega| \in (|\gamma|, 2|\gamma|)$ and $|\Omega| \in [2|\gamma|, \infty)$. In the two asymptotic limits, we obtain from (2.25):

$$E^2 = E_0^2 + \mathcal{O}(A^2) \quad \text{as} \quad A \to 0 \quad \text{and} \quad E^2 \to 0 \quad \text{as} \quad A^2 \to A_-^2.$$

See Figure 2.3(c).

Note that branches (b) and (c) coexist for $\Omega < -|\gamma|$. □

Remark 1. *The reduction (2.20) corresponds to the choice:*

$$E = 0, \quad \theta = -\frac{\pi}{4}, \quad 4A^2 + \Omega + \gamma = 0.$$

If $\gamma > 0$, this choice corresponds to $A = A_-$ for $\Omega \in (-2|\gamma|, -|\gamma|)$, that is, the point $E = 0$ on branch (c). If $\gamma < 0$, it corresponds to $A = A_+$ for any $\Omega < |\gamma|$, that is, the point $E = 0$ on branch (b).

Every solution of Lemma 4 can be extended to a breather on the chain $\mathbb{Z}$ which satisfies the spatial symmetry condition in addition to the $\mathcal{PT}$ symmetry:

$$U_{-n} = U_n = \bar{V}_n = \bar{V}_{-n}, \quad n \in \mathbb{Z}. \tag{2.30}$$

With two applications of the implicit function theorem (see Section 1.5.6), we prove the following main result of this section.

Theorem 6. *Fix $\gamma \neq 0$, $\Omega \neq -2|\gamma|$, and $E \neq \pm E_0$, where $E_0 := \sqrt{\Omega^2 - \gamma^2} > 0$ if $|\Omega| > |\gamma|$. There exists $\epsilon_0 > 0$ sufficiently small and $C_0 > 0$ such that for every $\epsilon \in (-\epsilon_0, \epsilon_0)$, there exists a unique solution $U \in l^2(\mathbb{Z})$ to the difference equation (2.22) satisfying the symmetry (2.30) and the bound*

$$\left|U_0 - Ae^{i\theta}\right| + \sup_{n\in\mathbb{N}} |U_n| \leq C_0|\epsilon|, \tag{2.31}$$

where A and θ are defined in Lemma 4. Moreover, the solution U is smooth in ϵ.

Proof. In the first application of the implicit function theorem, we consider the following system of algebraic equations

$$EU_n = \epsilon\left(\bar{U}_{n+1} - 2\bar{U}_n + \bar{U}_{n-1}\right) + \Omega\bar{U}_n + i\gamma U_n + 6|U_n|^2\bar{U}_n + 2U_n^3, \quad n \in \mathbb{N}, \tag{2.32}$$

where $U_0 \in \mathbb{C}$ is given, in addition to parameters γ, Ω, and E.

Let $x = \{U_n\}_{n\in\mathbb{N}}$, $X = \ell^2(\mathbb{N})$, $y = \epsilon$, $Y = \mathbb{R}$, and $Z = \ell^2(\mathbb{N})$. Then, we have $F(0,0) = 0$ and the Jacobian operator $D_xF(0,0)$ is given by identical copies of the matrix

$$\begin{bmatrix} E - i\gamma & -\Omega \\ -\Omega & E + i\gamma \end{bmatrix},$$

with the eigenvalues $\lambda_\pm := E \pm \sqrt{\Omega^2 - \gamma^2}$. By the assumption of the lemma, $\lambda_\pm \neq 0$, so that the Jacobian operator $D_xF(0,0)$ is one-to-one and onto. By the implicit function theorem, for every $U_0 \in \mathbb{C}$ and every $\epsilon \neq 0$ sufficiently small, there exists a unique small solution $U \in \ell^2(\mathbb{N})$ of the system (2.32) such that

$$\|U\|_{l^2(\mathbb{N})} \leq C_1|\epsilon||U_0|, \tag{2.33}$$

where the positive constant C_1 is independent from ϵ and U_0.

Thanks to the symmetry of the difference equation (2.22), we find that $U_{-n} = U_n$, $n \in \mathbb{N}$ satisfy the same system (2.32) with $-n \in \mathbb{N}$, with the same unique solution.

In the second application of the implicit function theorem, we consider the following algebraic equation

$$EU_0 = 2\epsilon\left(\bar{U}_1 - \bar{U}_0\right) + \Omega\bar{U}_0 + i\gamma U_0 + 6|U_0|^2\bar{U}_0 + 2U_0^3, \tag{2.34}$$

where $U_1 \in \mathbb{C}$ depends on U_0, γ, Ω, and E, satisfies the bound (2.33), and is uniquely defined by the previous result.

Let $x = U_0$, $X = \mathbb{C}$, $y = \epsilon$, $Y = \mathbb{R}$, and $Z = \mathbb{C}$. Then, we have $F(Ae^{i\theta}, 0) = 0$, where A and θ are defined in Lemma 4. The Jacobian operator $D_xF(Ae^{i\theta}, 0)$ is given by the matrix

$$\begin{aligned} &\begin{bmatrix} E - i\gamma - 6U_0^2 - 6\bar{U}_0^2 & -\Omega - 12|U_0|^2 \\ -\Omega - 12|U_0|^2 & E + i\gamma - 6U_0^2 - 6\bar{U}_0^2 \end{bmatrix}\Bigg|_{U_0 = Ae^{i\theta}} \\ = &\begin{bmatrix} E - i\gamma - \frac{12EA^2}{\Omega + 8A^2} & -\Omega - 12A^2 \\ -\Omega - 12A^2 & E + i\gamma - \frac{12EA^2}{\Omega + 8A^2} \end{bmatrix}. \end{aligned} \tag{2.35}$$

We show in Lemma 5 below that the matrix given by (2.35) is invertible under the conditions $\gamma \neq 0$ and $\Omega \neq -2|\gamma|$. By the implicit function theorem, for every $\epsilon \neq 0$ sufficiently small, there exists a unique solution $U_0 \in \mathbb{C}$ to the algebraic equation (2.34) near $Ae^{i\theta}$ such that

$$\left|U_0 - Ae^{i\theta}\right| \leq C_2|\epsilon|, \tag{2.36}$$

where the positive constant C_2 is independent from ϵ. The bound (2.31) holds thanks to the bounds (2.33) and (2.36). Since both equations (2.32) and (2.34) are smooth in ϵ, the solution U is smooth in ϵ. □

In the following result, we show that the matrix given by (2.35) is invertible for every branch of Lemma 4 with an exception of a single point $E = 0$ on branch (c) for $\Omega = -2|\gamma|$.

Lemma 5. *With the exception of the point $E = 0$ on branch (c) of Lemma 4 for $\Omega = -2|\gamma|$, the matrix given by (2.35) is invertible for every $\gamma \neq 0$.*

Proof. The matrix given by (2.35) has zero eigenvalue if and only if its determinant is zero, which happens at

$$\frac{E^2(\Omega - 4A^2)^2}{(\Omega + 8A^2)^2} + \gamma^2 - (\Omega + 12A^2)^2 = 0.$$

Eliminating E^2 by using parametrization (2.25) and simplifying the algebraic equation for nonzero A^2, we reduce it to the form

$$2(\Omega + 4A^2)^3 = \Omega\gamma^2. \tag{2.37}$$

We now check if this constraint can be satisfied for the three branches of Lemma 4.

(a) If $\Omega > |\gamma|$, the constraint (2.37) is not satisfied because the left-hand side

$$2(\Omega + 4A^2)^3 \geq 2\Omega^3 > 2\Omega\gamma^2$$

exceeds the right-hand side $\Omega\gamma^2$.

(b) If $\Omega < |\gamma|$ and $A^2 \geq A_+^2$, where A_+^2 is given by (2.27), the constraint (2.37) is not satisfied because the left-hand side

$$2(\Omega + 4A^2)^3 \geq 2(\Omega + 4A_+^2)^3 = 2|\gamma|^3$$

exceeds the left-hand side $\Omega\gamma^2$ both for $\Omega \in [0, |\gamma|)$ and for $\Omega < 0$.

(c) If $\Omega < -|\gamma|$ and $A^2 \leq A_-^2$, where A_-^2 is given by (2.28), the constraint (2.37) is not satisfied because the left-hand side is estimated by

$$2(4A^2 + \Omega)^3 \leq 2(4A_-^2 - |\Omega|)^3 = \min\{-2|\gamma|^3, -|\Omega|^3/4\}.$$

In the first case, we have $|\Omega| \in (|\gamma|, 2|\gamma|)$, so that the left-hand side is strictly smaller than $-|\Omega|\gamma^2$. In the second case, we have $|\Omega| > 2|\gamma|$, so that the left-hand side is also strictly smaller

than $-|\Omega|\gamma^2$. Only if $|\Omega| = 2|\gamma|$, the constraint (2.37) is satisfied at $E = 0$, when $A^2 = A_-^2$ and

$$2(4A^2 + \Omega)^3 = -2|\gamma|^3 = -|\Omega|\gamma^2 = \Omega\gamma^2.$$

Hence, the matrix (2.35) is invertible for all parameter values with one exceptional case. □

Remark 2. *In the asymptotic limit $E^2 = 64A^4 + \mathcal{O}(A^2)$ as $A \to \infty$, see Lemma 4, the matrix (2.35) is expanded asymptotically as*

$$-\frac{1}{2}\begin{bmatrix} E & 3|E| \\ 3|E| & E \end{bmatrix} + \mathcal{O}(1) \quad \text{as} \quad |E| \to \infty, \tag{2.38}$$

with the two eigenvalues $\lambda_1 = E$ and $\lambda_2 = -2E$. Thus, the matrix given by (2.38) is invertible for every branch extending to sufficiently large values of E.

2.4 Stability of zero equilibrium

Here we discuss the linear stability of the zero equilibrium in the $\mathcal{PT}$-symmetric dNLS equation (2.9). The following proposition yields a simple result.

Proposition 1. *The zero equilibrium of the $\mathcal{PT}$-symmetric dNLS equation (2.9) is linearly stable if $|\gamma| < \gamma_0$, where*

$$\gamma_0 := \begin{cases} \Omega - 4\epsilon, & \Omega > 0, \\ |\Omega|, & \Omega < 0. \end{cases} \tag{2.39}$$

The zero equilibrium is linearly unstable if $|\gamma| > \gamma_0$.

Proof. Truncating the $\mathcal{PT}$-symmetric dNLS equation (2.9) at the linear terms and using the Fourier transform

$$u_n(t) = \frac{1}{2\pi}\int_{-\pi}^{\pi} \hat{U}(k) e^{ikn + i\omega(k)t} dk, \tag{2.40}$$

we obtain the linear homogeneous system

$$\hat{D}(k)\begin{bmatrix} \hat{U}(k) \\ \hat{V}(k) \end{bmatrix} = \begin{bmatrix} 0 \\ 0 \end{bmatrix}, \quad \text{where} \quad \hat{D}(k) := \begin{bmatrix} -2\omega(k) - i\gamma & -\Omega + 4\epsilon\sin^2(k/2) \\ -\Omega + 4\epsilon\sin^2(k/2) & -2\omega(k) + i\gamma \end{bmatrix}.$$

The determinant of $\hat{D}(k)$ is zero if and only if $\omega(k)$ is found from the quadratic equation

$$4\omega^2(k) + \gamma^2 - \left(\Omega - 4\epsilon\sin^2\frac{k}{2}\right)^2 = 0. \tag{2.41}$$

For any $|\gamma| < \gamma_0$, where γ_0 is given by (2.39), the two branches $\pm\omega(k)$ found from the quadratic equation (2.41) are real-valued and non-degenerate for every $k \in [-\pi, \pi]$. Therefore, the zero equilibrium is linearly stable.

On the other hand, for any $|\gamma| > \gamma_0$, the values of $\omega(k)$ are purely imaginary either near $k = \pm\pi$ if $\Omega > 0$ or near $k = 0$ if $\Omega < 0$. Therefore, the zero equilibrium is linearly unstable. □

Remark 3. *The value γ_0 given by (2.39) represents the phase transition threshold and the $\mathcal{PT}$-symmetric dNLS equation (2.9) has broken $\mathcal{PT}$-symmetry for $|\gamma| > \gamma_0$.*

If $\epsilon = 0$, the zero equilibrium is only linearly stable for $|\gamma| < |\Omega|$. Since the localized breathers cannot be stable when the zero background is unstable, we shall study stability of breathers only for the case when $|\gamma| < |\Omega|$, that is, in the regime of unbroken $\mathcal{PT}$-symmetry.

2.5 Variational characterization of breathers

It follows from Theorem 6 that each interior point on the solution branches shown on Figure 2.3 generates a fundamental breather of the $\mathcal{PT}$-symmetric dNLS equation (2.9). We shall now characterize these breathers as relative equilibria of the energy function.

Thanks to the cross-gradient symplectic structure (2.16), the stationary $\mathcal{PT}$-symmetric dNLS equation (2.21) can be written in the gradient form

$$EU_n = \frac{\partial H_{u,v}}{\partial \bar{V}_n}, \quad EV_n = \frac{\partial H_{u,v}}{\partial \bar{U}_n}, \quad n \in \mathbb{Z}. \tag{2.42}$$

Keeping in mind the additional conserved quantity $Q_{u,v}$ given by (2.18), we conclude that the stationary solution (U, V) is a critical point of the combined energy function given by

$$H_E := H_{u,v} - EQ_{u,v}. \tag{2.43}$$

If we want to apply the Lyapunov method in order to study nonlinear stability of stationary solutions in Hamiltonian systems, we shall investigate convexity of the second variation of the combined energy functional H_E at (U, V). Using the expansion $u = U + \mathbf{u}$, $v = V + \mathbf{v}$ and introducing extended variables Φ and ϕ with the blocks

$$\Phi_n := (U_n, \bar{U}_n, V_n, \bar{V}_n), \quad \phi_n := (\mathbf{u}_n, \bar{\mathbf{u}}_n, \mathbf{v}_n, \bar{\mathbf{v}}_n), \tag{2.44}$$

we can expand the smooth function H_E up to the quadratic terms in ϕ:

$$H_E(\Phi + \phi) = H_E(\Phi) + \frac{1}{2} \langle \mathcal{H}_E'' \phi, \phi \rangle_{l^2} + \mathcal{O}(\|\phi\|_{l^2}^3), \tag{2.45}$$

where $\mathcal{H}_E''$ is the self-adjoint (Hessian) operator defined on $\ell^2(\mathbb{Z})$ and the scalar product was used in the following form:

$$\langle x, y \rangle_{l^2} = \sum_{k \in \mathbb{Z}} x_k \bar{y}_k.$$

Using (2.17) and (2.18), the Hessian operator can be computed explicitly as follows

$$\mathcal{H}_E'' = \mathcal{L} + \epsilon \Delta, \tag{2.46}$$

where blocks of $\mathcal{L}$ at each lattice node $n \in \mathbb{Z}$ are given by

$$\mathcal{L}_n = \begin{bmatrix} \Omega + 8|U_n|^2 & 2(U_n^2 + \bar{U}_n^2) & -E - i\gamma + 4(U_n^2 + \bar{U}_n^2) & 4|U_n|^2 \\ 2(U_n^2 + \bar{U}_n^2) & \Omega + 8|U_n|^2 & 4|U_n|^2 & -E + i\gamma + 4(U_n^2 + \bar{U}_n^2) \\ -E + i\gamma + 4(U_n^2 + \bar{U}_n^2) & 4|U_n|^2 & \Omega + 8|U_n|^2 & 2(U_n^2 + \bar{U}_n^2) \\ 4|U_n|^2 & -E - i\gamma + 4(U_n^2 + \bar{U}_n^2) & 2(U_n^2 + \bar{U}_n^2) & \Omega + 8|U_n|^2 \end{bmatrix}$$

and Δ is the discrete Laplacian operator applied to blocks of ϕ at each lattice node $n \in \mathbb{Z}$:

$$(\Delta\phi)_n = \phi_{n+1} - 2\phi_n + \phi_{n-1}.$$

In the expression for $\mathcal{L}_n$, we have used the $\mathcal{PT}$-symmetry condition $V = \bar{U}$ for the given stationary solution (U, V).

We study convexity of the combined energy functional H_E at (U, V). Since the zero equilibrium is linearly stable only for $|\gamma| < |\Omega|$ (if $\epsilon = 0$), we only consider breathers of Theorem 6 for $|\gamma| < |\Omega|$.

With an application of the perturbation theory for linear operators (see Section 1.5.6), we prove the following main result of this section.

Theorem 7. *Fix $\gamma \neq 0$, Ω, and E along branches of the $\mathcal{PT}$-symmetric breathers (U, V) given by Theorem 6 such that $|\Omega| > |\gamma|$ and $E \neq \pm E_0$, where $E_0 := \sqrt{\Omega^2 - \gamma^2} > 0$. For every $\epsilon > 0$ sufficiently small, the operator $\mathcal{H}_E''$ admits a one-dimensional kernel in $\ell^2(\mathbb{Z})$ spanned by the eigenvector $\sigma\Phi$ due to the gauge invariance, where the blocks of the eigenvector are given by*

$$(\sigma\Phi)_n := (U_n, -\bar{U}_n, V_n, -\bar{V}_n). \tag{2.47}$$

In addition,

- *If $|E| > E_0$, the spectrum of $\mathcal{H}_E''$ in $\ell^2(\mathbb{Z})$ includes infinite-dimensional positive and negative parts.*
- *If $|E| < E_0$ and $\Omega < -|\gamma|$, the spectrum of $\mathcal{H}_E''$ in $\ell^2(\mathbb{Z})$ includes an infinite-dimensional negative part and either three or one simple positive eigenvalues for branches (b) and (c) of Lemma 4 respectively.*

Proof. If $\epsilon = 0$, the breather solution of Theorem 6 is given by $U_n = 0$ for every $n \neq 0$ and $U_0 = Ae^{i\theta}$, where A and θ are defined by Lemma 4. In this case, the linear operator $\mathcal{H}_E'' = \mathcal{L}$ decouples into 4-by-4 blocks for each lattice node $n \in \mathbb{Z}$.

For $n = 0$, the 4-by-4 block of the linear operator $\mathcal{L}$ is given by

$$\mathcal{L}_0 = \begin{bmatrix} \Omega + 8A^2 & 4A^2\cos(2\theta) & -E - i\gamma + 8A^2\cos(2\theta) & 4A^2 \\ 4A^2\cos(2\theta) & \Omega + 8A^2 & 4A^2 & -E + i\gamma + 8A^2\cos(2\theta) \\ -E + i\gamma + 8A^2\cos(2\theta) & 4A^2 & \Omega + 8A^2 & 4A^2\cos(2\theta) \\ 4A^2 & -E - i\gamma + 8A^2\cos(2\theta) & 4A^2\cos(2\theta) & \Omega + 8A^2 \end{bmatrix}.$$

Using relations (2.24) and (2.25), as well as symbolic computations with MAPLE, we found that the 4-by-4 matrix block $\mathcal{L}_0$ admits a simple zero eigenvalue and three nonzero eigenvalues μ_1, μ_2, and

μ_3 given by

$$\mu_1 = 2(4A^2 + \Omega), \tag{2.48}$$

$$\mu_{2,3} = 12A^2 + \Omega \pm \sqrt{(4A^2 - \Omega)^2 + \frac{16\Omega A^2\gamma^2}{(4A^2 + \Omega)^2}}. \tag{2.49}$$

For each branch of Lemma 4 with $\gamma \neq 0$ and $E \neq \pm E_0$, we have $4A^2 + \Omega \neq 0$, so that $\mu_1 \neq 0$. Furthermore, either $\mu_2 = 0$ or $\mu_3 = 0$ if and only if

$$(12A^2 + \Omega)^2(4A^2 + \Omega)^2 = (16A^4 - \Omega^2)^2 + 16\Omega\gamma^2 A^2.$$

Expanding this equation for nonzero A yields constraint (2.37). With the exception of a single point $E = 0$ at $\Omega = -2|\gamma|$, we showed in Lemma 5 that the constraint (2.37) does not hold for any of the branches of Lemma 4. Therefore, $\mu_2 \neq 0$ and $\mu_3 \neq 0$ along each branch of Lemma 4 and the signs of μ_1, μ_2, and μ_3 for each branch of Lemma 4 can be obtained in the limit $A \to \infty$ for branches (a) and (b) or $A \to 0$ for branch (c). By means of these asymptotic computations as $A \to \infty$ or $A \to 0$, we obtain the following results for the three branches shown on Figure 2.3:

(a) $\mu_1, \mu_2, \mu_3 > 0$.

(b) $\mu_1, \mu_2, \mu_3 > 0$.

(c) $\mu_1 < 0$, $\mu_2 > 0$, and $\mu_3 < 0$.

For $n \in \mathbb{Z}\backslash\{0\}$, the 4-by-4 block of the linear operator $\mathcal{L}$ is given by

$$\mathcal{L}_n = \begin{bmatrix} \Omega & 0 & -E - i\gamma & 0 \\ 0 & \Omega & 0 & -E + i\gamma \\ -E + i\gamma & 0 & \Omega & 0 \\ 0 & -E - i\gamma & 0 & \Omega \end{bmatrix}. \tag{2.50}$$

Each block has two double eigenvalues μ_+ and μ_- given by

$$\mu_+ = \Omega + \sqrt{E^2 + \gamma^2}, \quad \mu_- = \Omega - \sqrt{E^2 + \gamma^2}.$$

Since there are infinitely many nodes with $n \neq 0$, the points μ_+ and μ_- have infinite multiplicity in the spectrum of the linear operator $\mathcal{L}$. Furthermore, we can sort up the signs of μ_+ and μ_- for each point on the three branches shown on Figure 2.3:

(1),(3) If $|E| > E_0 := \sqrt{\Omega^2 - \gamma^2}$, then $\mu_+ > 0$ and $\mu_- < 0$.

(2),(4) If $|E| < E_0$ and $\Omega < -|\gamma|$, then $\mu_+, \mu_- < 0$.

By using the perturbation theory for linear operators, we argue as follows:

- Since $\mathcal{H}_E''$ is Hermitian on $\ell^2(\mathbb{Z})$, its spectrum is a subset of the real line for every $\epsilon \neq 0$.

- The zero eigenvalue persists with respect to $\epsilon \neq 0$ at zero because the eigenvector (2.47) belongs to the kernel of $\mathcal{H}_E''$ due to the gauge invariance for every $\epsilon \neq 0$.
- The other eigenvalues of $\mathcal{L}$ are isolated away from zero. The spectrum of $\mathcal{H}_E''$ is continuous with respect to ϵ and includes infinite-dimensional parts near points μ_+ and μ_- for small $\epsilon > 0$ (which may include continuous spectrum and isolated eigenvalues) as well as simple eigenvalues near $\mu_{1,2,3}$ (if $\mu_{1,2,3}$ are different from $\mu_\pm$).

The statement of the theorem follows from the perturbation theory and the count of signs of $\mu_{1,2,3}$ and $\mu_\pm$ above. □

Remark 4. *In the asymptotic limit $E^2 = 64A^4 + \mathcal{O}(A^2)$ as $A \to \infty$, we can sort out eigenvalues of $\mathcal{H}_E''$ asymptotically as:*

$$\mu_1 \approx |E|, \quad \mu_2 \approx 2|E|, \quad \mu_3 \approx |E|, \quad \mu_+ \approx |E|, \quad \mu_- \approx -|E|, \tag{2.51}$$

where the remainder terms are $\mathcal{O}(1)$ as $|E| \to \infty$. The values μ_1, μ_3, and μ_+ are close to each other as $|E| \to \infty$.

Remark 5. *It follows from Theorem 7 that for $|E| > E_0$, the breather (U, V) is a saddle point of the energy functional H_E with infinite-dimensional positive and negative invariant subspaces of the Hessian operator $\mathcal{H}_E''$. This is very similar to the Hamiltonian systems of the Dirac type, where stationary states are located in the gap between the positive and negative continuous spectrum. This property holds for points 1 and 3 on branches (a) and (b) shown on Figure 2.3.*

Remark 6. *No branches other than $|E| > E_0$ exist for $\Omega > |\gamma|$. On the other hand, points 2 and 4 on branches (b) and (c) shown on Figure 2.3 satisfy $|E| < E_0$ and $\Omega < -|\gamma|$. The breather (U, V) is a saddle point of H_E for these points and it only has three (one) directions of positive energy in space $\ell^2(\mathbb{Z})$ for point 2 (point 4).*

2.6 Spectral and orbital stability of breathers

Spectral stability of breathers can be studied for small values of coupling constant ϵ by using the perturbation theory [115]. First, we linearize the $\mathcal{PT}$-symmetric dNLS equation (2.9) at the breather (2.19) by using the expansion

$$u(t) = e^{-\frac{1}{2}iEt}\left[U + \mathbf{u}(t)\right], \quad v(t) = e^{-\frac{1}{2}iEt}\left[V + \mathbf{v}(t)\right],$$

where $(\mathbf{u}, \mathbf{v})$ is a small perturbation satisfying the linearized equations

$$\begin{cases} 2i\dot{\mathbf{u}}_n + E\mathbf{u}_n = & \epsilon\left(\mathbf{v}_{n+1} - 2\mathbf{v}_n + \mathbf{v}_{n-1}\right) + \Omega\mathbf{v}_n + i\gamma\mathbf{u}_n \\ & +2\left[2\left(|U_n|^2 + |V_n|^2\right)\mathbf{v}_n + (U_n^2 + V_n^2)\bar{\mathbf{v}}_n\right. \\ & \left. + 2(\bar{U}_n V_n + U_n\bar{V}_n)\mathbf{u}_n + 2U_n V_n\bar{\mathbf{u}}_n\right], \\ 2i\dot{\mathbf{v}}_n + E\mathbf{v}_n = & \epsilon\left(\mathbf{u}_{n+1} - 2\mathbf{u}_n + \mathbf{u}_{n-1}\right) + \Omega\mathbf{u}_n - i\gamma\mathbf{v}_n \\ & +2\left[2\left(|U_n|^2 + |V_n|^2\right)\mathbf{u}_n + (U_n^2 + V_n^2)\bar{\mathbf{u}}_n\right. \\ & \left. +2\left(\bar{U}_n V_n + U_n\bar{V}_n\right)\mathbf{v}_n + 2U_n V_n\bar{\mathbf{v}}_n\right]. \end{cases} \tag{2.52}$$

The spectral stability problem arises from the linearized equations (2.52) after the separation of variables:

$$\mathbf{u}(t) = \varphi e^{\frac{1}{2}\lambda t}, \quad \bar{\mathbf{u}}(t) = \psi e^{\frac{1}{2}\lambda t}, \quad \mathbf{v}(t) = \chi e^{\frac{1}{2}\lambda t}, \quad \bar{\mathbf{v}}(t) = \nu e^{\frac{1}{2}\lambda t},$$

where $\phi := (\varphi, \psi, \chi, \nu)$ is the eigenvector corresponding to the spectral parameter λ. Note that (φ, ψ) and (χ, ν) are no longer complex conjugate to each other if λ has a nonzero imaginary part. The

spectral problem can be written in the explicit form

$$\begin{cases} (E+i\lambda-i\gamma)\varphi_n - \Omega\chi_n = \epsilon\left(\chi_{n+1}-2\chi_n+\chi_{n-1}\right) \\ \qquad\qquad + 2\left[2|U_n|^2(\psi_n+2\chi_n) + (U_n^2+\bar{U}_n^2)(2\varphi_n+\nu_n)\right], \\ (E-i\lambda+i\gamma)\psi_n - \Omega\nu_n = \epsilon\left(\nu_{n+1}-2\nu_n+\nu_{n-1}\right) \\ \qquad\qquad + 2\left[2|U_n|^2(\varphi_n+2\nu_n) + (U_n^2+\bar{U}_n^2)(2\psi_n+\chi_n)\right], \\ (E+i\lambda+i\gamma)\chi_n - \Omega\varphi_n = \epsilon\left(\varphi_{n+1}-2\varphi_n+\varphi_{n-1}\right) \\ \qquad\qquad + 2\left[2|U_n|^2(2\varphi_n+\nu_n) + (U_n^2+\bar{U}_n^2)(\psi_n+2\chi_n)\right], \\ (E-i\lambda-i\gamma)\nu_n - \Omega\psi_n = \epsilon\left(\psi_{n+1}-2\psi_n+\psi_{n-1}\right) \\ \qquad\qquad + 2\left[2|U_n|^2(2\psi_n+\chi_n) + (U_n^2+\bar{U}_n^2)(\varphi_n+2\nu_n)\right], \end{cases} \tag{2.53}$$

where we have used the condition $V = \bar{U}$ for the $\mathcal{PT}$-symmetric breathers. Recalling definition of the Hessian operator $\mathcal{H}_E''$ in (2.46), we can rewrite the spectral problem (2.53) in the Hamiltonian form:

$$\mathcal{S}\mathcal{H}_E''\phi = i\lambda\phi, \tag{2.54}$$

where $\mathcal{S}$ is a symmetric matrix with the blocks at each lattice node $n \in \mathbb{Z}$ given by

$$S := \begin{bmatrix} 0 & 0 & 1 & 0 \\ 0 & 0 & 0 & -1 \\ 1 & 0 & 0 & 0 \\ 0 & -1 & 0 & 0 \end{bmatrix}. \tag{2.55}$$

We note the Hamiltonian symmetry of the eigenvalues of the spectral problem (2.54).

Proposition 2. *Eigenvalues of the spectral problem (2.54) occur either as real or imaginary pairs or as quadruplets in the complex plane.*

Proof. Assume that $\lambda \in \mathbb{C}$ is an eigenvalue of the spectral problem (2.54) with the eigenvector $(\varphi, \psi, \chi, \nu)$. Then, $\bar{\lambda}$ is an eigenvalue of the same problem with the eigenvector $(\bar{\psi}, \bar{\varphi}, \bar{\nu}, \bar{\chi})$, whereas $-\lambda$ is also an eigenvalue with the eigenvector $(\nu, \chi, \psi, \varphi)$. □

If $\Omega < -|\gamma|$ and $|E| < E_0 := \sqrt{\Omega^2 - \gamma^2}$ (points 2 and 4 shown on Figure 2.3), Theorem 7 implies that the self-adjoint operator $\mathcal{H}_E''$ in $\ell^2(\mathbb{Z})$ is negative-definite with the exception of either three (point 2) or one (point 4) simple positive eigenvalues. In this case, we can apply Hamilton–Krein index theorem (see Section 1.5.6) in order to characterize the spectrum of $S\mathcal{H}_E''$.

Lemma 6. *Fix $\gamma \neq 0$, $\Omega < -|\gamma|$, and $0<|E|<E_0$, where $E_0 := \sqrt{\Omega^2 - \gamma^2} > 0$. For every $\epsilon > 0$ sufficiently small, $K_{HAM} = 2$ for branch (b) of Lemma 4 and $K_{HAM} = 0$ for branch (c) of Lemma 4 with $\Omega < -2\sqrt{2}|\gamma|$. For branch (c) with $\Omega \in (-2\sqrt{2}|\gamma|, -|\gamma|)$, there exists a value $E_s \in (0, E_0)$ such that $K_{HAM} = 1$ for $0 < |E| < E_s$ and $K_{HAM} = 0$ for $E_s < |E| < E_0$.*

Proof. If $\gamma \neq 0$, $\Omega < -|\gamma|$, $|E| < E_0$, and $\epsilon > 0$ is sufficiently small, Theorem 7 implies that the spectrum of $\mathcal{H}_E''$ in $\ell^2(\mathbb{Z})$ has finitely many positive eigenvalues and a simple zero eigenvalue with eigenvector $\sigma\Phi$. Therefore, the Hamilton–Krein index theorem is applied in $\ell^2(\mathbb{Z})$ for $L = -\mathcal{H}_E''$, $J = i\mathcal{S}$, and $v_0 = \sigma\Phi$. We shall verify that

$$\mathcal{H}_E''(\sigma\Phi) = 0, \quad \mathcal{S}\mathcal{H}_E''(\partial_E\Phi) = \sigma\Phi, \tag{2.56}$$

where $\sigma\Phi$ is given by (2.47) and $\partial_E\Phi$ denotes derivative of Φ with respect to parameter E. The first equation $\mathcal{H}_E''(\sigma\Phi) = 0$ follows by Theorem 7. By differentiating equations (2.21) in E, we obtain $\mathcal{H}_E''(\partial_E\Phi) = \mathcal{S}\sigma\Phi$ for every E, for which the solution Φ is differentiable in E. For $\epsilon = 0$, the limiting solution of Lemma 4 is differentiable in E for every $E \neq 0$ and $E \neq \pm E_0$. Due to smoothness of the continuation in ϵ by Theorem 7, this property holds for every $\epsilon > 0$ sufficiently small.

By using (2.56) with $\mathcal{S}^{-1} = \mathcal{S}$, we obtain

$$\begin{aligned} D &= -\langle (\mathcal{H}_E'')^{-1}\mathcal{S}\sigma\Phi, \mathcal{S}\sigma\Phi\rangle_{\ell^2} = -\langle \partial_E\Phi, \mathcal{S}\sigma\Phi\rangle_{\ell^2} \\ &= -\sum_{n\in\mathbb{Z}} \partial_E\left(U_n\bar{V}_n + \bar{U}_n V_n\right) = -\frac{dQ_{u,v}}{dE}, \end{aligned} \tag{2.57}$$

where we have used the definition of $Q_{u,v}$ in (2.18). We compute the slope condition at $\epsilon = 0$:

$$\left.\frac{dQ_{u,v}}{dE}\right|_{\epsilon=0} = 2\frac{d}{dE}\frac{A^2E}{8A^2+\Omega} = 4(8A^2+\Omega)\frac{dA^2}{dE^2}\left[1 - \frac{\Omega\gamma^2}{(4A^2+\Omega)^3}\right], \tag{2.58}$$

where relations (2.24) and (2.25) have been used.

For branch (b) of Lemma 4 with $\Omega < -|\gamma|$, we have $dA^2/dE^2 > 0$ and $|\Omega| < 4A^2$, so that $dQ_{u,v}/dE > 0$. By continuity, $dQ_{u,v}/dE$ remains strictly positive for small $\epsilon > 0$. Thus, $D < 0$ and $K_{HAM} = 2$ by the Hamilton–Krein index theorem.

For branch (c) of Lemma 4 with $\Omega < -|\gamma|$, we have $dA^2/dE^2 < 0$ and $|\Omega| > 8A^2$. Therefore, we only need to inspect the sign of the expression $(4A^2+\Omega)^3 - \Omega\gamma^2$. If $\Omega < -2\sqrt{2}|\gamma|$, then for every

$A^2 \in (0, A_-^2)$, we have

$$(4A^2+\Omega)^3 - \Omega\gamma^2 \leq (4A_-^2+\Omega)^3 - \Omega\gamma^2 = \frac{1}{8}\Omega^3 - \Omega\gamma^2 \leq \frac{1}{8}\Omega(\Omega^2 - 8\gamma^2) < 0,$$

therefore, $D < 0$ and $K_{HAM} = 0$ by the Hamilton–Krein index theorem.

On the other hand, if $-2\sqrt{2}|\gamma| < \Omega < -|\gamma|$, we have $(4A^2+\Omega)^3 - \Omega\gamma^2 < 0$ at $A = 0$ ($E = E_0$) and $(4A^2+\Omega)^3 - \Omega\gamma^2 > 0$ at $A = A_-$ ($E = 0$). Since the dependence of A versus E is monotonic, there exists a value $E_s \in (0, E_0)$ such that $K_{HAM} = 1$ for $0 < |E| < E_s$ and $K_{HAM} = 0$ for $E_s < |E| < E_0$. □

If $K_{HAM} = 0$ and $D \neq 0$, orbital stability of a critical point of H_E in space $\ell^2(\mathbb{Z})$ can be proved from the Hamilton–Krein theorem (see [68] and references therein). Orbital stability of breathers is understood in the following sense.

Definition 10. *We say that the breather solution (2.19) is orbitally stable in $\ell^2(\mathbb{Z})$ if for every $\nu > 0$ sufficiently small, there exists $\delta > 0$ such that if $\psi(0) \in \ell^2(\mathbb{Z})$ satisfies $\|\psi(0) - \Phi\|_{\ell^2} \leq \delta$, then the unique global solution $\psi(t) \in \ell^2(\mathbb{Z})$, $t \in \mathbb{R}$ to the $\mathcal{PT}$-symmetric dNLS equation (2.9) satisfies the bound*

$$\inf_{\alpha\in\mathbb{R}} \|e^{i\alpha}\psi(t) - \Phi\|_{\ell^2} \leq \nu, \quad \text{for every } \ t \in \mathbb{R}. \tag{2.59}$$

The definition of instability of breathers is given by negating Definition 10. The following result gives orbital stability or instability for branch (c) shown on Figure 2.3.

Theorem 8. *Fix $\gamma \neq 0$, $\Omega < -|\gamma|$, and $0 < |E| < E_0$. For every $\epsilon > 0$ sufficiently small, the breather (U, V) for branch (c) of Lemma 4 is orbitally stable in $\ell^2(\mathbb{Z})$ if $\Omega < -2\sqrt{2}|\gamma|$. For every $\Omega \in (-2\sqrt{2}|\gamma|, -|\gamma|)$, there exists a value $E_s \in (0, E_0)$ such that the breather (U, V) is orbitally stable in $\ell^2(\mathbb{Z})$ if $E_s < |E| < E_0$ and unstable if $0 < |E| < E_s$.*

Proof. The theorem is a corollary of Lemma 6 for branch (c) of Lemma 4 and the orbital stability theory from [68]. □

Orbital stability of breathers for branches (a) and (b) of Lemma 4 does not follow from the standard theory because $K_{HAM} = \infty$ for $|E| > E_0$ and $K_{HAM} = 2 > 0$ for branch (b) with $|E| < E_0$. Nevertheless, by using smallness of parameter ϵ and the construction of the breather (U, V) in Theorem 6, spectral stability of breathers can be considered directly. Spectral stability and instability of breathers is understood in the following sense.

Definition 11. *We say that the breather solution (2.19) is spectrally stable if $\lambda \in i\mathbb{R}$ for every bounded solution of the spectral problem (2.54). On the other hand, if the spectral problem (2.54) admits an eigenvalue $\lambda \notin i\mathbb{R}$ with an eigenvector in $\ell^2(\mathbb{R})$, we say that the breather solution (2.19) is spectrally unstable.*

The following theorem gives spectral stability of breathers for branches (a) and (b) shown on Figure 2.3.

Theorem 9. *Fix $\gamma \neq 0$, $|\Omega| > |\gamma|$, and E along branches (a) and (b) of Lemma 4 with $E \neq 0$ and $E \neq \pm E_0$. For every $\epsilon > 0$ sufficiently small, the spectral problem (2.54) admits a double zero eigenvalue with the generalized eigenvectors*

$$\mathcal{H}_E''(\sigma\Phi) = 0, \quad \mathcal{S}\mathcal{H}_E''(\partial_E\Phi) = \sigma\Phi, \tag{2.60}$$

where the eigenvector $\sigma\Phi$ is given by (2.47) and the generalized eigenvector $\partial_E\Phi$ denotes derivative of Φ with respect to parameter E. For every E such that the following non-degeneracy condition is satisfied,

$$2\sqrt{(4A^2+\Omega)^2 - \frac{\Omega\gamma^2}{4A^2+\Omega}} \neq E \pm \sqrt{\Omega^2-\gamma^2}, \tag{2.61}$$

the breather (U, V) is spectrally stable.

Proof. If $\epsilon = 0$, the breather solution of Theorem 6 is given by $U_n = 0$ for every $n \neq 0$ and $U_0 = Ae^{i\theta}$, where A and θ are defined by Lemma 4. In this case, the spectral problem (2.53) decouples into 4-by-4 blocks for each lattice node $n \in \mathbb{Z}$. Recall that $\mathcal{H}_E'' = \mathcal{L}$ at $\epsilon = 0$.

For $n = 0$, eigenvalues λ are determined by the 4-by-4 matrix block $-iS\mathcal{L}_0$. Using relations (2.24) and (2.25), as well as symbolic computations with MAPLE, we found that the 4-by-4 matrix block $-iS\mathcal{L}_0$ has a double zero eigenvalue and a pair of simple eigenvalues at $\lambda = \pm\lambda_0$, where

$$\lambda_0 = 2i\sqrt{(4A^2+\Omega)^2 - \frac{\Omega\gamma^2}{4A^2+\Omega}}. \tag{2.62}$$

For $n \in \mathbb{Z}\backslash\{0\}$, eigenvalues λ are determined by the 4-by-4 matrix block $-iS\mathcal{L}_n$, where $\mathcal{L}_n$ is given by (2.50). If $|\gamma| < |\Omega|$, $E \neq 0$, and $E \neq \pm E_0$, where $E_0 := \sqrt{\Omega^2-\gamma^2}$, each block has four simple eigenvalues $\pm\lambda_+$ and $\pm\lambda_-$, where

$$\lambda_\pm := i(E \pm E_0), \tag{2.63}$$

so that $\lambda_\pm \in i\mathbb{R}$. Since there are infinitely many nodes with $n \neq 0$, the four eigenvalues are semi-simple and have infinite multiplicity.

If $\epsilon > 0$ is sufficiently small, we use perturbation theory for linear operators from Section 2.5.

- The double zero eigenvalue persists with respect to $\epsilon \neq 0$ at zero because of the gauge invariance of the breather (U, V) (with respect to rotation of the complex phase). Indeed, $\mathcal{H}_E''(\sigma\Phi) = 0$ follows from the result of Theorem 7. The generalized eigenvector is defined by equation $\mathcal{S}\mathcal{H}_E''\Psi = \sigma\Phi$, which is equivalent to equation $\mathcal{H}_E''\Psi = (V, \bar{V}, U, \bar{U})^T$. Differentiating equations (2.21) in E, we obtain $\Psi = \partial_E\Phi$. Since $\dim[\mathrm{Ker}(\mathcal{H}_E'')] = 1$ and

$$\langle \sigma\Phi, \mathcal{S}\partial_E\Phi\rangle_{\ell^2} = \sum_{n\in\mathbb{Z}} \partial_E\left(U_n\bar{V}_n + \bar{U}_nV_n\right) = \frac{dQ_{u,v}}{dE}, \tag{2.64}$$

  the second generalized eigenvector $\tilde{\Psi} \in \ell^2(\mathbb{Z})$ exists as a solution of equation $\mathcal{S}\mathcal{H}_E''\tilde{\Psi} = \partial_E\Phi$ if and only if $dQ_{u,v}/dE = 0$. It follows from the explicit computation (2.58) that if $\epsilon = 0$,

then $dQ_{u,v}/dE \neq 0$ for every E along branches (a) and (b) of Lemma 4. By continuity, $dQ_{u,v}/dE \neq 0$ for small $\epsilon > 0$. Therefore, the zero eigenvalue of the operator $-i\mathcal{S}\mathcal{H}_E''$ is exactly double for small $\epsilon > 0$.

- Using the same computation (2.58), it is clear that $\lambda_0 \in i\mathbb{R}$ for every E along branches (a) and (b) of Lemma 4. Assume that $\lambda_0 \neq \pm\lambda_+$ and $\lambda_0 \neq \pm\lambda_-$, which is expressed by the non-degeneracy condition (2.61). Then, the pair $\pm\lambda_0$ is isolated from the rest of the spectrum of the operator $-i\mathcal{S}\mathcal{H}_E''$ at $\epsilon = 0$. Since the eigenvalues $\lambda = \pm\lambda_0$ are simple and purely imaginary, they persist on the imaginary axis for $\epsilon \neq 0$ because they cannot leave the imaginary axis by the Hamiltonian symmetry of Proposition 2.

- If $|\gamma| < |\Omega|$, $E \neq 0$, and $E \neq \pm E_0$, the semi-simple eigenvalues $\pm\lambda_+$ and $\pm\lambda_-$ of infinite multiplicity are nonzero and located at the imaginary axis at different points for $\epsilon = 0$. They persist on the imaginary axis for $\epsilon \neq 0$ according to the following perturbation argument. First, for the central site $n = 0$, the spectral problem (2.53) can be written in the following abstract form

$$(S\mathcal{L}_0(\epsilon) - 2\epsilon S - i\lambda I)\,\phi_0 = -\epsilon S(\phi_1 + \phi_{-1}),$$

where $\mathcal{L}_0(\epsilon)$ denotes a continuation of $\mathcal{L}_0$ in ϵ. Thanks to the non-degeneracy condition (2.61) as well as the condition $\lambda_\pm \neq 0$, the matrix $S\mathcal{L}_0 - i\lambda_\pm I$ is invertible. By continuity, the matrix $S\mathcal{L}_0(\epsilon) - i\lambda I$ is invertible for every ϵ and λ near $\epsilon = 0$ and $\lambda = \lambda_\pm$. Therefore, there is a unique ϕ_0 given by

$$\phi_0 = -\epsilon\,(S\mathcal{L}_0(\epsilon) - 2\epsilon S - i\lambda I)^{-1}\,S(\phi_1 + \phi_{-1}),$$

which satisfies $|\phi_0| \leq C\epsilon(|\phi_1| + |\phi_{-1}|)$ near $\epsilon = 0$ and $\lambda = \lambda_\pm$, where C is a positive ϵ- and λ-independent constant. Next, for either $n \in \mathbb{N}$ or $-n \in \mathbb{N}$, the spectral problem (2.53) can be represented in the form

$$S\mathcal{L}_n(\epsilon)\phi_n + \epsilon S(\Delta\phi)_n - i\lambda\phi_n = -\delta_{n,\pm 1}\epsilon S\phi_0, \quad \pm n \in \mathbb{N},$$

where $\mathcal{L}_n(\epsilon)$ denotes a continuation of $\mathcal{L}_n$ given by (2.50) in ϵ, whereas the operator Δ is applied with zero end-point condition at $n = 0$. We have $\mathcal{L}_n(\epsilon) = \mathcal{L}_n + \mathcal{O}(\epsilon^2)$ and $\epsilon S\phi_0 = \mathcal{O}(\epsilon^2)$ near $\epsilon = 0$ and $\lambda = \lambda_\pm$. Therefore, up to the first order of the perturbation theory, the spectral parameter λ near $\lambda_\pm$ is defined from the truncated eigenvalue problem

$$S\mathcal{L}_n\phi_n + \epsilon S(\Delta\phi)_n = i\lambda\phi_n, \quad \pm n \in \mathbb{N}, \tag{2.65}$$

which is solved with the discrete Fourier transform (2.40). In order to satisfy the Dirichlet end-point condition at $n = 0$, the sine–Fourier transform must be used, which does not affect the characteristic equation for the purely continuous spectrum of the spectral problem (2.65). By means of routine computations, we obtain the characteristic equation in the form, see also equation (2.41):

$$(E \pm i\lambda)^2 + \gamma^2 - \left(\Omega - 4\epsilon\sin^2\frac{k}{2}\right)^2 = 0, \tag{2.66}$$

where $k \in [-\pi, \pi]$ is the parameter of the discrete Fourier transform (2.40). Solving the characteristic equation (2.66), we obtain four branches of the continuous spectrum

$$\lambda = \pm i \left(E \pm \sqrt{\left(\Omega - 4\epsilon \sin^2 \frac{k}{2} \right)^2 - \gamma^2} \right), \tag{2.67}$$

where the two sign choices are independent from each other. If $|\Omega| > |\gamma|$ is fixed and $\epsilon > 0$ is small, the four branches of the continuous spectrum are located on the imaginary axis near the points $\pm\lambda_+$ and $\pm\lambda_-$ given by (2.63).

In addition to the continuous spectrum given by (2.66), there may exist isolated eigenvalues near $\pm\lambda_+$ and $\pm\lambda_-$, which are found from the second-order perturbation theory [111]. Under the condition $E \neq 0$ and $E \neq \pm E_0$, these eigenvalues are purely imaginary. Therefore, the infinite-dimensional part of the spectrum of the operator $-i\mathcal{S}\mathcal{H}_E''$ persists on the imaginary axis for $\epsilon \neq 0$ near the points $\pm\lambda_+$ and $\pm\lambda_-$ of infinite algebraic multiplicity.

The statement of the lemma follows from the perturbation theory and the fact that all isolated eigenvalues and the continuous spectrum of $-i\mathcal{S}\mathcal{H}_E''$ are purely imaginary. □

Remark 7. *In the asymptotic limit $E^2 = 64A^4 + \mathcal{O}(A^2)$ as $A \to \infty$, the eigenvalues λ_0 and $\lambda_\pm$ defined by (2.62) and (2.63) are given asymptotically by*

$$\lambda_0 \approx i|E|, \quad \lambda_+ \approx iE, \quad \lambda_- \approx iE, \tag{2.68}$$

where the remainder terms are $\mathcal{O}(1)$ as $|E| \to \infty$. The values λ_0, λ_+, and λ_- are close to each other as $E \to +\infty$.

Remark 8. *Computations in the proof of Theorem 9 can be extended to the branch (c) of Lemma 4. Indeed, $\lambda_0 \in i\mathbb{R}$ for branch (c) with either $\Omega < -2\sqrt{2}|\gamma|$ or $\Omega \in (-2\sqrt{2}|\gamma|, -|\gamma|)$, and E near $\pm E_0$. On the other hand, $\lambda_0 \in \mathbb{R}$ if $\Omega \in (-2\sqrt{2}|\gamma|, -|\gamma|)$ and E near 0. As a result, branch (c) is spectrally stable in the former case and is spectrally unstable in the latter case, in agreement with Theorem 8.*

Remark 9. *Observe in the proof of Theorem 9 that $\lambda_\pm \notin i\mathbb{R}$ if $|\Omega| < |\gamma|$. In this case, branch (b) of Lemma 4 is spectrally unstable. This instability corresponds to the instability of the zero equilibrium for $|\Omega| < |\gamma|$, in agreement with the result of Proposition 1.*

Before presenting numerical approximations of eigenvalues of the spectral problem (2.54), we compute the Krein signature of wave continuum. This helps to interpret instabilities and resonances that arise when isolated eigenvalues $\pm\lambda_0$ cross the continuous bands near points $\pm\lambda_+$ and $\pm\lambda_-$. The Krein signature of simple isolated eigenvalues is defined as follows.

Definition 12. *Let $\phi \in \ell^2(\mathbb{Z})$ be an eigenvector of the spectral problem (2.54) for an isolated simple eigenvalue $\lambda_0 \in i\mathbb{R}$. Then, the energy quadratic form $\langle \mathcal{H}_E'' \phi, \phi \rangle_{\ell^2}$ is nonzero and its sign is called the Krein signature of the eigenvalue λ_0.*

Definition 12 is used to simplify the presentation. Similarly, one can define the Krein signature of isolated multiple eigenvalues and the Krein signature of the continuous spectral bands in the spectral problem (2.54) [68]. The following lemma characterizes Krein signatures of the spectral points arising in the proof of Theorem 9.

Lemma 7. *Fix $\gamma \neq 0$, $|\Omega| > |\gamma|$, and $E > 0$ with $E \neq \pm E_0$. Assume the non-degeneracy condition (2.61). For every $\epsilon > 0$ sufficiently small, we have the following for the corresponding branches of Lemma 4:*

(a) the subspaces of $-i\mathcal{S}\mathcal{H}_E''$ in $\ell^2(\mathbb{Z})$ near $\pm\lambda_+$, $\pm\lambda_-$, and $\pm\lambda_0$ have positive, negative, and positive Krein signature, respectively;

(b) the subspaces of $-i\mathcal{S}\mathcal{H}_E''$ in $\ell^2(\mathbb{Z})$ near $\pm\lambda_+$, $\pm\lambda_-$, and $\pm\lambda_0$ have negative, positive (if $E > E_0$) or negative (if $E < E_0$), and positive Krein signature, respectively;

(c) all subspaces of $-i\mathcal{S}\mathcal{H}_E''$ in $\ell^2(\mathbb{Z})$ near $\pm\lambda_+$, $\pm\lambda_-$, and $\pm\lambda_0$ (if $\lambda_0 \in i\mathbb{R}$) have negative Krein signature.

Proof. We proceed by the perturbation arguments from the limit $\epsilon = 0$, where $-i\mathcal{S}\mathcal{H}_E'' = -i\mathcal{S}\mathcal{L}$ is a block-diagonal operator consisting of 4×4 blocks. In particular, we consider the blocks for $n \in \mathbb{Z}\backslash\{0\}$, where $\mathcal{L}_n$ is given by (2.50). Solving (2.53) at $\epsilon = 0$ and $\lambda = \lambda_\pm$, we obtain the eigenvector

$$\varphi_n = -\Omega, \quad \psi_n = 0, \quad \chi_n = \pm E_0 + i\gamma, \quad \nu_n = 0, \quad n \in \mathbb{Z}\backslash\{0\}.$$

As a result, we obtain for the eigenvector $\phi_n = (\varphi_n, \psi_n, \chi_n, \nu_n)$:

$$\begin{aligned} K_n := \langle \mathcal{L}_n\phi_n, \phi_n\rangle_{\ell^2} &= \Omega(|\varphi_n|^2 + |\chi_n|^2) - (E + i\gamma)\chi_n\bar{\varphi}_n - (E - i\gamma)\varphi_n\bar{\chi}_n \\ &= 2\Omega E_0(E_0 \pm E). \end{aligned}$$

For branch (a), $\Omega > |\gamma|$ and $E > E_0$. Therefore, $K_n > 0$ for $\lambda = \lambda_+$ and $K_n < 0$ for $\lambda = \lambda_-$.

For branch (b), $\Omega < -|\gamma|$ and either $E > E_0$ or $E \in (0, E_0)$. In either case, $K_n < 0$ for $\lambda = \lambda_+$. On the other hand, for $\lambda = \lambda_-$, $K_n > 0$ if $E > E_0$ and $K_n < 0$ if $E \in (0, E_0)$.

For branch (c), $\Omega < -|\gamma|$ and $E \in (0, E_0)$. In this case, $K_n < 0$ for either $\lambda = \lambda_+$ or $\lambda = \lambda_-$.

Finally, the Krein signature for the eigenvalue $\lambda = \lambda_0$ denoted by K_0 follows from the computations of eigenvalues $\mu_{1,2,3}$ in the proof of Theorem 7. We have $K_0 > 0$ for branches (a) and (b) because $\mu_{1,2,3} > 0$ and we have $K_0 < 0$ for branch (c) because $\mu_{1,3} < 0$, whereas the eigenvalue $\mu_2 > 0$ is controlled by the result of Lemma 6.

The signs of all eigenvalues are nonzero and continuous with respect to parameter ϵ. Therefore, the count above extends to the case of small nonzero ϵ. □

The spectrum of $-i\mathcal{S}\mathcal{H}_E''$ is shown at Figure 2.4. Panels (a), (b) and (c) correspond to branches shown at Figure 2.3.

(a) We can see on panel (a) of Figure 2.4 that $\lambda_0, \lambda_\pm$ do not intersect for every $E > E_0$ and are located within fixed distance $\mathcal{O}(1)$, as $|E| \to \infty$. Note that the upper-most λ_0 and λ_+ have positive Krein signature, whereas the lowest λ_- has negative Krein signature, as is given by Lemma 7.

(b) We observe on panel (b) of Figure 2.4 that λ_+ intersects λ_0, creating a small bubble of instability in the spectrum. The insert shows that the bubble shrinks as $\epsilon \to 0$, in agreement with Theorem

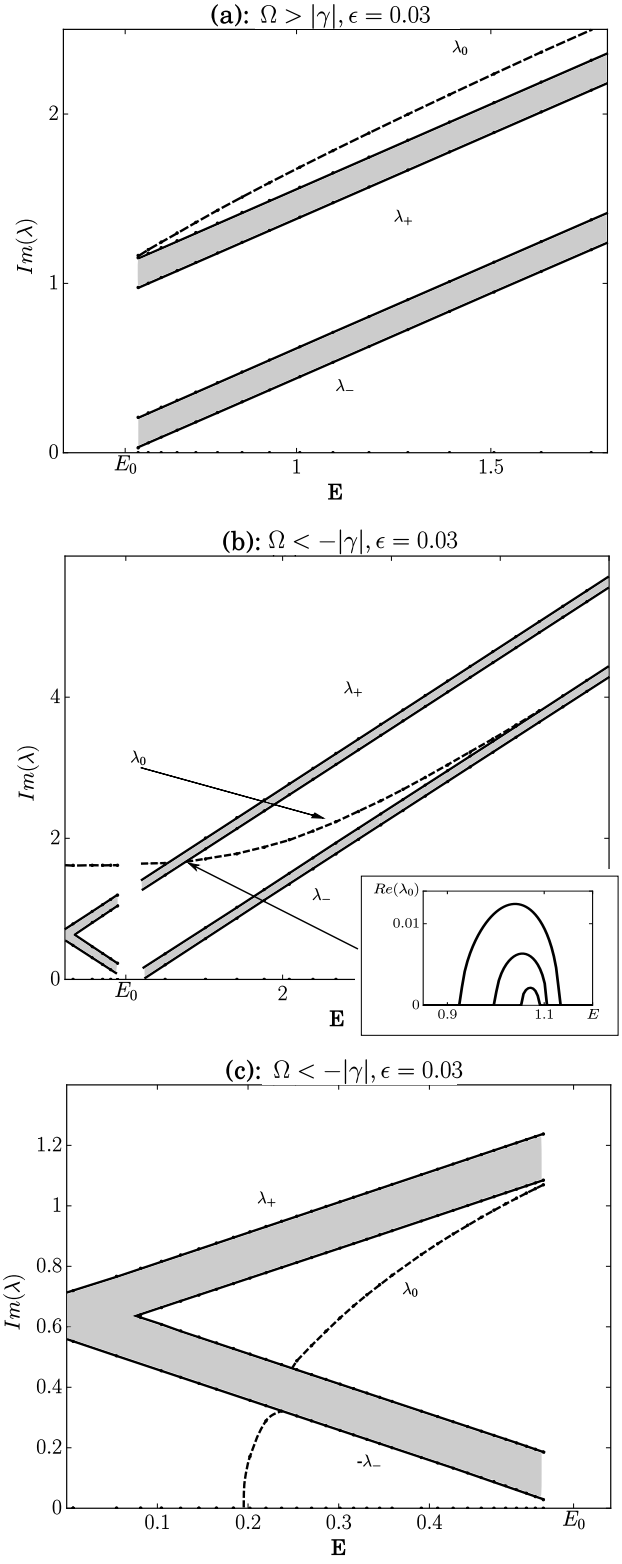

Figure 2.4: The spectrum of $-i\mathcal{S}\mathcal{H}''_E$ for different branches of breathers.

9. There is also an intersection between λ_- and λ_0, which does not create instability. These results are explained by the Krein signature computations in Lemma 7. Instability is induced by opposite Krein signatures between λ_+ and λ_0, whereas crossing of λ_- and λ_0 with the same Krein signatures is safe of instabilities. Note that for small E, the isolated eigenvalue λ_0 is located above both the spectral bands near λ_+ and λ_-. The gap in the numerical data near $E = E_0$ indicates failure to continue the breather solution numerically in ϵ, in agreement with the proof of Theorem 6.

(c) We observe from panel (c) of Figure 2.4 that λ_0 and $-\lambda_-$ intersect but do not create instabilities, since all parts of the spectrum have the same signature, as is given by Lemma 7. In fact, the branch is both spectrally and orbitally stable as long as $\lambda_0 \in i\mathbb{R}$, in agreement with Theorem 8. On the other hand, there is $E_s \in (0, E_0)$, if $\Omega \in (-2\sqrt{2}|\gamma|, -|\gamma|)$, such that $\lambda_0 \in \mathbb{R}$ for $E \in (0, E_s)$, which indicates instability of branch (c), again, in agreement with Theorem 8.

As we see on panel (b) of Figure 2.4, λ_0 intersects λ_+ for some $E = E_* > E_0$. In the remainder of this section, we study whether this crossing point is always located on the right of E_0. In fact, the answer to this question is negative. We shall prove for branch (b) that the intersection of λ_0 with either λ_+ or $-\lambda_-$ occurs either for $E_* > E_0$ or for $E_* < E_0$, depending on parameters γ and Ω.

Lemma 8. *Fix $\gamma \neq 0$, $\Omega < -|\gamma|$, and $E > 0$ along branch (b) of Lemma 4. There exists a resonance $\lambda_0 = \lambda_+$ at $E = E_*$ with $E_* > E_0$ if $\Omega \in (\Omega_*, -|\gamma|)$ and $E_* \in (0, E_0)$ if $\Omega \in (-5|\gamma|, \Omega_*)$, where*

$$\Omega_* := -\frac{\sqrt{1+5\sqrt{2}}}{\sqrt{2}}|\gamma|. \tag{2.69}$$

Moreover, if $\Omega < -5|\gamma|$, there exists a resonance $\lambda_0 = -\lambda_-$ at $E = E_*$ with $E_* \in (0, E_0)$.

Proof. Let us first assume that there exists a resonance $\lambda_0 = \lambda_+$ at $E = E_* = E_0$ and find the condition on γ and Ω, when this is possible. From the definitions (2.62) and (2.63), we obtain the constraint on A^2:

$$(4A^2+\Omega)^2 - \frac{\Omega\gamma^2}{4A^2+\Omega} = E_0^2 = \Omega^2 - \gamma^2.$$

After canceling $4A^2$ since $A^2 \geq A_+^2 > 0$ with A_+^2 given by (2.27), we obtain

$$16A^4 + 12\Omega A^2 + 2\Omega^2 + \gamma^2 = 0,$$

which has two roots

$$A^2 = -\frac{3}{8}\Omega \pm \frac{1}{8}\sqrt{\Omega^2 - 4\gamma^2}.$$

Since $A^2 \geq A_+^2$, the lower sign is impossible because this leads to a contradiction

$$\sqrt{|\Omega| - 2|\gamma|} - \sqrt{|\Omega| + 2|\gamma|} \geq 0.$$

The upper sign is possible if $|\Omega| \geq 2|\gamma|$. Using the parametrization (2.25), we substitute the root for A^2 to the equation $E_0^2 = E^2$ and simplify it:

$$\begin{aligned}
\Omega^2 - \gamma^2 &= \left(2|\Omega| + \sqrt{\Omega^2 - 4\gamma^2}\right)^2 \left[1 - \frac{4\gamma^2}{\left(|\Omega| + \sqrt{\Omega^2 - 4\gamma^2}\right)^2}\right] \\
&= \frac{2\sqrt{\Omega^2 - 4\gamma^2}\left(2|\Omega| + \sqrt{\Omega^2 - 4\gamma^2}\right)^2}{\left(|\Omega| + \sqrt{\Omega^2 - 4\gamma^2}\right)}.
\end{aligned}$$

This equation further simplifies to the form:

$$\sqrt{\Omega^2 - 4\gamma^2}(9\Omega^2 - 7\gamma^2) + \Omega(31\gamma^2 - 7\Omega^2) = 0.$$

Squaring it up, we obtain

$$8\Omega^6 - 4\Omega^4\gamma^2 - 102\Omega^2\gamma^4 - 49\gamma^6 = 0,$$

which has only one positive root for Ω^2 given by

$$\Omega^2 = \frac{1+5\sqrt{2}}{2}\gamma^2.$$

This root yields a formula for Ω_* in (2.69). Since there is a unique value for $\Omega \in (-\infty, -|\gamma|)$, for which the case $E_* = E_0$ is possible, we shall now consider whether $E_* > E_0$ or $E_* < E_0$ for $\Omega \in (-\infty, \Omega_*)$ or $\Omega \in (\Omega_*, -|\gamma|)$.

To inspect the range $E_* < E_0$, we consider a particular case, for which the intersection $\lambda_0 = \lambda_+ = -\lambda_-$ happens at $E = 0$. In this case, $A^2 = A_+^2$ given by (2.27), so that the condition $\lambda_0^2 = -E_0^2$ can be rewritten as

$$4(\gamma^2 - |\gamma|\Omega) = \Omega^2 - \gamma^2.$$

There is only one negative root for Ω and it is given by $\Omega = -5|\gamma|$. By continuity, we conclude that $\lambda_0 = \lambda_+$ for $\Omega \in (-5|\gamma|, \Omega_*)$ and $\lambda_0 = -\lambda_-$ for $\Omega \in (-\infty, -5|\gamma|)$, both cases correspond to $E_* \in (0, E_0)$.

Finally, we verify that the case $\lambda_0 = \lambda_+$ occurs for $E_* > E_0$ if $\Omega \in (\Omega_*, -|\gamma|)$. Indeed, $\lambda_0 = i(8A^2 + 2\Omega + \mathcal{O}(A^{-2}))$ and $\lambda_+ = i(8A^2 + \Omega + E_0 + \mathcal{O}(A^{-2}))$ as $A \to \infty$, so that $\text{Im}(\lambda_0) < \text{Im}(\lambda_+)$ as $E \to \infty$. On the other hand, the previous estimates suggest that $\text{Im}(\lambda_0) > \text{Im}(\lambda_+)$ for every $E \in (0, E_0)$ if $\Omega \in (\Omega_*, -|\gamma|)$. Therefore, there exists at least one intersection $\lambda_0 = \lambda_+$ for $E_* > E_0$ if $\Omega \in (\Omega_*, -|\gamma|)$. □

Remark 10. *The existence of the resonance at $E = 0$ for some parameter configurations predicted by Lemma 8 is in agreement with the numerical results in [135, 136] on the scalar parametrically forced dNLS equation that follows from system (2.5) under the reduction (2.6). It was reported in [135, 136] that the instability bubble for breather solutions may appear for every nonzero coupling constant $\epsilon = 0$ in a narrow region of the parameter space.*

2.7 Summary

We have reduced Newton's equation of motion for coupled pendula shown on Figure 2.1 under a resonant periodic force to the $\mathcal{PT}$-symmetric dNLS equation (2.9). We have shown that this system is Hamiltonian with conserved energy (2.17) and an additional constant of motion (2.18). We have studied breather solutions of this model, which generalize symmetric synchronized oscillations of coupled pendula that arise if $E = 0$. We showed existence of three branches of breathers shown on Figure 2.3. We also investigated their spectral stability analytically and numerically. The spectral information on each branch of solutions is shown on Figure 2.4. For branch (c), we were also able to prove orbital stability and instability from the energy method. The technical results of this Chapter are summarized in Table 1 and described as follows.

For branch (a), we found that it is disconnected from the symmetric synchronized oscillations at $E = 0$. Along this branch, breathers of small amplitudes A are connected to breathers of large amplitudes A. Every point on the branch corresponds to the saddle point of the energy function between two wave continua of positive and negative energies. Every breather along the branch is spectrally stable and is free of resonance between isolated eigenvalues and continuous spectrum. In Chapter 3, we will prove long-time orbital stability of breathers along this branch.

For branch (b), we found that the large-amplitude breathers as $E \to \infty$ are connected to the symmetric synchronized oscillations at $E = 0$, which have the smallest (but nonzero) amplitude

Table 2.1: A summary of results on breather solutions for small ϵ. Here, IB is a narrow instability bubble seen on panel (b) of Figure 2.4.

Parameter intervals	$\|E\| > E_0$		$\|E\| < E_0$	
	$\Omega > \|\gamma\|$	$\Omega < -\|\gamma\|$	$\Omega < -\|\gamma\|$	$\Omega < -\|\gamma\|$
Existence on Figure 2.3	point 1 on branch (a)	point 3 on branch (b)	point 2 on branch (b)	point 4 on branch (c)
Continuum	Sign-indefinite	Sign-indefinite	Negative	Negative
Spectral stability	Yes	Yes (IB)	Yes (IB)	Depends on parameters
Orbital stability	No	No	Yes if $\|\lambda_0\| > \|\lambda_\pm\|$	Yes if spectrally stable

$A = A_+$. Breathers along the branch are spectrally stable except for a narrow instability bubble, where the isolated eigenvalue λ_0 is in resonance with the continuous spectrum. The instability bubble can occur either for $E > E_0$, where the breather is a saddle point of the energy function between two wave continua of opposite energies or for $E < E_0$, where the breather is a saddle point between the two negative-definite wave continua and directions of positive energy. When the isolated eigenvalue of positive energy λ_0 is above the continuous spectrum near λ_+ and $\pm\lambda_-$, orbital stability of breathers can be proved by using the technique in [42], which was developed for the dNLS equation.

Finally, for branch (c), we found that the small-amplitude breathers at $E \to E_0$ are connected to the symmetric synchronized oscillations at $E = 0$, which have the largest amplitude $A = A_-$. Breathers are either spectrally stable near $E = E_0$ or unstable near $E = 0$, depending on the detuning frequency Ω and the amplitude of the periodic resonant force γ. When breathers are spectrally stable, they are also orbitally stable for infinitely long times.

Chapter 3

Metastability in Discrete Systems

3.1 Background

We consider the system of amplitude equations (2.9), which is reproduced here for convenience without factor 2 for the time derivatives:

$$\begin{cases} i\frac{du_n}{dt} = \epsilon\left(v_{n+1} - 2v_n + v_{n-1}\right) + i\gamma u_n + \Omega v_n + 2\left[\left(2|u_n|^2 + |v_n|^2\right)v_n + u_n^2\bar{v}_n\right], \\ i\frac{dv_n}{dt} = \epsilon\left(u_{n+1} - 2u_n + u_{n-1}\right) - i\gamma v_n + \Omega u_n + 2\left[\left(|u_n|^2 + 2|v_n|^2\right)u_n + \bar{u}_n v_n^2\right], \end{cases} \tag{3.1}$$

where $\{u_n, v_n\}_{n\in\mathbb{Z}}$ are complex-valued amplitudes that depend on time $t \in \mathbb{R}$, whereas $(\Omega, \gamma, \epsilon)$ are real-valued parameters arising in a physical context described below. We assume $\Omega \neq 0$, $\gamma > 0$, and $\epsilon > 0$ throughout this Chapter.

The remarkable property of the $\mathcal{PT}$-symmetric dNLS equation (3.1) is the existence of the cross–gradient symplectic structure (2.16) with two conserved quantities (2.17) and (2.18) bearing the meaning of the energy and charge functions. For convenience, we reproduce again the cross-gradient symplectic structure

$$i\frac{du_n}{dt} = \frac{\partial H}{\partial \bar{v}_n}, \quad i\frac{dv_n}{dt} = \frac{\partial H}{\partial \bar{u}_n}, \quad n \in \mathbb{Z}, \tag{3.2}$$

and the Hamiltonian function

$$\begin{aligned} H &= \sum_{n\in\mathbb{Z}} (|u_n|^2 + |v_n|^2)^2 + (u_n\bar{v}_n + \bar{u}_n v_n)^2 + \Omega(|u_n|^2 + |v_n|^2) \\ &\quad -\epsilon|u_{n+1} - u_n|^2 - \epsilon|v_{n+1} - v_n|^2 + i\gamma(u_n\bar{v}_n - \bar{u}_n v_n). \end{aligned} \tag{3.3}$$

The Hamiltonian system (3.2) has an additional gauge symmetry, with respect to the transformation $\{u_n, v_n\}_{n\in\mathbb{Z}} \to \{e^{i\alpha}u_n, e^{i\alpha}v_n\}_{n\in\mathbb{Z}}$, where $\alpha \in \mathbb{R}$. The charge function related to the gauge symmetry is written in the form

$$Q = \sum_{n\in\mathbb{Z}} (u_n\bar{v}_n + \bar{u}_n v_n). \tag{3.4}$$

The energy and charge functions H and Q are conserved in the time evolution of the Hamiltonian

system (3.2). Compared to the other physically relevant $\mathcal{PT}$-symmetric dNLS equations [79, 114, 115], where the Hamiltonian structure is not available and analysis of nonlinear stability of the zero equilibrium and time-periodic localized breathers is barely possible, we are able to address these questions for the $\mathcal{PT}$-symmetric dNLS equation (3.1), thanks to the Hamiltonian structure (3.2) with two conserved quantities (3.3) and (3.4).

The temporal evolution of the $\mathcal{PT}$-symmetric dNLS equation (3.1) is studied in sequence space $\ell^2(\mathbb{Z})$ for sequences (u, v) as functions of time. Global existence of solutions in $\ell^2(\mathbb{Z})$ follows from an easy application of Picard's method and energy estimates (Proposition 3). The global solution in $\ell^2(\mathbb{Z})$ may still grow at most exponentially in time, due to the destabilizing properties of the gain-damping terms in the system (3.1). However, thanks to coercivity of the energy function (3.3) near the zero equilibrium, we can still obtain a global bound on the $\ell^2(\mathbb{Z})$ norm of the solution near the zero equilibrium, provided it is linearly stable. Moreover, for $\Omega > (\gamma+4\epsilon)$, the global bound holds for arbitrary initial data. The corresponding result is given by the following theorem (proved in Section 2). A similar result for a single dimer is deemed as the *spontaneous $\mathcal{PT}$-symmetry restoration* in [16].

Theorem 10. *For every $\Omega > (\gamma + 4\epsilon)$ and every initial data $(u(0), v(0)) \in \ell^2(\mathbb{Z})$, there is a positive constant C that depends on parameters and Ω, γ, ϵ and $(\|u(0)\|_{\ell^2}, \|v(0)\|_{\ell^2})$ such that*

$$\|u(t)\|_{\ell^2}^2 + \|v(t)\|_{\ell^2}^2 \leq C, \quad \text{for every } \ t \in \mathbb{R}. \tag{3.5}$$

The bound (3.5) also holds for every $\Omega < -\gamma$ and every $(u(0), v(0)) \in \ell^2(\mathbb{Z})$ with sufficiently small $\ell^2(\mathbb{Z})$ norm.

Remark 11. *As shown in Chapter 2, the zero equilibrium of the $\mathcal{PT}$-symmetric dNLS equation (3.1) is linearly stable if $|\gamma| < \gamma_0$, where the $\mathcal{PT}$ phase transition threshold γ_0 is given by*

$$\gamma_0 := \begin{cases} \Omega - 4\epsilon, & \Omega > 0 \\ |\Omega|, & \Omega < 0. \end{cases}$$

The zero equilibrium is linearly unstable if $|\gamma| \geq \gamma_0$. Thus, the constraints on parameters in Theorem 10 coincide with the criterion of linear stability of the zero equilibrium.

We shall now characterize *breathers* supported by the $\mathcal{PT}$-symmetric dNLS equation (3.1). These are solutions of the form

$$u(t) = Ue^{-iEt}, \quad v(t) = Ve^{-iEt}, \tag{3.6}$$

where the frequency parameter E is considered to be real and the sequence $(U, V) \in \ell^2(\mathbb{Z})$ is time-independent. By continuous embedding, we note that $(U, V) \in \ell^2(\mathbb{Z})$ implies the decay at infinity: $|U_n| + |V_n| \to 0$ as $|n| \to \infty$. The breather is considered to be $\mathcal{PT}$-symmetric with respect to the operators in (2.11) if $V = \bar{U}$.

Thanks to the cross-gradient symplectic structure (3.2), $(U, V) \in \ell^2(\mathbb{Z})$ in (3.6) is a critical point of the extended energy function $H_E : \ell^2(\mathbb{Z}) \to \mathbb{R}$ given by

$$H_E := H - EQ, \tag{3.7}$$

where H and Q are given by (3.3) and (3.4). The Euler–Lagrange equations for H_E produce the stationary $\mathcal{PT}$-symmetric dNLS equation:

$$EU_n = \epsilon\left(\bar{U}_{n+1} - 2\bar{U}_n + \bar{U}_{n-1}\right) + i\gamma U_n + \Omega\bar{U}_n + 6|U_n|^2\bar{U}_n + 2U_n^3, \tag{3.8}$$

which corresponds to the reduction of the $\mathcal{PT}$-symmetric dNLS equation (3.1) for the breather solution (3.6) under the $\mathcal{PT}$ symmetry $V = \bar{U}$.

We denote a solution of the $\mathcal{PT}$-symmetric dNLS equation (3.1) in $\ell^2(\mathbb{Z})$ by $\psi = (u, v)$ and the localized solution of the stationary dNLS equation (3.8) by $\Phi = (U, V)$. We fix parameters $\gamma > 0$, $\Omega > \gamma$, and $E \in (-\infty, -E_0) \cup (E_0, \infty)$. The following theorem (proved in Section 3) formulates the main result of this Chapter.

Theorem 11. *For every $\nu > 0$ sufficiently small, there exists $\epsilon_0 > 0$ and $\delta > 0$ such that for every $\epsilon \in (0, \epsilon_0)$ the following is true. If $\psi(0) \in \ell^2(\mathbb{Z})$ satisfies $\|\psi(0) - \Phi\|_{l^2} \leq \delta$, then there exist a positive time $t_0 \lesssim \epsilon^{-1/2}$ and a C^1 function $\alpha(t) : [0, t_0] \to \mathbb{R}/(2\pi\mathbb{Z})$ such that the unique solution $\psi(t) : [0, t_0] \to \ell^2(\mathbb{Z})$ to the $\mathcal{PT}$-symmetric dNLS equation (3.1) satisfies the bound*

$$\|e^{i\alpha(t)}\psi(t) - \Phi\|_{l^2} \leq \nu, \quad \text{for every } \ t \in [0, t_0]. \tag{3.9}$$

Moreover, there exists a positive constant C such that $|\dot{\alpha} - E| \leq C\nu$, for every $t \in [0, t_0]$.

Remark 12. *The statement of Theorem 11 remains true for $\epsilon = 0$. In this (anti-continuum) limit, Theorem 11 gives nonlinear stability of the standing localized state Φ compactly supported at the central site $n = 0$. The bound (3.9) is extended in the case $\epsilon = 0$ for all times $t \in \mathbb{R}$.*

Remark 13. *It becomes clear from the proof of Theorem 11 for $\epsilon \neq 0$, see inequality (3.59) below, that the bound (3.9) on the perturbation ϕ to the stationary solution Φ is defined within the size of $\mathcal{O}(\epsilon^{1/2} + \delta)$. Therefore, if $\Phi_n = \mathcal{O}(\epsilon^{|n|})$ for every $n \neq 0$ (Proposition 4), then the perturbation term is $\phi_n = \mathcal{O}(\epsilon^{1/2} + \delta)$ for every $n \in \mathbb{Z}$. This is a limitation of the result of Theorem 11. Not only it holds for long but finite times $t_0 = \mathcal{O}(\epsilon^{-1/2})$ but also it gives a larger than expected bound on the perturbation term ϕ. It may be quite possible to improve the approximation result with a sequence of normal form transformations, similar to what was done recently in [110].*

Remark 14. *The statement of Theorem 11 can be improved on a shorter time scale $t_0 = \mathcal{O}(1)$. In this case, see inequality (3.58) below, the perturbation term ϕ has the size of $\mathcal{O}(\epsilon + \delta)$. Thus, the perturbation term ϕ_n at $n = \pm 1$ is comparable with the standing localized state Φ_n at $n = \pm 1$, but it is still much larger than Φ_n for every n such that $|n| \geq 2$.*

Remark 15. *Theorem 11 cannot be extended to the solution branch with $\Omega < -\gamma < 0$ and $|E| > E_0$ (point 3 on Figure 2.3) because the second variation of Λ_E at (U, V) is not coercive and does not control the size of perturbation terms. This analytical difficulty reflects the unfortunate location of the discrete and continuous spectra that leads to a resonance studied in Chapter 2. No resonance was found for the solution branch with $\Omega > \gamma > 0$ and $|E| > E_0$ (point 1 on Figure 2.3) and this numerical result from Chapter 2 is in agreement with the analytical method used in the proof of Theorem 11.*

The remainder of this Chapter is devoted to the proof of Theorems 10 and 11.

3.2 Proof of the global bound

The following proposition gives the global existence result for the $\mathcal{PT}$-symmetric dNLS equation (3.1).

Proposition 3. *For every $(u^{(0)}, v^{(0)}) \in \ell^2(\mathbb{Z})$, there exists a unique solution $(u, v)(t) \in C^1(\mathbb{R}, \ell^2(\mathbb{Z}))$ of the $\mathcal{PT}$-symmetric dNLS equation (3.1) such that $(u, v)(0) = (u^{(0)}, v^{(0)})$. The unique solution depends continuously on initial data $(u^{(0)}, v^{(0)}) \in \ell^2(\mathbb{Z})$.*

Proof. Since discrete Laplacian is a bounded operator in $\ell^2(\mathbb{Z})$ and the sequence space $\ell^2(\mathbb{Z})$ forms a Banach algebra with respect to pointwise multiplication, the local well-posedness of the initial-value problem for the $\mathcal{PT}$-symmetric dNLS equation (3.1) follows from the standard Picard's method. The local solution $(u, v)(t)$ exists in $C^0([-t_0, t_0], \ell^2(\mathbb{Z}))$ for some finite $t_0 > 0$. Thanks again to the boundedness of the discrete Laplacian operator in $\ell^2(\mathbb{Z})$, bootstrap arguments extend this solution in $C^1([-t_0, t_0], \ell^2(\mathbb{Z}))$.

The local solution is continued globally by using the energy method. For any solution $(u, v)(t)$ in $C^1([-t_0, t_0], \ell^2(\mathbb{Z}))$, we obtain the following balance equation from system (3.1):

$$\frac{d}{dt}\sum_{n\in\mathbb{Z}}(|u_n|^2 + |v_n|^2) = -\gamma\sum_{n\in\mathbb{Z}}(|u_n|^2 - |v_n|^2).$$

Integrating this equation in time and applying Gronwall's inequality, we get

$$\|u(t)\|_{l^2}^2 + \|v(t)\|_{l^2}^2 \leq \left(\|u(0)\|_{l^2}^2 + \|v(0)\|_{l^2}^2\right) e^{|\gamma t|}, \quad t \in [-t_0, t_0].$$

Therefore $\|u(t)\|_{l^2}$ and $\|v(t)\|_{l^2}$ cannot blow up in a finite time, so that the local solution $(u, v)(t) \in C^1([-t_0, t_0], \ell^2(\mathbb{Z}))$ is continued for every $t_0 > 0$. □

A critical question also addressed in [79, 115] for other $\mathcal{PT}$-symmetric dNLS equations is whether the $\ell^2(\mathbb{Z})$ norms of the global solution of Proposition 3 remain bounded as $t \to \infty$. In the context of the Hamiltonian $\mathcal{PT}$-symmetric dNLS equation (3.1), this question can be addressed by using the energy function given by (3.3). In what follows, we use coercivity of the energy function and prove the result stated in Theorem 10.

Proof of Theorem 10. We use $\gamma > 0$ and $\epsilon > 0$ everywhere in the proof. If $\Omega > (\gamma + 4\epsilon)$, the following lower bound is available for the energy function H given by (3.3) using Cauchy–Schwarz inequality:

$$H \geq (\Omega - \gamma - 4\epsilon)\left(\|u\|_{\ell^2}^2 + \|v\|_{\ell^2}^2\right). \tag{3.10}$$

Since H is time-independent and bounded for any $(u, v)(t) \in C^1(\mathbb{R}, \ell^2(\mathbb{Z}))$ due to the continuous embedding $\|u\|_{\ell^4} \leq \|u\|_{\ell^2}$, we obtain the time-independent bound (3.5) for any $\Omega > (\gamma + 4\epsilon)$.

If $\Omega < -\gamma$, the following lower bound is available for the energy function $-H$:

$$-H \geq (|\Omega| - \gamma)\left(\|u\|_{\ell^2}^2 + \|v\|_{\ell^2}^2\right) - \left(\|u\|_{\ell^2}^2 + \|v\|_{\ell^2}^2\right)^2, \tag{3.11}$$

where the continuous embedding $\|u\|_{\ell^4} \leq \|u\|_{\ell^2}$ has been used. If $\|u(0)\|_{\ell^2} + \|v(0)\|_{\ell^2}$ is sufficiently small, then $|H|$ is sufficiently small, and the bound (3.5) with sufficiently small C holds for every $t \in \mathbb{R}$. □

Remark 16. *For every $\Omega \leq (\gamma + 4\epsilon)$, the energy functions H or $-H$ do not produce a useful lower bound, which would result in a time-independent bound on the $\ell^2(\mathbb{Z})$ norm for the global solution $(u, v)(t)$. This is because the continuous embedding*

$\|u\|_{\ell^4} \leq \|u\|_{\ell^2}$ is not sufficient to control H or $-H$ from below. If the lattice is truncated on a finitely many (say, N) sites, then the bound $\|u\|_{\ell^2} \leq N^{1/4}\|u\|_{\ell^4}$ can be used to obtain from (3.3):

$$H \geq \left(\|u\|_{\ell^4}^4 + \|v\|_{\ell^4}^4\right) - (\gamma + 4\epsilon - \Omega)N^{1/2}\left(\|u\|_{\ell^4}^2 + \|v\|_{\ell^4}^2\right).$$

Thus, the time-independent bound on the $\ell^4(\mathbb{Z}_N)$ (and then $\ell^2(\mathbb{Z}_N)$) norms for the global solution $(u, v)(t)$ restricted on N sites of the lattice $\mathbb{Z}$ is available for every Ω. However, the control becomes impossible in the limit $N \to \infty$ if $\Omega \leq (\gamma + 4\epsilon)$.

Remark 17. *It is an interesting open question to investigate if the global dynamics of the $\mathcal{PT}$-symmetric dNLS equation (3.1) on the infinite lattice is globally bounded in time for $\Omega \leq (\gamma + 4\epsilon)$. This open question would include the case $-\gamma \leq \Omega \leq (\gamma + 4\epsilon)$, when the zero equilibrium is linearly unstable, and the case $\Omega < -\gamma$ with sufficiently large initial data $(u(0), v(0)) \in \ell^2(\mathbb{Z})$, when the zero equilibrium is linearly stable but the bound (3.11) can no longer be closed. This open question is addressed numerically for a similar model without phase invariance in [46], where it was shown that l^2 norm of the solution grows while l^∞ norm remains finite.*

3.3 Proof of metastability

We divide the proof of Theorem 11 into several subsections.

3.3.1 Characterization of the localized solutions

For $\epsilon = 0$, a solution to the stationary dNLS equation (3.8) is supported on the central site $n = 0$ and satisfies

$$(E - i\gamma)U_0 - \Omega\bar{U}_0 = 6|U_0|^2\bar{U}_0 + 2U_0^3. \tag{3.12}$$

The parameters γ and Ω are considered to be fixed, and parameter E is thought to parameterize a continuous branch of solutions of the nonlinear algebraic equation (3.12). Substituting the decomposition $U_0 = Ae^{i\theta}$ with $A > 0$ and $\theta \in [0, 2\pi)$ into the algebraic equation (3.12), we obtain

$$\sin(2\theta) = \frac{\gamma}{4A^2 + \Omega}, \quad \cos(2\theta) = \frac{E}{8A^2 + \Omega}, \tag{3.13}$$

from which the solution branches of E versus A are obtained in Chapter 2 as shown on Figure 2.3. The dependence of E versus A is given analytically by

$$E^2 = (\Omega + 8A^2)^2\left[1 - \frac{\gamma^2}{(\Omega + 4A^2)^2}\right]. \tag{3.14}$$

Persistence of the central dimer in the unbounded lattice with respect to the coupling parameter ϵ is given by the following proposition.

Proposition 4. *Fix $\gamma > 0$, $\Omega > \gamma$, and $E \neq \pm E_0$, where $E_0 := \sqrt{\Omega^2 - \gamma^2} > 0$. There exist $\epsilon_0 > 0$ sufficiently small and $C_0 > 0$ such that for every $\epsilon \in (-\epsilon_0, \epsilon_0)$, there exists a unique solution*

$U \in l^2(\mathbb{Z})$ to the difference equation (3.8) such that

$$\left|U_0 - Ae^{i\theta}\right| \leq C_0|\epsilon|, \quad |U_n| \leq C_0|\epsilon|^{|n|}, \quad n \neq 0, \tag{3.15}$$

where A and θ are defined in (3.13). Moreover, the solution U is smooth in ϵ.

Proof. Persistence and smoothness of a solution $U \in l^2(\mathbb{Z})$ to the difference equation (3.8) in ϵ, as well as the first bound in (3.15), were proved in Theorem 6.

It remains to prove the second bound in (3.15), for which we employ the implicit function theorem (see Section 1.5.6). Inspecting the difference equation (3.8) shows that if $U_{\pm 1} = \mathcal{O}(|\epsilon|)$ according to the bound (2.33), then $U_n = U_{-n}$ can be expressed by using the scaling transformation

$$U_n = \epsilon^{|n|} W_{|n|}, \quad \pm n \in \mathbb{N}, \tag{3.16}$$

where the sequence $W \in \ell^2(\mathbb{N})$ is found from the system

$$EW_n - i\gamma W_n - \Omega \bar{W}_n = \bar{W}_{n-1} + \epsilon^2 \bar{W}_{n+1} - 2\epsilon \bar{W}_n + 6\epsilon^{2|n|}|W_n|^2 \bar{W}_n + 2\epsilon^{2|n|} W_n^3, \quad n \in \mathbb{N}, \tag{3.17}$$

with $W_0 = U_0$ given by the previous result. Let $x = \{W_n\}_{n\in\mathbb{N}}$, $X = \ell^2(\mathbb{N})$, $y = \epsilon$, $Y = \mathbb{R}$, and $Z = \ell^2(\mathbb{N})$ in the definition of system $F : X \times Y \to Z$. Then, we have $F(x_0, 0) = 0$, where $x_0 = \{W_n^{(0)}\}_{n\in\mathbb{N}}$ is a unique solution of the recurrence equation

$$EW_n^{(0)} - i\gamma W_n^{(0)} - \Omega \bar{W}_n^{(0)} = \bar{W}_{n-1}^{(0)}, \quad n \in \mathbb{N}, \tag{3.18}$$

starting with a given $W_0^{(0)} = U_0$. Indeed, each block in the left-hand side of system (3.18) is given by the invertible matrix

$$\begin{bmatrix} E - i\gamma & -\Omega \\ -\Omega & E + i\gamma \end{bmatrix},$$

with eigenvalues $\lambda_\pm = E \pm E_0 \neq 0$. Hence, a unique solution for $W^{(0)} \in \ell^\infty(\mathbb{N})$ is found from the recurrence relation (3.18). Moreover, since $D_x F(0, 0) : X \to Z$ is one-to-one and onto (as a lower block-triangular matrix with invertible diagonal blocks), the solution $W^{(0)}$ is actually in $X = \ell^2(\mathbb{N})$. By the implicit function theorem, for every $\epsilon \neq 0$ sufficiently small, there exists a unique solution $W \in \ell^2(\mathbb{N})$ to the system (3.17) such that

$$\|W - W^{(0)}\|_{\ell^2(\mathbb{N})} < C'''|\epsilon|, \tag{3.19}$$

where a positive constant C''' is independent of ϵ. Thus, the second bound in (3.15) is proved from (3.16) and (3.19). □

3.3.2 Decomposition of the solution

Let $\psi = (u, \bar{u}, v, \bar{v})$ denote a solution of the $\mathcal{PT}$-symmetric dNLS equation (3.1) in $\ell^2(\mathbb{Z})$ given by Proposition 3. Let $\Phi = (U, \bar{U}, V, \bar{V})$ denote a localized solution of the stationary dNLS equation (3.8) given by Proposition 4. Let $\phi = \psi - \Phi = (\mathbf{u}, \bar{\mathbf{u}}, \mathbf{v}, \bar{\mathbf{v}})$ denote a perturbation to Φ. Note that these

are extended 4-component variables at each lattice site (concatenated by the complex conjugate functions) compared to the two-component variables used in the formulation of Theorem 11. The extended variables are more suitable for dealing with the energy functions such as (3.7) or (6.3), which we reproduce here for convenience:

$$\Lambda_E := H - E(u_0\bar{v}_0 + \bar{u}_0 v_0). \tag{3.20}$$

By using the energy function (3.20), we introduce the energy difference function

$$\Delta := \Lambda_E(\Phi + \phi) - \Lambda_E(\Phi). \tag{3.21}$$

Let us write the expansion for Δ explicitly:

$$\Delta = N_1(\phi) + N_2(\phi) + N_3(\phi) + N_4(\phi), \tag{3.22}$$

where the linear part is

$$N_1(\phi) = E \sum_{n\in\mathbb{Z}\setminus\{0\}} \left(\bar{V}_n \mathbf{u}_n + V_n \bar{\mathbf{u}}_n + \bar{U}_n \mathbf{v}_n + U_n \bar{\mathbf{v}}_n\right), \tag{3.23}$$

the quadratic part is

$$N_2(\phi) = \frac{1}{2}\langle \mathcal{H}_E'' \phi, \phi\rangle_{l^2} + E \sum_{n\in\mathbb{Z}\setminus\{0\}} \left(\bar{\mathbf{v}}_n \mathbf{u}_n + \mathbf{v}_n \bar{\mathbf{u}}_n\right), \tag{3.24}$$

whereas the cubic and quartic parts of Δ denoted by $N_3(\phi)$ and $N_4(\phi)$ are not important for estimates, thanks to the bounds

$$|N_3(\phi)| \leq C_3 \|\phi\|_{l^2}^3, \quad |N_4(\phi)| \leq C_4 \|\phi\|_{l^2}^4, \tag{3.25}$$

where C_3, C_4 are positive constants and we have used continuous embedding $\|u\|_{\ell^p} \leq \|u\|_{\ell^2}$ for any $p \geq 2$.

In the next three subsections, we show that the quadratic part $N_2(\phi)$ is positive, the linear part $N_1(\phi)$ can be removed by a local transformation, and the time evolution of Δ can be controlled on a long but finite time interval.

In what follows, all constants depend on parameters $\gamma > 0$, $\Omega > \gamma$, and $E \in (-\infty, -E_0) \cup (E_0, \infty)$. The parameter $\epsilon > 0$ is sufficiently small, and unless it is stated otherwise, the constants do not depend on the small parameter ϵ.

3.3.3 Positivity of the quadratic part of Δ

The quadratic part (3.24) can be analyzed by a parameter continuation from the case $\epsilon = 0$. Compared to the self-adjoint (Hessian) operator $\mathcal{H}_E'' : \ell^2(\mathbb{Z}) \to \ell^2(\mathbb{Z})$ which is a second variation of H_E

in (3.7), the Hessian operator for $N_2(\phi)$ denoted by $\Lambda_E'' : \ell^2(\mathbb{Z}) \to \ell^2(\mathbb{Z})$ is given by

$$\Lambda_E'' = \tilde{\mathcal{M}} + \epsilon\mathcal{L}, \tag{3.26}$$

where $\mathcal{L}$ is the discrete Laplacian operator applied to blocks of ϕ at each lattice site $n \in \mathbb{Z}$:

$$(\mathcal{L}\phi)_n = \phi_{n+1} - 2\phi_n + \phi_{n-1},$$

and the blocks of $\tilde{\mathcal{M}}$ at each site $n \in \mathbb{Z}$ are given differently for $n = 0$ and $n \neq 0$. For $n = 0$, the 4-by-4 matrix block of $\tilde{\mathcal{M}}_0$ is given by

$$\tilde{\mathcal{M}}_0 = \begin{bmatrix} \Omega + 8A^2 & 4A^2\cos(2\theta) & -E - i\gamma + 8A^2\cos(2\theta) & 4A^2 \\ 4A^2\cos(2\theta) & \Omega + 8A^2 & 4A^2 & -E + i\gamma + 8A^2\cos(2\theta) \\ -E + i\gamma + 8A^2\cos(2\theta) & 4A^2 & \Omega + 8A^2 & 4A^2\cos(2\theta) \\ 4A^2 & -E - i\gamma + 8A^2\cos(2\theta) & 4A^2\cos(2\theta) & \Omega + 8A^2 \end{bmatrix},$$

whereas for $n \neq 0$, we have

$$\tilde{\mathcal{M}}_n = \begin{bmatrix} \Omega + 8|U_n|^2 & 2(U_n^2 + \bar{U}_n^2) & -i\gamma + 4(U_n^2 + \bar{U}_n^2) & 4|U_n|^2 \\ 2(U_n^2 + \bar{U}_n^2) & \Omega + 8|U_n|^2 & 4|U_n|^2 & +i\gamma + 4(U_n^2 + \bar{U}_n^2) \\ +i\gamma + 4(U_n^2 + \bar{U}_n^2) & 4|U_n|^2 & \Omega + 8|U_n|^2 & 2(U_n^2 + \bar{U}_n^2) \\ 4|U_n|^2 & -i\gamma + 4(U_n^2 + \bar{U}_n^2) & 2(U_n^2 + \bar{U}_n^2) & \Omega + 8|U_n|^2 \end{bmatrix}.$$

The following proposition characterizes eigenvalues of $\tilde{\mathcal{M}}$ at $\epsilon = 0$.

Proposition 5. *Fix $\epsilon = 0$, $\gamma > 0$, $\Omega > \gamma$, and $E \neq \pm E_0$, where $E_0 := \sqrt{\Omega^2 - \gamma^2} > 0$. The matrix block of $\tilde{\mathcal{M}}_n$ has three positive and one zero eigenvalues for $n = 0$ and two double positive eigenvalues for every $n \neq 0$.*

Proof. If $\epsilon = 0$, the stationary state of Proposition 4 is given by $U_n = 0$ for every $n \neq 0$ and $U_0 = Ae^{i\theta}$, where A and θ are defined by the parametrization (3.13).

Using relations (3.13) and (3.14), as well as symbolic computations with MAPLE, we found that the 4-by-4 matrix block $\tilde{\mathcal{M}}_0$ has a simple zero eigenvalue and three nonzero eigenvalues μ_1, μ_2, and μ_3 given by

$$\begin{aligned} \mu_1 &= 2(\Omega + 4A^2), \\ \mu_{2,3} &= \Omega + 12A^2 \pm \sqrt{(\Omega - 4A^2)^2 + \frac{16\Omega A^2\gamma^2}{(\Omega + 4A^2)^2}}. \end{aligned}$$

It is shown in Chapter 2 that $\mu_1, \mu_2, \mu_3 > 0$ for every point on the solution branch with $\Omega > \gamma > 0$, and $|E| > E_0$.

For every $n \in \mathbb{Z}\backslash\{0\}$, the 4-by-4 matrix block of $\tilde{\mathcal{M}}_n$ is given by

$$\tilde{\mathcal{M}}_n = \begin{bmatrix} \Omega & 0 & -i\gamma & 0 \\ 0 & \Omega & 0 & +i\gamma \\ +i\gamma & 0 & \Omega & 0 \\ 0 & -i\gamma & 0 & \Omega \end{bmatrix}.$$

Each block has two double eigenvalues μ_+ and μ_- given by

$$\mu_+ = \Omega + \gamma, \quad \mu_- = \Omega - \gamma,$$

which are positive since $\Omega > \gamma$. □

By Proposition 5, if $\epsilon = 0$, then $N_2(\phi) \geq 0$ for every $\phi \in \ell^2(\mathbb{Z})$ and, moreover, $N_2(\phi) = 0$ if and only if ϕ is proportional to an eigenvector supported at $n = 0$. The existence of the zero eigenvalue at $\epsilon = 0$ is related to the gauge symmetry of the $\mathcal{PT}$-symmetric dNLS equation (3.1). Both for $\epsilon = 0$ and $\epsilon \neq 0$, there exists a nontrivial kernel of the Hessian operator $\mathcal{H}_E'' : \ell^2(\mathbb{Z}) \to \ell^2(\mathbb{Z})$ associated with the standing localized state (U, V), thanks to the identity

$$\mathcal{H}_E''(\sigma\Phi) = 0, \tag{3.27}$$

where the blocks of the eigenvector $\sigma\Phi$ are given by

$$(\sigma\Phi)_n := (U_n, -\bar{U}_n, V_n, -\bar{V}_n), \quad n \in \mathbb{Z}. \tag{3.28}$$

In the limit of $\epsilon \to 0$, the eigenvector $\sigma\Phi$ is supported at the central site $n = 0$ and it corresponds to the zero eigenvalue of the matrix block $\tilde{\mathcal{M}}_0$. By using Proposition 5 and identity (3.27), we can now state that if $\epsilon = 0$, then $N_2(\phi) = 0$ if and only if $\phi \in \text{span}\{\sigma\Phi\}$.

By the perturbation theory for linear operators (see Section 1.5.6), the strictly positive part of Λ_E'' remains strictly positive for a sufficiently small ϵ. On the other hand, the simple zero eigenvalue may drift away from zero if $\epsilon \neq 0$.

In order to avoid a problem of degeneracy (or even slight negativity) of Λ_E'', we introduce a constrained subspace of $\ell^2(\mathbb{Z})$ by

$$l_c^2(\mathbb{Z}) = \{\phi \in l^2(\mathbb{Z}) : \quad \langle \sigma\Phi, \phi \rangle_{l^2} = 0\}. \tag{3.29}$$

If $\epsilon = 0$ and ϕ belongs to $l_c^2(\mathbb{Z})$, then the quadratic form $N_2(\phi)$ in (3.24) is strictly positive and coercive. By the perturbation theory for linear operators (Appendix A), for $\epsilon \neq 0$ sufficiently small, the quadratic part $N_2(\phi)$ given by (3.24) for $\phi \in l_c^2(\mathbb{Z})$, remains strictly positive and coercive. This argument yields the proof of the following proposition.

Proposition 6. *Fix $\gamma > 0$, $\Omega > \gamma$, and $E \neq \pm E_0$. There exist $\epsilon_0 > 0$ sufficiently small and $C_2 > 0$ such that for every $\epsilon \in (-\epsilon_0, \epsilon_0)$,*

$$N_2(\phi) \geq C_2 \|\phi\|_{\ell^2}^2 \quad \text{for every} \quad \phi \in l_c^2(\mathbb{Z}), \tag{3.30}$$

where $l_c^2(\mathbb{Z})$ is given by (3.29).

Bounds (3.25) and (3.30) allow us to estimate the principal part of Δ in (3.22) from below, e.g.

$$|\Delta - N_1(\phi)| \geq \left(C_2 - C_3\|\phi\|_{\ell^2} - C_4\|\phi\|_{\ell^2}^2\right) \|\phi\|_{\ell^2}^2 \quad \text{for every} \quad \phi \in l_c^2(\mathbb{Z}).$$

However, the linear part $N_1(\phi)$ is an obstacle for such estimates. Therefore, we need to remove the obstacle by a local transformation.

3.3.4 Removal of the linear part of Δ

Let us define

$$\phi = \tilde{\phi} + \rho, \tag{3.31}$$

where $\tilde{\phi} = (\tilde{\mathbf{u}}_n, \overline{\tilde{\mathbf{u}}_n}, \tilde{\mathbf{v}}_n, \overline{\tilde{\mathbf{v}}}_n)$ is a new variable and $\rho = (a, \bar{a}, b, \bar{b})$ is a correction term to be found uniquely by removing the linear term $N_1(\phi)$. Since the breather is $\mathcal{PT}$-symmetric with $V = \bar{U}$, we shall look for a $\mathcal{PT}$-symmetric correction term with $b = \bar{a}$.

The easiest way of finding $a \in \ell^2(\mathbb{Z})$ is to write the Euler–Lagrange equations for the energy function Λ_E given by (3.20). For the $\mathcal{PT}$-symmetric solution with $v = \bar{u}$, the Euler–Lagrange equations for Λ_E take the form

$$Eu_n\delta_{n,0} = \epsilon\left(\bar{u}_{n+1} - 2\bar{u}_n + \bar{u}_{n-1}\right) + i\gamma u_n + \Omega\bar{u}_n + 6|u_n|^2\bar{u}_n + 2u_n^3, \tag{3.32}$$

where $\delta_{n,0}$ is the Kronecker symbol supported at $n = 0$. Let $u = U + a$, where U is a solution of the stationary dNLS equation (3.8). Then, a satisfies the nonlinear equation

$$\begin{aligned} &Ea_n\delta_{n,0} - \Omega\bar{a}_n - i\gamma a_n - \epsilon(\bar{a}_{n+1} - 2\bar{a}_n + \bar{a}_{n-1}) - 12|U_n|^2\bar{a}_n \\ &\quad -6(U_n^2 + \bar{U}_n^2)a_n - 6U_n(a_n^2 + \bar{a}_n^2) - 12\bar{U}_n|a_n|^2 - 6|a_n|^2\bar{a}_n - 2a_n^3 = EU_n(1 - \delta_{n,0}), \end{aligned} \tag{3.33}$$

where $n \in \mathbb{Z}$. Thanks to the bounds (3.15) Proposition 4, the right-hand side of system (3.33) is small in ϵ. The following proposition characterizes a unique solution to system (3.33). This solution with $b = \bar{a}$ defines a unique ρ in the transformation (3.31).

Proposition 7. *Fix $\gamma > 0$, $\Omega > \gamma$, and $E \neq \pm E_0$. There exist $\epsilon_0 > 0$ sufficiently small and $C_1 > 0$ such that for every $\epsilon \in (-\epsilon_0, \epsilon_0)$, there exists a unique solution $a \in \ell^2(\mathbb{Z})$ to the system (3.33) such that*

$$|a_0| \leq C_1 \epsilon^2, \quad |a_n| \leq C_1 |\epsilon|^{|n|}, \quad n \in \mathbb{Z} \backslash \{0\}. \tag{3.34}$$

Proof. The proof repeats the three steps in the proof of Proposition 4. On the sites $n \in \mathbb{Z}\backslash\{0\}$, the Jacobian operator $D_x F(0,0)$ is block-diagonal with identical blocks given by

$$\begin{bmatrix} -i\gamma & -\Omega \\ -\Omega & i\gamma \end{bmatrix}. \tag{3.35}$$

Each block is invertible thanks to the constraint $\Omega > \gamma$. On the central site $n = 0$, the Jacobian operator $D_x F(Ae^{i\theta}, 0)$ coincides with the block (2.35), which is invertible for every $\gamma \neq 0$, $\Omega > \gamma > 0$, and $|E| > E_0$ (see Theorem 6 in Chapter 2). Thus, existence and uniqueness of solutions to the nonlinear system (3.33) for small ϵ is established with two applications of the implicit function theorem.

In order to justify the bound (3.34), we use (3.16) and substitute

$$a_0 = \epsilon^2 A_0, \quad a_n = \epsilon^{|n|} A_{|n|}, \quad \pm n \in \mathbb{N} \tag{3.36}$$

to the system (3.33). The sequence $\{A_n\}_{n \in \mathbb{N}}$ is found from the system

$$\begin{aligned} &-\Omega \bar{A}_n - i\gamma A_n - \epsilon^2 \bar{A}_{n+1} + 2\epsilon \bar{A}_n - \bar{A}_{n-1}(1 - \delta_{n,1}) - \epsilon^2 A_0 \delta_{n,1} \\ &-6\epsilon^{2|n|}(W_n^2 + \bar{W}_n^2) A_n - 12\epsilon^{2|n|} |W_n|^2 \bar{A}_n - 6\epsilon^{2|n|} W_n (A_n^2 + \bar{A}_n^2) \\ &\qquad -12\epsilon^{2|n|} \bar{W}_n |A_n|^2 - 6\epsilon^{2|n|} |A_n|^2 \bar{A}_n - 2\epsilon^{2|n|} A_n^3 \ = EW_n, \end{aligned} \tag{3.37}$$

whereas the term A_0 satisfies the nonlinear equation

$$\begin{aligned} &EA_0 - \Omega \bar{A}_0 - i\gamma A_0 - 2\bar{A}_1 + 2\epsilon \bar{A}_0 - 6(U_0^2 + \bar{U}_0^2) A_0 - 12 |U_0|^2 \bar{A}_0 \\ &\qquad -6\epsilon^2 U_0 (A_0^2 + \bar{A}_0^2) - 12\epsilon^2 \bar{U}_0 |A_0|^2 - 6\epsilon^4 |A_0|^2 \bar{A}_0 - 2\epsilon^2 A_0^3 \ = 0. \end{aligned} \tag{3.38}$$

It follows from the invertibility of the block (2.35) that there exists a unique solution to the nonlinear equation (3.38) for $A_0 \in \mathbb{C}$ if ϵ is sufficiently small and $A_1 \in \mathbb{C}$ is given. The solution satisfies the bound

$$|A_0| \leq C' |A_1|, \tag{3.39}$$

where the positive constant C' is ϵ-independent. By substituting this solution for $A_0 \in \mathbb{C}$ to the system (3.37), we observe that the leading-order system is given by the recurrence equation

$$-\Omega \bar{A}_n^{(0)} - i\gamma A_n^{(0)} - \bar{A}_{n-1}^{(0)}(1 - \delta_{n,1}) = EW_n, \quad n \in \mathbb{N}. \tag{3.40}$$

Since $\Omega > \gamma$, there exists a unique solution $A^{(0)} \in \ell^\infty(\mathbb{N})$ of the leading-order system (3.40). Moreover, because the Jacobian operator $D_x F(0,0)$ is one-to-one and onto, the solution $A^{(0)}$ is actually

in $\ell^2(\mathbb{N})$. By using the implicit function theorem again, for $\epsilon \neq 0$ sufficiently small, there exists a unique solution $A \in \ell^2(\mathbb{N})$ to the system (3.37) satisfying the bound

$$\|A - A^{(0)}\|_{\ell^2(\mathbb{N})} < C''|\epsilon|, \tag{3.41}$$

where the positive constant C'' is ϵ-independent. Combining bounds (3.39), (3.41) with the representation (3.36) yields the bounds (3.34). □

By using the transformation (3.31), we rewrite the expansion (3.22) in the following equivalent form

$$\Delta = \Delta_0 + \Delta_2(\tilde{\phi}) + \Delta_3(\tilde{\phi}) + \Delta_4(\tilde{\phi}), \tag{3.42}$$

where the $\tilde{\phi}$-independent term Δ_0 is given by

$$\Delta_0 := N_1(\rho) + N_2(\rho) + N_3(\rho) + N_4(\rho),$$

the quadratic and cubic parts $\Delta_2(\tilde{\phi})$ and $\Delta_3(\tilde{\phi})$ are ϵ-close to $N_2(\tilde{\phi})$ and $N_3(\tilde{\phi})$, while $\Delta_4(\tilde{\phi}) = N_4(\tilde{\phi})$. The following proposition characterizes each term of the decomposition (3.42). The new definitions of constants override the previous definitions of constants.

Proposition 8. *Fix $\gamma > 0$, $\Omega > \gamma$, and $E \neq \pm E_0$. There exist $\epsilon_0 > 0$ sufficiently small and $C_0, C_1, C_2, C_3, C_4 > 0$ such that for every $\epsilon \in (-\epsilon_0, \epsilon_0)$, we have*

$$|\Delta_0| \leq C_0 \epsilon^2, \tag{3.43}$$

$$\|\tilde{\phi}\|_{l^2} \leq \|\phi\|_{l^2} + C_1 \epsilon, \quad \|\phi\|_{l^2} \leq \|\tilde{\phi}\|_{l^2} + C_1 \epsilon, \tag{3.44}$$

$$\|\Delta_3(\tilde{\phi})\|_{l^2} \leq C_3 \|\tilde{\phi}\|_{l^2}^3, \quad \|\Delta_4(\tilde{\phi})\|_{l^2} \leq C_4 \|\tilde{\phi}\|_{l^2}^4, \tag{3.45}$$

and

$$\Delta_2(\tilde{\phi}) \geq C_2 \|\tilde{\phi}\|_{\ell^2}^2 \quad \text{for every } \tilde{\phi} \in l_c^2(\mathbb{Z}). \tag{3.46}$$

Proof. Since ρ is constructed in Proposition 7 with the $\mathcal{PT}$-symmetric correction term $b = \bar{a}$, it is true that $\rho \in \ell_c^2(\mathbb{Z})$. Therefore, the condition $\phi \in \ell_c^2(\mathbb{Z})$ is satisfied if and only if $\tilde{\phi} \in \ell_c^2(\mathbb{Z})$. Since the constants C_2, C_3, and C_4 in the bounds (3.25) and (3.30) are ϵ-independent, whereas Δ_2, Δ_3, and Δ_4 are ϵ-close to N_2, N_3, and N_4 in space $\ell^2(\mathbb{Z})$, then the bounds (3.45) and (3.46) follow from the bounds (3.25) and (3.30) respectively, thanks to the smallness of ϵ.

In order to obtain the bounds (3.43) and (3.44), we use the bounds (3.15) and (3.34) and obtain

$$|N_1(\rho)| \leq C \sum_{n \in \mathbb{Z} \setminus \{0\}} \epsilon^{2|n|} \leq C' \epsilon^2, \quad \|\rho\|_{l^2}^2 \leq C \left(\epsilon^4 + \sum_{n \in \mathbb{Z} \setminus \{0\}} \epsilon^{2|n|} \right) \leq C' \epsilon^2, \tag{3.47}$$

where the positive constants C, C' are ϵ-independent and ϵ is sufficiently small. Since N_2, N_3, and N_4 are quadratic, cubic, and quartic respectively, the bound (3.43) is obtained from the triangle inequality and the estimates (3.47). The bounds (3.44) follow from the triangle inequality and the second estimate (3.47). □

3.3.5 Time evolution of Δ

We recall that H given by (3.3) is a constant of motion for the $\mathcal{PT}$-symmetric dNLS equation (3.1). On the other hand, the part of Q at $n = 0$ satisfies the balance equation

$$i \frac{d}{dt} \left(u_0 \bar{v}_0 + \bar{u}_0 v_0 \right) = \epsilon \left[\bar{u}_0 (u_1 + u_{-1}) - u_0 (\bar{u}_1 + \bar{u}_{-1}) + \bar{v}_0 (v_1 + v_{-1}) - v_0 (\bar{v}_1 + \bar{v}_{-1}) \right]. \tag{3.48}$$

If the initial data $\psi(0) \in l^2(\mathbb{Z})$ is close to Φ in the sense of the bound $\|\psi(0) - \Phi\|_{\ell^2} \leq \delta$, then the unique solution $\psi(t) \in C^1(\mathbb{R}, l^2(\mathbb{Z}))$ to the $\mathcal{PT}$-symmetric dNLS equation (3.1) with the same initial data can be defined in the modulation form

$$\psi(t) = e^{-i\alpha(t)\sigma} \left[\Phi + \phi(t) \right], \tag{3.49}$$

as long as the solution remains close to the orbit of Φ under the phase rotation in the sense of the bound (3.9). Note again that the vectors ψ, Φ, and ϕ are extended 4-component vectors at each lattice site compared to the 2-component vectors used in the formulation of Theorem 11. As a result, the gauge symmetry is represented by the matrix operator σ defined by (3.28).

The decomposition (3.49) is defined uniquely only if a constraint is imposed to $\phi(t) \in \ell^2(\mathbb{R})$. In agreement with the definition (3.29) on the constrained space $\ell^2_c(\mathbb{R})$, we impose the orthogonality condition:

$$\langle \sigma\Phi, \phi(t) \rangle_{l^2} = 0. \tag{3.50}$$

The decomposition (3.49) under the orthogonality condition (3.50) and the modulation equation for α are justified in the next section. Here we estimate how the time-dependent energy quantity Δ changes along the solution $\psi(t) \in C^1(\mathbb{R}, l^2(\mathbb{Z}))$ represented by the decomposition (3.49).

The rate of change of Δ defined by (3.21) along the solution $\psi(t)$ represented by (3.49) is obtained from (3.48) as follows:

$$\left| \frac{d\Delta}{dt} \right| \leq C_E \epsilon \|\Phi_0 + \phi_0\| \left(\|\Phi_1 + \phi_1\| + \|\Phi_{-1} + \phi_{-1}\| \right) \tag{3.51}$$

where C_E is a positive ϵ-independent constant. By using the bounds (3.15) and (3.34), the transformation (3.31), and the triangle inequality (3.44), we obtain from (3.51):

$$\begin{aligned} \left| \frac{d\Delta}{dt} \right| &\leq C_E \epsilon \left(1 + \|\tilde{\phi}_0\| \right) \left(\epsilon + \|\tilde{\phi}_1\| + \|\tilde{\phi}_{-1}\| \right) \\ &\leq C'_E \epsilon \left(\epsilon + \|\tilde{\phi}_0\| + \|\tilde{\phi}_1\| + \|\tilde{\phi}_{-1}\| + \|\tilde{\phi}_0\|^2 + \|\tilde{\phi}_1\|^2 + \|\tilde{\phi}_{-1}\|^2 \right), \end{aligned} \tag{3.52}$$

where C'_E is another positive ϵ-independent constant.

Let us now define a ball in the space $\ell^2_c(\mathbb{Z})$ of a finite size $K > 0$ by

$$\mathcal{M}_K := \left\{ \phi \in \ell^2_c(\mathbb{Z}) : \quad \|\phi\|_{\ell^2} \leq K \right\}. \tag{3.53}$$

From estimates (3.45) and (3.46), there is a positive K-dependent constant C_K such that

$$\Delta - \Delta_0 \geq C_K \|\tilde{\phi}\|^2_{\ell^2} \quad \text{for every } \tilde{\phi} \in \mathcal{M}_K. \tag{3.54}$$

By using coercivity (3.54) in the ball $\mathcal{M}_K$ and the Young inequality

$$|ab| \leq \frac{\alpha}{2} a^2 + \frac{1}{2\alpha} b^2, \quad a, b \in \mathbb{R},$$

where $\alpha \in \mathbb{R}^+$ is arbitrary, we estimate

$$\|\tilde{\phi}_0\| + \|\tilde{\phi}_1\| + \|\tilde{\phi}_{-1}\| \leq \sqrt{C_K^{-1}(\Delta - \Delta_0)} \leq \frac{\alpha}{2C_K} + \frac{1}{2\alpha}(\Delta - \Delta_0),$$

where $\Delta - \Delta_0 \geq 0$ follows from (3.54). Substituting this estimate to (3.52) yields

$$\left| \frac{d\Delta}{dt} \right| \leq C_E \epsilon \left(\epsilon + \alpha + (\Delta - \Delta_0) + \alpha^{-1}(\Delta - \Delta_0) \right), \tag{3.55}$$

for another constant $C_E > 0$. In what follows, we will set the scaling parameter α such that $\alpha \to 0$ as $\epsilon \to 0$. Therefore, the constant α^{-1} is much larger compared to unity. Integrating (3.55) with an

integrating factor,

$$\left| \frac{d}{dt} e^{-C_E \epsilon \alpha^{-1} t} (\Delta - \Delta_0) \right| \leq C_E \epsilon (\epsilon + \alpha) e^{-C_E \epsilon \alpha^{-1} t},$$

we obtain with the Gronwall's inequality:

$$\begin{aligned} \Delta(t) - \Delta_0 &\leq e^{C_E \epsilon \alpha^{-1} t} \left(\Delta(0) - \Delta_0 + C_E \epsilon (\epsilon + \alpha) \int_0^t e^{-C_E \epsilon \alpha^{-1} s} ds \right) \\ &\leq e^{C_E \epsilon \alpha^{-1} t} \left(\Delta(0) - \Delta_0 + \alpha(\epsilon + \alpha) \right). \end{aligned} \tag{3.56}$$

It is clear from the estimate (3.56) that $\Delta(t) - \Delta_0$ is small only if $\alpha \to 0$ as $\epsilon \to 0$. If $\alpha = \epsilon$, then

$$\alpha = \epsilon : \quad \Delta(t) - \Delta_0 \leq e^{C_E t} \left(\Delta(0) + C_0 \epsilon^2 \right),$$

where the bound (3.43) has been used and C_0 is an ϵ-independent constant. Therefore, if $\Delta(0)$ is small, then $\Delta(t)$ remains small on the time scale $t = \mathcal{O}(1)$ as $\epsilon \to 0$. On the other hand, if $\alpha = \epsilon^{1/2}$, then the estimate (3.56) yields

$$\alpha = \epsilon^{1/2} : \quad \Delta(t) - \Delta_0 \leq e^{C_E \epsilon^{1/2} t} \left(\Delta(0) + C_0 \epsilon \right),$$

so that $\Delta(t)$ remains small on the time scale $t = \mathcal{O}(\epsilon^{-1/2})$.

The initial value for $\Delta(0)$ is estimated from (3.42), (3.43), and (3.44). By (3.44), for every $\phi(0) \in \mathcal{M}_\delta$ with $\delta > 0$ sufficiently small, we have $\tilde{\phi}(0) \in \mathcal{M}_K$ with $K = \delta + \epsilon$ and there are positive (ϵ,δ)-independent constants C, C' such that

$$|\Delta(0)| \leq C \left(\epsilon^2 + \|\tilde{\phi}(0)\|_{\ell^2}^2 \right) \leq C'(\epsilon^2 + \delta^2). \tag{3.57}$$

By using the triangle inequality (3.44), coercivity (3.54), and the bound (3.57), we finally obtain the following two estimates:

$$\alpha = \epsilon : \quad \|\phi(t)\|_{\ell^2}^2 \leq C e^{C_E t} \left(\epsilon^2 + \delta^2 \right)$$

and

$$\alpha = \epsilon^{1/2} : \quad \|\phi(t)\|_{\ell^2}^2 \leq C e^{C_E \epsilon^{1/2} t} \left(\epsilon + \delta^2 \right),$$

where the positive constant C is independent of ϵ and δ. Comparing with the bound (3.9) stated in Theorem 11, we obtain

$$\alpha = \epsilon, \quad t_0 \lesssim 1 : \quad C(\epsilon + \delta) \leq \nu \tag{3.58}$$

and

$$\alpha = \epsilon^{1/2}, \quad t_0 \lesssim \epsilon^{-1/2} : \quad C \left(\epsilon^{1/2} + \delta \right) \leq \nu, \tag{3.59}$$

where t_0 is the final time in the bound (3.9) and C is another positive (ϵ,δ)-independent constant. For every $\nu > 0$, there exist $\epsilon_0 > 0$ and $\delta > 0$ such that inequalities (3.58) and (3.59) can be satisfied for every $\epsilon \in (0, \epsilon_0)$. The statement of Theorem 11 is formulated on the extended time scale corresponding to the inequality (3.59). The short time scale corresponding to the inequality (3.58) is mentioned in Remark 14.

3.3.6 Modulation equations in $\ell^2_c(\mathbb{Z})$

It remains to show how we can define the decomposition (3.49) under the constraint (3.50) for a solution to the $\mathcal{PT}$-symmetric dNLS equation (3.1) and how the evolution of α in time t can be estimated from the modulation equation. Here we modify standard results on modulation equations, see, e.g., Lemmas 6.1 and 6.3 in [56] for similar analysis. For reader's convenience, we only give the main ideas behind the proofs.

Proposition 9. *There exist constants $\nu_0 \in (0,1)$ and $C_0 \geq 1$ such that, for any $\psi \in l^2(\mathbb{Z})$ satisfying*

$$d := \inf_{\alpha \in \mathbb{R}} \|e^{i\alpha\sigma}\psi - \Phi\|_{l^2} \leq \nu_0, \tag{3.60}$$

one can find modulation parameter $\alpha \in \mathbb{R}/(2\pi\mathbb{Z})$ such that $\psi = e^{-i\alpha\sigma}(\Phi+\phi)$ with $\phi \in \ell^2_c(\mathbb{Z})$ satisfying $d \leq \|\phi\|_{l^2} \leq C_0 d$.

Proof. We consider a function $f : \mathbb{R} \to \mathbb{R}$ given by

$$f(\alpha) := \langle \sigma\Phi, e^{i\alpha\sigma}\psi - \Phi\rangle_{\ell^2} = 0.$$

Let $\alpha_0 \in \mathbb{R}/(2\pi\mathbb{Z})$ be the argument of the infimum in (3.60). Then, $|f(\alpha_0)| \leq d\|\Phi\|_{\ell^2}$ by the Cauchy–Schwartz inequality. On the other hand, the derivative $f'(\alpha_0)$ is bounded away from zero because

$$f'(\alpha_0) = \langle \sigma\Phi, i\sigma e^{i\alpha_0\sigma}\psi\rangle_{\ell^2} = i\|\Phi\|^2_{\ell^2} + i\langle \Phi, e^{i\alpha_0\sigma}\psi - \Phi\rangle_{\ell^2},$$

where the second term is bounded by $d\|\Phi\|_{\ell^2}$ and the first term is d-independent. The function $f : \mathbb{R} \to \mathbb{R}$ is smooth in α. By the implicit function theorem, for any $d > 0$ sufficiently small, there is a unique solution of the equation $f(\alpha) = 0$ for α near α_0 such that $|\alpha - \alpha_0| \leq Cd$, where C is d-independent. By the triangle inequality, $\|\phi\|_{l^2} \leq C_0 d$, where C_0 is also d-independent. □

Proposition 10. *Assume that the solution $\psi(t)$ to the $\mathcal{PT}$-symmetric dNLS equation (3.1) satisfies $d(t) \leq \nu$ for every $t \in [0, t_0]$, where $d(t)$ is given by (3.60). Then the modulation parameter $\alpha(t)$ defined by (3.49) in Proposition 9 is a continuously differentiable function of t and there is a positive constant C such that $|\dot{\alpha} - E| \leq C\nu$, for every $t \in [0, t_0]$.*

Proof. Let $\psi(t) \in C^1(\mathbb{R}, l^2(\mathbb{Z}))$ be a solution to the $\mathcal{PT}$-symmetric dNLS equation (3.1). Substituting the decomposition (3.49) into the $\mathcal{PT}$-symmetric dNLS equation (3.1), we obtain the evolution equation in the form

$$i\dot{\phi} = \mathcal{S}\mathcal{H}''_E\phi + (E - \dot{\alpha})\sigma(\Phi + \phi) + N(\phi), \tag{3.61}$$

where the bounded invertible operator $\mathcal{S} : \ell^2(\mathbb{Z}) \to \ell^2(\mathbb{Z})$ represents the symplectic structure (3.2) of the $\mathcal{PT}$-symmetric dNLS equation (3.1), $N(\phi)$ contains quadratic and cubic terms in ϕ, and the gauge invariance of the $\mathcal{PT}$-symmetric dNLS equation (3.1) has been used. From the condition (3.50), projecting the evolution equation (3.61) to $\sigma\Phi$ yields

$$\dot{\alpha} - E = \frac{\langle \mathcal{H}''_E\mathcal{S}\sigma\Phi, \phi\rangle_{\ell^2} + \langle \sigma\Phi, N(\phi)\rangle_{\ell^2}}{\|\Phi\|^2_{\ell^2} + \langle \Phi, \phi\rangle_{\ell^2}}. \tag{3.62}$$

By Proposition 9, if $d(t) \leq \nu$ is sufficiently small for every $t \in [0, t_0]$, then $\|\phi(t)\|_{\ell^2} \leq C_0 d(t)$ for a positive constant C_0. Then, the denominator in (3.62) is bounded away from zero, whereas the numerator is bounded by $Cd(t)$, which yields the bound $|\dot{\alpha} - E| \leq C\nu$, for every $t \in [0, t_0]$. □

Chapter 4

Krein signature in Hamiltonian Systems

4.1 Background

We consider the prototypical example of the one-dimensional Gross-Pitaevskii (GP) equation arising in the context of cigar-shaped Bose–Einstein (BEC) condensates [116, 119]. The model takes the form of the following defocusing nonlinear Schrödinger (NLS) equation with a harmonic potential [31, 76]:

$$i\partial_t u = -\partial_x^2 u + V(x)u + |u|^2 u, \tag{4.1}$$

where u represents the complex wave function and V characterizes the external potential. The probability density of finding atoms at a given location and time is characterized by $|u|^2$.

In the case of magnetic trapping of the BECs [116, 119], the potential V is real-valued and is given by

$$V(x) = \Omega^2 x^2, \tag{4.2}$$

where Ω is the ratio of longitudinal to transverse confinement strengths of the parabolic trapping. The NLS equation (4.1) with the potential (4.2) is a Hamiltonian system written in the symplectic form

$$i\frac{\partial u}{\partial t} = \frac{\delta H}{\delta \bar{u}}, \tag{4.3}$$

where H is the following real-valued Hamiltonian function

$$H(u) = \int_{\mathbb{R}} \left[|\partial_x u|^2 + V(x)|u|^2 + \frac{1}{2}|u|^4 \right] dx. \tag{4.4}$$

In the setting of the NLS equation (4.1) with the potential (4.2), the linear Hamiltonian system can be formulated as the spectral problem

$$J\mathcal{L}v = \lambda v, \tag{4.5}$$

where $\mathcal{L}$ is a self-adjoint unbounded operator in the space of square-integrable functions $L^2(\mathbb{R})$ with a dense domain in $L^2(\mathbb{R})$ and J is a skew-adjoint bounded operator in $L^2(\mathbb{R})$. The operators $\mathcal{L}$ and J are assumed to satisfy $J^2 = -I$ and $J\mathcal{L} + \bar{\mathcal{L}}\bar{J} = 0$, thanks to the Hamiltonian symmetry.

If $\lambda_0 \in \mathbb{C}$ is an eigenvalue of the spectral problem (4.5), then it is neutrally stable if $\text{Re}(\lambda_0) = 0$ and unstable if $\text{Re}(\lambda_0) > 0$. Thanks to the Hamiltonian symmetry of $\mathcal{L}$ and J, the eigenvalues appear in symmetric pairs relative to the axis $\text{Re}(\lambda) = 0$. Indeed, if v is an eigenvector of the spectral problem (4.5) for the eigenvalue λ, then $w = -J\bar{v}$ is an eigenvector of the same spectral problem (4.5) with the eigenvalue $-\bar{\lambda}$. Indeed, substituting $v = \bar{J}\bar{w}$ into (4.5) yields

$$J\mathcal{L}\bar{J}\bar{w} = \lambda\bar{J}\bar{w} \quad \Leftrightarrow \quad \bar{\mathcal{L}}\bar{w} = \lambda\bar{J}\bar{w} \quad \Leftrightarrow \quad \bar{J}\bar{\mathcal{L}}\bar{w} = -\lambda\bar{w} \quad \Leftrightarrow \quad J\mathcal{L}w = -\bar{\lambda}w.$$

Definition 13. *For a nonzero eigenvalue $\lambda_0 \in \mathbb{C}$ of the spectral problem (4.5) with the eigenvector v_0 in the domain of $\mathcal{L}$, we define the Krein quantity $K(\lambda_0)$ by*

$$K(\lambda_0) := \langle \mathcal{L}v_0, v_0 \rangle, \tag{4.6}$$

where $\langle \cdot, \cdot \rangle$ is the standard inner product in $L^2(\mathbb{R})$.

Proposition 11. *Krein quantity in (4.6) satisfies the following properties:*

1. *$K(\lambda_0)$ is real if $\lambda_0 \in i\mathbb{R}$.*
2. *$K(\lambda_0)$ is nonzero if $\lambda_0 \in i\mathbb{R}\backslash\{0\}$ is simple.*
3. *$K(\lambda_0)$ is zero if $\lambda_0 \in \mathbb{C}\backslash\{i\mathbb{R}\}$.*

The Krein signature is defined as the sign of the Krein quantity $K(\lambda_0)$ for a simple neutrally stable eigenvalue $\lambda_0 \in i\mathbb{R}\backslash\{0\}$. If parameters of the NLS equation (4.1) change, parameters of the spectral problem (4.5) change, however, the simple eigenvalue $\lambda_0 \in i\mathbb{R}$ remains on the axis $\text{Re}(\lambda) = 0$ unless it coalesces with another eigenvalue or a part of the continuous spectrum, thanks to the preservation of its multiplicity and the Hamiltonian symmetry of eigenvalues. In this case, the eigenvalue λ_0 and its Krein quantity $K(\lambda_0)$ are at least continuous functions of the parameters of the NLS equation (4.1).

It is quite typical in the parameter continuations of the spectral problem (4.5) to see that the simple eigenvalue $\lambda_0 \in i\mathbb{R}$ coalesces at a bifurcation point with another simple eigenvalue $\lambda_0' \in i\mathbb{R}$ and that both eigenvalues split into the complex plane as unstable eigenvalues past the bifurcation point. The Krein signature is a helpful tool towards predicting this instability bifurcation in the sense of the following necessary condition.

Theorem 12 (Necessary condition for instability bifurcation.)**.** *Under some non-degeneracy constraints, the double eigenvalue $\lambda_0 = \lambda_0' \in i\mathbb{R}$ of the spectral problem (4.5) with a bifurcation parameter $\varepsilon \in \mathbb{R}$ splits into a pair of complex eigenvalues symmetric relative to $\text{Re}(\lambda) = 0$ for $\varepsilon > 0$ only if there exist two simple eigenvalues $\lambda_0, \lambda_0' \in i\mathbb{R}$ with the opposite Krein signature for $\varepsilon < 0$.*

In other words, if two neutrally stable eigenvalues of the same Krein signature move towards each other in the parameter continuation of the spectral problem (4.5), then their coalescence will not result in the onset of instability, whereas if the two neutrally stable eigenvalues have the opposite Krein signature, their coalescence is likely to result in the onset of instability, subject to technical non-degeneracy constraints.

The concept of Krein signature in the infinite-dimensional setting, e.g. for the NLS equation, was introduced independently in works [68, 107]. It was justified in a number of mathematical publications [38, 70] and it remains a practical tool to trace instability bifurcations in physically relevant Hamiltonian systems [113, 130] (see review in [83]).

The purpose of this Chapter is to explain definitions and properties of the Krein signature on the prototypical example of the NLS equation (4.1) with the potential (4.2).

4.2 Krein signature for the NLS equation

In the context of the NLS equation (4.1) with the potential (4.2), we consider the nonlinear stationary states of the form $u(x,t) = e^{-i\mu t}\phi(x)$, where $\mu \in \mathbb{R}$ is referred to as the chemical potential [45] and the real-valued function ϕ satisfies the differential equation

$$\mu\phi(x) = -\phi''(x) + x^2\phi(x) + \phi(x)^3, \tag{4.7}$$

where we have set $\Omega = 1$ without loss of generality. In the linear (small-amplitude) limit, we obtain the quantum harmonic oscillator with the eigenvalues $\mu_n = 1 + 2n$, $n \in \mathbb{N}_0 := \{0, 1, 2, ...\}$ and the L^2-normalized eigenfunctions

$$\varphi_n(x) = \frac{1}{\sqrt{2^n n!\sqrt{\pi}}} H_n(x) e^{-x^2/2}, \tag{4.8}$$

where H_n is the Hermite polynomial of degree n, e.g., $H_0(x) = 1$, $H_1(x) = 2x$, $H_2(x) = 4x^2 - 2$, etc.

Each eigenfunction φ_n for a simple eigenvalue μ_n generates a branch of solutions bifurcating in the stationary problem (4.7). This follows from the general Crandall–Rabinowitz bifurcation theory [41] and is generally used in physics community, see, e.g., [51, 143]. Each branch can be approximated by the following expansion in terms of the small parameter ϵ:

$$\begin{cases} \mu = \mu_n + \epsilon^2 \mu_n^{(2)} + \ldots, \\ \phi = \epsilon\varphi_n + \epsilon^3 \varphi_n^{(3)} + \ldots, \end{cases} \tag{4.9}$$

where (μ_n, φ_n) is the n-th eigenvalue–eigenfunction pair, $(\mu_n^{(2)}, \varphi_n^{(3)})$ are the next-order correction terms to be found, and the dots denote the higher-order corrections terms. The n-th branch of the nonlinear stationary states is smooth with respect to the small parameter ϵ, which parameterizes both μ and ϕ, whereas it has a square-root singularity when it is written in terms of the parameter $\mu - \mu_n$.

The formal solvability condition for the correction terms $(\mu_n^{(2)}, \varphi_n^{(3)})$ yields

$$\mu_n^{(2)} = \int_{\mathbb{R}} \varphi_n(x)^4 dx > 0, \tag{4.10}$$

which implies that the branch of nonlinear stationary states extends towards $\mu > \mu_n$. The limit $\mu \to \infty$ can be rescaled as the semi-classical limit of the stationary NLS equation. Each n-th branch of the nonlinear stationary states is uniquely extended to the limit $\mu \to \infty$, where it is matched with the asymptotic approximation involving bound states of n dark solitons on the background of V in (4.2) [40, 106].

When considering the stability of the nonlinear stationary state of the form $u(x,t) = e^{-i\mu t}\phi(x)$, we linearize the NLS equation (4.1) with the expansion

$$u(x,t) = e^{-i\mu t}\left[\phi(x) + \delta\left(a(x)e^{-\lambda t} + \bar{b}(x)e^{-\bar{\lambda} t}\right) + \ldots\right], \tag{4.11}$$

where δ is a formal small parameter. To the leading order in δ, the eigenvalue–eigenvector pair (λ, v) with $v = (a,b)^T$ is found from the spectral problem

$$\mathcal{L}v = -i\lambda\sigma_3 v, \tag{4.12}$$

where $\sigma_3 = \text{diag}(1,-1)$ and the linear operator $\mathcal{L}$ is written in the differential form:

$$\mathcal{L} = \begin{bmatrix} -\partial_x^2 + x^2 - \mu + 2\phi(x)^2 & \phi(x)^2 \\ \phi(x)^2 & -\partial_x^2 + x^2 - \mu + 2\phi(x)^2 \end{bmatrix}. \tag{4.13}$$

The operator $\mathcal{L}$ is extended to a self-adjoint operator in $L^2(\mathbb{R})$ with the domain $H^2(\mathbb{R}) \cap L^{2,2}(\mathbb{R})$ (see [62], Ch. 4, p.37), where $H^2(\mathbb{R})$ is the Sobolev space of square integrable functions and their second derivatives and $L^{2,2}(\mathbb{R})$ is the space of square integrable functions multiplied by $(1+x^2)$. The spectrum of $\mathcal{L}$ is purely discrete (see [121], Ch. XIII, Theorem 16 on p.120).

The spectral problem (4.12) takes the abstract form (4.5) with the self-adjoint operator $\mathcal{L}$ given by (4.13) and the skew-symmetric operator $J = i\sigma_3$. The Hamiltonian symmetry $J^2 = -I$ and $J\mathcal{L} + \bar{\mathcal{L}}\bar{J} = 0$ (or, equivalently, $\sigma_3\mathcal{L} = \bar{\mathcal{L}}\sigma_3$) is satisfied. The eigenvalues are symmetric relative to the imaginary axis. To be precise, if λ_0 is an eigenvalue with the eigenvector $v_0 = (a,b)^T$, then $-\overline{\lambda}_0$ is another eigenvalue with the eigenvector $\sigma_3\bar{v}_0 = (\overline{a}, -\overline{b})^T$ by the Hamiltonian symmetry $\sigma_3\mathcal{L} = \bar{\mathcal{L}}\sigma_3$.

In addition to the Hamiltonian symmetry, the operator $\mathcal{L}$ in (4.13) satisfies $\sigma_1\mathcal{L} = \bar{\mathcal{L}}\sigma_1$, which implies that the eigenvalues are symmetric relative to the real axis. Indeed, if λ_0 is an eigenvalue with the eigenvector $v_0 = (a,b)^T$, then $\bar{\lambda}_0$ is another eigenvalue with the eigenvector $\sigma_1\bar{v}_0 = (\bar{b}, \bar{a})$. Hence, the unstable eigenvalues with $\text{Re}(\lambda_0) > 0$ occur either as pairs on the real axis or as quadruplets in the complex plane, whereas the neutrally stable eigenvalues with $\text{Re}(\lambda_0) = 0$ occur as pairs on the imaginary axis.

For each nonzero eigenvalue $\lambda_0 \in \mathbb{C}$ of the spectral problem (4.12) with the eigenvector $v_0 = (a,b)^T \in H^2(\mathbb{R}) \cap L^{2,2}(\mathbb{R})$, the Krein quantity $K(\lambda_0)$ introduced in (4.6) can be written explicitly as

follows:

$$K(\lambda_0) = \langle \mathcal{L} v_0, v_0 \rangle = -i\lambda_0 \langle \sigma_3 v_0, v_0 \rangle = -i\lambda_0 \int_{\mathbb{R}} (|a(x)|^2 - |b(x)|^2) dx. \tag{4.14}$$

If $K(\lambda_0)$ is nonzero and real, the sign of $K(\lambda_0)$ is referred to as the Krein signature. In what follows, we only consider eigenvalues with $\lambda_0 \in i\mathbb{R}_+$, for which $-i\lambda_0 > 0$.

Let us verify the three main properties of the Krein quantity $K(\lambda_0)$.

Proof of Proposition 11.

1. If $\lambda_0 \in i\mathbb{R}$, then $(-i\lambda_0) \in \mathbb{R}$. The integral in (4.14) is also real. Hence, $K(\lambda_0)$ is real.

2. Let us write the eigenvalue problem (4.13) for the generalized eigenvector v_g:

$$(\mathcal{L} + i\lambda_0 \sigma_3) v_g = \sigma_3 v_0. \tag{4.15}$$

   If $\lambda_0 \in i\mathbb{R}\backslash\{0\}$, then v_0 is in the kernel of the adjoint operator $(\mathcal{L} + i\lambda_0\sigma_3)^*$, and Fredholm solvability condition of the above equation is $\langle \sigma_3 v_0, v_0 \rangle = 0$. If $K(\lambda_0) = 0$, then there exists a solution to the nonhomogeneous equation (4.15), so that λ_0 is not simple. Hence, $K(\lambda_0) \neq 0$.

3. Using self-adjoint property of $\mathcal{L}$, one can write

$$\langle \mathcal{L} v_0, v_0 \rangle = \langle v_0, \mathcal{L} v_0 \rangle,$$

   which can be expanded as

$$-i\lambda_0 \langle \sigma_3 v_0, v_0 \rangle = i\bar{\lambda}_0 \langle v_0, \sigma_3 v_0 \rangle,$$

   where the equality holds either for $\lambda_0 \in i\mathbb{R}$ or $\langle \sigma_3 v_0, v_0 \rangle = 0$. Hence $K(\lambda_0) = 0$ for $\lambda_0 \notin i\mathbb{R}$.

□

Let us now illustrate how the Krein signatures can be used to predict instability bifurcations from multiple neutrally stable eigenvalues of the spectral problem (4.12). We restrict consideration to the small-amplitude limit. If $\epsilon = 0$ and $\mu = \mu_n$, the linear operator (4.13) becomes diagonal:

$$\mathcal{L}_0 = \begin{bmatrix} -\partial_x^2 + x^2 - \mu_n & 0 \\ 0 & -\partial_x^2 + x^2 - \mu_n \end{bmatrix} \tag{4.16}$$

and the eigenvalues are located at $\sigma(\mathcal{L}_0) = \{2(m-n), \ \ m \in \mathbb{N}_0\}$, where $n \in \mathbb{N}_0$ is fixed. Because of the skew-symmetric operator $J = i\sigma_3$ in the right-hand side of the spectral problem (4.12), these eigenvalues are mapped to the imaginary axis in the pairs $\lambda \in \pm i\{2(m-n), \ m \in \mathbb{N}_0\}$.

If $n = 0$, the ground state branch (4.9) leads to a double zero eigenvalue and a set of simple eigenvalues in pairs $\lambda \in \pm i\{2m, \ m \in \mathbb{N}_0\backslash\{0\}\}$. The double zero eigenvalue is preserved in ϵ due to gauge symmetry, whereas the simple neutrally stable eigenvalues are preserved on the imaginary axis due to Hamiltonian symmetry (at least for small ϵ). Moreover, each eigenvalue has a positive Krein signature, therefore, by the necessary condition for instability bifurcations, no complex eigenvalue

quartets can arise in parameter continuations of solutions to the spectral problem (4.12) in ϵ. These spectral stability properties are natural for the ground state solution.

If $n = 1$, the first excited state branch (4.9) associated with a single dark soliton [40, 106] leads to a double zero eigenvalue, a pair of double eigenvalues $\lambda = \pm 2i$, and a set of simple eigenvalues in pairs $\lambda \in \pm i\{2(m-1),\ m \in \mathbb{N}_0 \backslash \{0, \pm 1\}\}$. The double zero eigenvalue is again preserved in ϵ due to gauge symmetry but the pair of nonzero double eigenvalues $\lambda = \pm 2i$ may split if $\epsilon \neq 0$. Note that two linearly independent eigenvectors exist for $\lambda_0 = 2i$:

$$v_1 = \begin{bmatrix} \varphi_2 \\ 0 \end{bmatrix}, \quad v_2 = \begin{bmatrix} 0 \\ \varphi_0 \end{bmatrix}. \tag{4.17}$$

The two eigenvectors induce opposite Krein signatures for the coalescent double eigenvalue since $K(\lambda_0) > 0$ for v_1 and $K(\lambda_0) < 0$ for v_2. Therefore, by the necessary condition on the splitting of the double eigenvalues, we may anticipate unstable eigenvalues for small ϵ.

Similarly, if $n = 2$, the second excited state branch (4.9) associated with two dark solitons [40, 106] leads to a double zero eigenvalue, two pairs of double eigenvalues $\lambda = \pm 2i$ and $\lambda = \pm 4i$, and a set of simple eigenvalues in pairs $\lambda \in \pm i\{2(m-2),\ \ m \in \mathbb{N}_0 \backslash \{0, \pm 1, \pm 2\}\}$. The double zero eigenvalue is again preserved in ϵ due to gauge symmetry but the pairs of nonzero double eigenvalues $\lambda = \pm 2i$ and $\lambda = \pm 4i$ may split if $\epsilon \neq 0$. Note that two linearly independent eigenvectors exist as follows:

$$\lambda_0 = 2i: \quad v_1 = \begin{bmatrix} \varphi_3 \\ 0 \end{bmatrix}, \quad v_2 = \begin{bmatrix} 0 \\ \varphi_1 \end{bmatrix} \tag{4.18}$$

and

$$\lambda_0 = 4i: \quad v_1 = \begin{bmatrix} \varphi_4 \\ 0 \end{bmatrix}, \quad v_2 = \begin{bmatrix} 0 \\ \varphi_0 \end{bmatrix}. \tag{4.19}$$

Again, the two eigenvectors induce opposite Krein signatures for each coalescent double eigenvalue, hence by the necessary condition on the splitting of the double eigenvalues, we may anticipate unstable eigenvalues for small ϵ.

In order to compute definite predictions whether or not the double eigenvalues produce instability bifurcations for the first and second excited states, we shall proceed using perturbation theory arguments. We substitute expansion (4.9) into the spectral problem (4.12) and expand it into powers of ϵ^2 as follows:

$$(\mathcal{L}_0 + \epsilon^2 \mathcal{L}_1 + \ldots)v = -i\lambda\sigma_3 v, \tag{4.20}$$

where

$$\mathcal{L}_1 = \begin{bmatrix} 2\varphi_n(x)^2 - \mu_n^{(2)} & \varphi_n(x)^2 \\ \varphi_n(x)^2 & 2\varphi_n(x)^2 - \mu_n^{(2)} \end{bmatrix}. \tag{4.21}$$

Let $-i\lambda = \omega_0 + \epsilon^2\omega_1 + \ldots$, where ω_0 is a coalescent double eigenvalue and ω_1 is a correction term. Representing $v = c_1 v_1 + c_2 v_2 + \ldots$ and projecting the perturbed spectral problem (4.20) to

the eigenvectors v_1 and v_2 yield the matrix eigenvalue problem

$$M \begin{bmatrix} c_1 \\ c_2 \end{bmatrix} = \omega_1 \sigma_3 \begin{bmatrix} c_1 \\ c_2 \end{bmatrix}, \tag{4.22}$$

where $M_{ij} = \langle \mathcal{L}_1 v_i, v_j \rangle$, $1 \leq i, j \leq 2$, and the L^2 normalization of eigenvectors has been taken into account.

Let us consider the first excited state $n = 1$ bifurcating from $\mu_1 = 3$. For $\epsilon = 0$, the eigenvalue at $\omega_0 = 2$ is double with two eigenvectors (4.17). However, there exists a linear combination of v_1 and v_2 which produces the so-called dipolar oscillation (also known as the Kohn mode, see explicit solutions in [77]) and thus the eigenvalue at $\omega_0 = 2$ related to this linear combination is independent of the variations of the chemical potential in ϵ. The shift of the eigenvalue for another linear combination of v_1 and v_2 has been the subject of intense scrutiny as it is associated with the oscillation frequency of the dark soliton in the parabolic trap [28, 109].

By using (4.10) for $n = 1$, we find $\mu_1^{(2)} = 3/(4\sqrt{2\pi})$. The matrix M in the matrix eigenvalue problem (4.22) is computed explicitly as

$$M = \begin{bmatrix} \frac{1}{8\sqrt{2\pi}} & \frac{1}{8\sqrt{\pi}} \\ \frac{1}{8\sqrt{\pi}} & \frac{1}{4\sqrt{2\pi}} \end{bmatrix}. \tag{4.23}$$

Computations of eigenvalues of the matrix eigenvalue problem (4.22) yield 0 and $-1/(8\sqrt{2\pi})$. The zero eigenvalue corresponds to the dipolar oscillations. The nonzero eigenvalue near $\omega_0 = 2$ is given by the following expansion:

$$\omega = 2 - \frac{1}{6}(\mu - 3) + \ldots \tag{4.24}$$

Numerical results on the top left panel of Figure 4.1 confirm this prediction. The smallest nonzero eigenvalue remains below $\omega_0 = 2$ and approaches $\omega \to \sqrt{2}$ as $\mu \to \infty$, in agreement with the previous results [28, 109].

It is relevant to indicate that the asymptotic limit of the eigenfrequencies of the ground state solution with $n = 0$ can be computed in the limit of large μ [132] (see also [77] for a recent account of the relevant analysis). These modes include the so-called dipolar oscillation, quadrupolar oscillation, etc. (associated, respectively, to $m = 1$, $m = 2$, etc.) and the corresponding eigenfrequencies are given by the analytical expression in the limit $\mu \to \infty$:

$$\omega_m = \sqrt{2m(m+1)}, \quad m \in \mathbb{N}. \tag{4.25}$$

We can see from the top left panel of Fig. 4.1 that these frequencies of the ground state solution are present in the linearization of the first excited state in addition to the eigenfrequency $\omega_* = \sqrt{2}$, which corresponds to the oscillation of the dark soliton inside the trap.

While the example of the first excited state is instructive, it does not show any instability bifurcations due to coalescence of eigenvalues of the opposite Krein signatures. This is because although the eigenfrequency at $\omega_0 = 2$ is double, the dipolar oscillations do not allow the manifestation of an

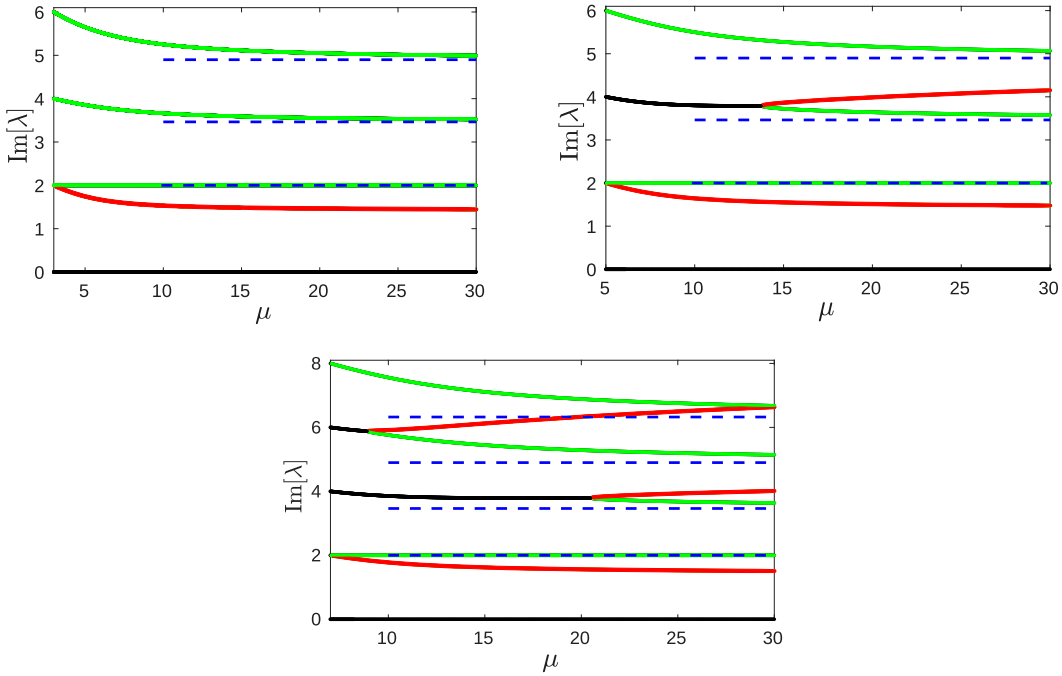

Figure 4.1: The top left panel corresponds to the case of the first excited state, the top right one corresponds to the second excited state, while the bottom panel corresponds to the third excited state. Eigenvalues of negative (positive) Krein signature are shown in red (green), complex eigenvalues are shown in black. For the first excited state, only the lowest nonzero eigenfrequency has a negative Krein signature (but its linear degeneracy with a symmetry mode yields no instability). For the second excited state, there are two degenerate modes at 2 and 4. Only the latter yields the quartet of complex eigenvalues. For the third excited states, there are three degenerate modes at 2, 4, and 6, the last two yield quartets of complex eigenvalues.

instability as a result of resonance. However, the onset of instability can still be found for the other excited states, e.g. for the second excited state corresponding to $n = 2$ bifurcating out of $\mu_2 = 5$.

By using (4.10) for $n = 2$, we find $\mu_2^{(2)} = 41/(64\sqrt{2\pi})$. At $\epsilon = 0$, the eigenvalue at $\omega_0 = 2$ is double with the two eigenvectors (4.18). The dipolar oscillation mode is present again and corresponds to the eigenvalue at $\omega_0 = 2$ independently of the variations of the chemical potential in ϵ. The other eigenvalue at $\omega_0 = 2$ is shifted for small ϵ. The matrix M in the matrix eigenvalue problem (4.22) is computed explicitly as

$$M = \begin{bmatrix} \frac{5}{32\sqrt{2\pi}} & \frac{15}{64\sqrt{3\pi}} \\ \frac{15}{64\sqrt{3\pi}} & \frac{15}{64\sqrt{2\pi}} \end{bmatrix}. \tag{4.26}$$

Computations of eigenvalues of the matrix eigenvalue problem (4.22) yield 0 and $-5/(64\sqrt{2\pi})$. The nonzero eigenvalue near $\omega_0 = 2$ is given by the following expansion:

$$\omega = 2 - \frac{5}{41}(\mu - 5) + \dots \tag{4.27}$$

While the degeneracy at $\omega_0 = 2$ does not lead to the onset of instability, let us consider the

double eigenvalue at $\omega_0 = 4$ with the two eigenvectors (4.19). The matrix M in the matrix eigenvalue problem (4.22) is computed explicitly as

$$M = \begin{bmatrix} \frac{1}{512\sqrt{2\pi}} & \frac{9}{128\sqrt{3\pi}} \\ \frac{9}{128\sqrt{3\pi}} & \frac{7}{64\sqrt{2\pi}} \end{bmatrix}. \tag{4.28}$$

The complex eigenvalues of the matrix eigenvalue problem (4.22) are given by $(-55 \pm 3\sqrt{23}i)/(2048\sqrt{2\pi})$. The complex eigenvalues near $\omega_0 = 4$ are given by the following expansion:

$$\omega = 4 + \frac{-55 \pm 3\sqrt{23}i}{656}(\mu - 5) + \dots \tag{4.29}$$

The eigenvalues remain complex for values of $\mu \gtrsim 5$ but coalesce again on the imaginary axis at $\mu \approx 13.75$ and reappear as pairs of imaginary eigenvalues of the opposite Krein signatures. This reversed instability bifurcation takes place in a complete agreement with the necessary condition for the instability bifurcations.

In the large chemical potential limit, the eigenfrequencies of the linearization at the excited state with $n = 2$ include the same eigenfrequencies of the linearization at the ground state with $n = 0$ given by (4.25), see the top right panel of Fig. 4.1. In addition, two modes with negative Krein signature appear due to the dynamics of the two dark solitary waves on the ground state. One mode represents the in-phase oscillation of the two dark solitons and it is continued from the eigenvalue expanded by (4.27) to the limit $\mu \to \infty$, where it approaches $\omega_* = \sqrt{2}$. The other mode represents the out-of-phase oscillation of the two dark solitons and it appears from the complex pair (4.29) which reappears back on the imaginary axis for higher values of the chemical potential μ. Asymptotic approximation of the out-of-phase oscillation in the limit $\mu \to \infty$ is reported in [40].

This pattern continues for other excited states with $n \geq 3$. The bottom panel on Fig. 4.1 shows the case $n = 3$. For every $n \geq 3$, there are n double eigenvalues with opposite Krein signature at $\epsilon = 0$. If $\epsilon \neq 0$, the lowest double eigenvalue does not lead to instability due to its linear degeneracy with the dipolar symmetry mode. The remaining $n - 1$ double eigenvalues may yield instability bifurcations with complex eigenvalues. For large μ, these eigenvalues reappear on the imaginary axis after the reversed instability bifurcations in agreement with the necessary condition for the instability bifurcation. The n eigenvalues of negative Krein signature characterize n dark solitons on the top of the ground state solution. As such, they provide a rather lucid example of the nature and relevance the negative Krein signature concept. Further details can be found in [40] for the large μ case and in [74] for the small μ case.

Chapter 5

Krein signature in $\mathcal{PT}$-symmetric systems

5.1 Background

In this Chapter, we address the following nonlinear Schrödinger's equation (NLSE) with a general complex potential:

$$i\partial_t\psi + \partial_x^2\psi - (V(x) + i\gamma W(x))\psi + g|\psi|^2\psi = 0, \tag{5.1}$$

where $\gamma \in \mathbb{R}$ is a gain–loss parameter, $g = +1$ ($g = -1$) defines focusing (defocusing) nonlinearity, and the real potentials V and W satisfy the even and odd symmetry, respectively:

$$V(x) = V(-x), \quad W(-x) = -W(x), \quad x \in \mathbb{R}. \tag{5.2}$$

In quantum physics, the complex potential $V+i\gamma W$ is used to describe effects observed when quantum particles are loaded in an open system [32, 45]. The intervals with positive and negative imaginary part correspond to the gain and loss of quantum particles, respectively. When gain exactly matches loss, which happens under the symmetry condition (5.2), the potential $V + i\gamma W$ is $\mathcal{PT}$-symmetric with respect to the parity operator $\mathcal{P}$ and the time reversal operator $\mathcal{T}$, defined in Chapter 1. The NLSE (5.1) is $\mathcal{PT}$-symmetric under the condition (5.2) in the sense that if $\psi(x,t)$ is a solution to (5.1), then

$$\widetilde{\psi}(x,t) = \mathcal{PT}\psi(x,t) = \overline{\psi(-x,-t)}$$

is also a solution to (5.1).

The NLSE (5.1) with a $\mathcal{PT}$-symmetric potential is also used in the paraxial nonlinear optics. In that context, time and space have a meaning of longitudinal and transverse coordinates, and complex potential models the complex refractive index [124]. Another possible application of the NLSE (5.1) is Bose-Einstein condensate, where it models the dynamics of the self-gravitating boson gas trapped in a confining potential V. Intervals, where W is positive and negative, allow one to compensate atom injection and particle leakage, correspondingly [32].

Here we deal with the stationary states in the NLSE (5.1) and introduce Krein signature of isolated eigenvalues in the spectrum of their linearization. We prove that the necessary condition for the onset of instability of the stationary states from a defective eigenvalue of algebraic multiplicity two is the *opposite* Krein signature of the two simple isolated eigenvalues prior to their coalescence. Compared to the Hamiltonian system in Chapter 4, or the linear Schrödinger equation in [105], the Krein signature of eigenvalues cannot be computed from the eigenvectors in the linearized problem, as the adjoint eigenvectors need to be computed separately and the sign of the adjoint eigenvector needs to be chosen by a continuity argument.

5.2 Stationary states, eigenvalues of the linearization, and Krein signature

Let us define the stationary state of the NLSE (5.1) by $\psi(x,t) = \Phi(x)e^{-i\mu t}$, where $\mu \in \mathbb{R}$ is a parameter. In the context of Bose-Einstein condensate, μ has the meaning of the chemical potential [45]. The function $\Phi(x) : \mathbb{R} \to \mathbb{C}$ is a suitable solution of the stationary NLSE in the form

$$-\Phi''(x) + (V(x) + i\gamma W(x))\Phi(x) - g|\Phi(x)|^2\Phi(x) = \mu\Phi(x), \tag{5.3}$$

where $x \in \mathbb{R}$. We say that Φ is a $\mathcal{PT}$-symmetric stationary state if Φ satisfies the $\mathcal{PT}$ symmetry:

$$\Phi(x) = \mathcal{PT}\Phi(x) = \overline{\Phi(-x)}, \quad x \in \mathbb{R}. \tag{5.4}$$

In addition to the symmetry constraints on the potentials V and W in (5.2), our basic assumptions are given below. Here and in what follows, we denote the Sobolev space of square integrable functions with square integrable second derivatives by $H^2(\mathbb{R})$ and the weighted L^2 space with a finite second moment by $L^{2,2}(\mathbb{R})$.

Assumption 1. *We assume that the linear Schrödinger operator $L_0 := -\partial_x^2 + V$ in $L^2(\mathbb{R})$ admits a self-adjoint extension with a dense domain $D(L_0)$ in $L^2(\mathbb{R})$.*

Remark 18. *If $V \in L^2(\mathbb{R}) \cap L^\infty(\mathbb{R})$ as in (5.43), then Assumption 1 is satisfied with $D(L_0) = H^2(\mathbb{R})$ (see [63], Ch. 14, p.143). If V is harmonic as in (5.44), then Assumption 1 is satisfied with $D(L_0) = H^2(\mathbb{R}) \cap L^{2,2}(\mathbb{R})$ (see [62], Ch. 4, p.37).*

Assumption 2. *We assume that W is a bounded and exponentially decaying potential satisfying*

$$|W(x)| \leq Ce^{-\kappa|x|}, \quad x \in \mathbb{R},$$

for some $C > 0$ and $\kappa > 0$.

Remark 19. *Both examples in (5.43) and (5.44) satisfy Assumption 2. By Assumption 2, the potential $i\gamma W$ is a relatively compact perturbation to L_0 (see [121], Ch. XIII, p.113). This implies that the continuous spectrum of $L_0 + i\gamma W$ is the same as L_0. If $V \in L^2(\mathbb{R}) \cap L^\infty(\mathbb{R})$, then the*

continuous spectrum of L_0 is located on the positive real line. If V is harmonic, then the continuous spectrum of L_0 is empty (see [121], Ch. XIII, Theorem 16 on p.120).

Assumption 3. *We assume that for a given $\mu \in \mathbb{R}$, there exist $\gamma_* > 0$ and a bounded, exponentially decaying, and $\mathcal{PT}$-symmetric solution $\Phi \in D(L_0) \subset L^2(\mathbb{R})$ to the stationary NLSE (5.3) with $\gamma \in (-\gamma_*, \gamma_*)$ satisfying (5.4) and*

$$|\Phi(x)| \leq Ce^{-\kappa|x|}, \quad x \in \mathbb{R},$$

for some $C > 0$ and $\kappa > 0$. Moreover, the map $(-\gamma_*, \gamma_*) \ni \gamma \mapsto \Phi \in D(L_0)$ is real-analytic.

Remark 20. *Since the nonlinear equation (5.3) is real-analytic in γ, the Implicit Function Theorem (see [142], Ch. 4, Theorem 4.E on p.250) provides real analyticity of the map $(-\gamma_*, \gamma_*) \ni \gamma \mapsto \Phi \in D(L_0)$ as long as the Jacobian operator*

$$\mathcal{L} := \begin{bmatrix} -\partial_x^2 + V + i\gamma W - \mu - 2g|\Phi|^2 & -g\Phi^2 \\ -g\overline{\Phi}^2 & -\partial_x^2 + V - i\gamma W - \mu - 2g|\Phi|^2 \end{bmatrix} \tag{5.5}$$

is invertible in the space of $\mathcal{PT}$-symmetric functions in $L^2(\mathbb{R})$.

Remark 21. *Under Assumption 3, we treat μ as a fixed parameter and γ as a varying parameter in the interval $(-\gamma_*, \gamma_*)$. The interval includes the Hamiltonian case $\gamma = 0$. In the context of the example of V in (5.43), it will be more natural to fix the value of γ and to consider the parameter continuation of $\Phi \in D(L_0)$ with respect to μ. The continuation results for the latter case are analogous to what we present here under Assumption 3.*

We perform the standard linearization of the NLSE (5.1) near the stationary state Φ by substituting

$$\psi(x,t) = e^{-i\mu t}\left[\Phi(x) + u(x,t)\right]$$

into (5.1) and truncating at the linear terms in u:

$$\begin{cases} iu_t = (-\partial_x^2 + V + i\gamma W - \mu - 2g|\Phi|^2)u - g\Phi^2\overline{u}, \\ -i\bar{u}_t = (-\partial_x^2 + V - i\gamma W - \mu - 2g|\Phi|^2)\overline{u} - g\overline{\Phi}^2 u. \end{cases}$$

Using $u = Ye^{-\lambda t}$ and $\overline{u} = Ze^{-\lambda t}$ with the spectral parameter λ yields the spectral stability problem in the form

$$\mathcal{L}\begin{bmatrix} Y \\ Z \end{bmatrix} = -i\lambda\sigma_3\begin{bmatrix} Y \\ Z \end{bmatrix}, \tag{5.6}$$

where $\sigma_3 = \mathrm{diag}(1,-1)$ is the third Pauli's matrix and $\mathcal{L}$ is given by (5.5). Note that if $\lambda \notin \mathbb{R}$, then $Z \neq \overline{Y}$.

Lemma 9. *The continuous spectrum of the operator $i\sigma_3\mathcal{L} : D(L_0) \times D(L_0) \to L^2(\mathbb{R}) \times L^2(\mathbb{R})$, if it exists, is a subset of $i\mathbb{R}$.*

Proof. Thanks to the Assumptions 1, 2 and 3, W and Φ^2 terms in (5.5) are relatively compact perturbations to the diagonal unbounded operator $\mathcal{L}_0 := \text{diag}(L_0 - \mu, L_0 - \mu)$, where $L_0 = -\partial_x^2 + V$ is introduced in Assumption (A1). Therefore,

$$\sigma_c(i\sigma_3\mathcal{L}) = \sigma_c(i\sigma_3\mathcal{L}_0) \subset i\mathbb{R},$$

where $\sigma_c(A)$ denotes the absolutely continuous part of the spectrum of the operator $A : D(A) \subset L^2(\mathbb{R}) \to L^2(\mathbb{R})$. □

Remark 22. *If $V \in L^2(\mathbb{R}) \cap L^\infty(\mathbb{R})$ and $\mu < 0$, then*

$$\sigma_c(i\sigma_3\mathcal{L}) = i(-\infty, -|\mu|] \cup i[|\mu|, \infty).$$

If V is harmonic, then $\sigma_c(i\sigma_3\mathcal{L})$ is empty.

Definition 14. *We say that the stationary state Φ is spectrally stable if every nonzero solution $(Y, Z) \in D(L_0) \times D(L_0)$ to the spectral problem (5.6) corresponds to $\lambda \in i\mathbb{R}$.*

We note the quadruple symmetry of eigenvalues in the spectral problem (5.6).

Lemma 10. *If λ_0 is an eigenvalue of the spectral problem (5.6), so are $-\lambda_0$, $\bar{\lambda}_0$, and $-\bar{\lambda}_0$.*

Proof. We note the symmetry of $\mathcal{L}$ and σ_3:

$$\mathcal{L} = \sigma_1\overline{\mathcal{L}}\sigma_1, \quad \sigma_3 = -\sigma_1\sigma_3\sigma_1, \tag{5.7}$$

where $\sigma_1 = \text{antidiag}(1, 1)$ is the first Pauli's matrix. If λ_0 is an eigenvalue of the spectral problem (5.6) with the eigenvector $v_0 := (Y, Z)$, then so is $\overline{\lambda}_0$ with the eigenvector $\sigma_1\overline{v}_0 = (\overline{Z}, \overline{Y})$. We note the second symmetry of $\mathcal{L}$ and σ_3:

$$\mathcal{L} = \mathcal{P}\overline{\mathcal{L}}\mathcal{P}, \quad \sigma_3 = \mathcal{P}\sigma_3\mathcal{P}. \tag{5.8}$$

If λ_0 is an eigenvalue of the spectral problem (5.6) with the eigenvector $v_0 := (Y, Z)$, then so is $-\overline{\lambda}_0$ with the eigenvector $\mathcal{P}\mathcal{T}v_0(x) = (\overline{Y(-x)}, \overline{Z(-x)})$. As a consequence of the two symmetries (5.7) and (5.8), $-\lambda_0$ is also an eigenvalue with the eigenvector $\mathcal{P}\sigma_1 v_0(x) = (Z(-x), Y(-x))$. □

Besides the spectral problem (5.6), we also introduce the adjoint spectral problem with the adjoint eigenvector denoted by $(Y^\#, Z^\#)$:

$$\mathcal{L}^* \begin{bmatrix} Y^\# \\ Z^\# \end{bmatrix} = -i\lambda\sigma_3 \begin{bmatrix} Y^\# \\ Z^\# \end{bmatrix}, \tag{5.9}$$

where

$$\mathcal{L}^* := \begin{bmatrix} -\partial_x^2 + V - i\gamma W - \mu - 2g|\Phi|^2 & -g\Phi^2 \\ -g\overline{\Phi}^2 & -\partial_x^2 + V + i\gamma W - \mu - 2g|\Phi|^2 \end{bmatrix}.$$

Remark 23. *Unless $\gamma = 0$ or $\Phi = 0$, the adjoint eigenvector $(Y^\#, Z^\#)$ cannot be related to the eigenvector (Y, Z) for the same eigenvalue λ.*

Our next assumption is on the existence of a nonzero isolated eigenvalue of the spectral problem (5.6).

Assumption 4. *We assume that there exists a simple isolated eigenvalue $\lambda_0 \in \mathbb{C}\backslash\{0\}$ of the spectral problems (5.6) and (5.9) with the eigenvector $v_0 := (Y, Z) \in D(L_0) \times D(L_0)$ and the adjoint eigenvector $v_0^\# := (Y^\#, Z^\#) \in D(L_0) \times D(L_0)$, respectively.*

Lemma 11. *Under Assumption 4, if $\lambda_0 \in i\mathbb{R}$, then the corresponding eigenvectors $v_0 := (Y, Z)$ and $v_0^\# := (Y^\#, Z^\#)$ can be normalized to satisfy*

$$Y(x) = \overline{Y(-x)}, \quad Z(x) = \overline{Z(-x)}, \quad x \in \mathbb{R} \tag{5.10}$$

and

$$Y^\#(x) = \overline{Y^\#(-x)}, \quad Z^\#(x) = \overline{Z^\#(-x)}, \quad x \in \mathbb{R}. \tag{5.11}$$

Proof. By Lemma 10, if $\lambda_0 \in i\mathbb{R}$ is a nonzero eigenvalue with the eigenvector $v_0 := (Y, Z)$, so is $-\overline{\lambda}_0 = \lambda_0$ with the eigenvector $\mathcal{PT}v_0$. Since λ_0 is a simple eigenvalue, there is a constant $C \in \mathbb{C}$ such that $v_0 = C\mathcal{PT}v_0$. Taking norms on both sides, we have $|C| = 1$. Therefore $C = e^{i\alpha}$ for some $\alpha \in [0, 2\pi]$, and α can be chosen so that v_0 satisfies $v_0 = \mathcal{PT}v_0$ as in (5.10). The same argument applies to the adjoint eigenvector $v_0^\# := (Y^\#, Z^\#)$. □

We shall now introduce the main object of our study, the Krein signature of the simple nonzero isolated eigenvalue λ_0 in Assumption 4.

Definition 15. *The Krein signature of the eigenvalue λ_0 in Assumption 4 is the sign of the Krein quantity $K(\lambda_0)$ defined by*

$$K(\lambda_0) = \langle v_0, \sigma_3 v_0^\# \rangle = \int_{\mathbb{R}} \left[Y(x)\overline{Y^\#(x)} - Z(x)\overline{Z^\#(x)} \right] dx. \tag{5.12}$$

The following lemma states the main properties of the Krein quantity $K(\lambda_0)$.

Lemma 12. *Assume (A4) and define $K(\lambda_0)$ by (5.12). Then,*

1. *$K(\lambda_0)$ is real if $\lambda_0 \in i\mathbb{R}\backslash\{0\}$.*
2. *$K(\lambda_0) \neq 0$ if $\lambda_0 \in i\mathbb{R}\backslash\{0\}$.*
3. *$K(\lambda_0) = 0$ if $\lambda_0 \in \mathbb{C}\backslash\{i\mathbb{R}\}$.*

Proof. First, we prove that if f and g are $\mathcal{PT}$-symmetric functions, then their inner product $\langle f, g\rangle$ is real-valued. Indeed, this follows from

$$\begin{aligned}\langle f, g\rangle &= \int_{\mathbb{R}} f(x)\overline{g(x)}dx = \int_0^{+\infty} \big(f(x)\overline{g(x)} + f(-x)\overline{g(-x)}\big)dx \\ &= \int_0^{+\infty} \big(f(x)\overline{g(x)} + \overline{f(x)}g(x)\big)dx.\end{aligned}$$

Since $\lambda_0 \in i\mathbb{R}\backslash\{0\}$ is simple by Assumption 4, then the eigenvectors $v_0 := (Y, Z)$ and $v_0^{\#} := (Y^{\#}, Z^{\#})$ satisfy the $\mathcal{PT}$-symmetry (5.10) and (5.11) by Lemma 11. Hence, the inner products in the definition of $K(\lambda_0)$ in (5.12) are real.

Next, we prove that $K(\lambda_0) \neq 0$ if $\lambda_0 \in i\mathbb{R}\backslash\{0\}$ is simple. Consider a generalized eigenvector problem for the spectral problem (5.6):

$$(\mathcal{L} + i\lambda_0\sigma_3)\begin{bmatrix} Y_g \\ Z_g \end{bmatrix} = \sigma_3 \begin{bmatrix} Y \\ Z \end{bmatrix}. \tag{5.13}$$

Since $\lambda_0 \notin \sigma_c(i\sigma_3\mathcal{L})$ is isolated and simple by Assumption 4, there exists a solution $v_g := (Y_g, Z_g) \in D(L_0) \times D(L_0)$ to the nonhomogeneous equation (5.13) if and only if $\sigma_3 v_0$ is orthogonal to $v_0^{\#}$, which is the kernel of adjoint operator $\mathcal{L}^* + i\lambda_0\sigma_3$. The orthogonality condition coincides with $K(\lambda_0) = 0$. However, no v_g exists since $\lambda_0 \in i\mathbb{R}\backslash\{0\}$ is simple by Assumption 4. Hence $K(\lambda_0) \neq 0$.

Finally, we show that $K(\lambda_0) = 0$ if $\lambda_0 \in \mathbb{C}\backslash\{i\mathbb{R}\}$. Taking inner products for the spectral problems (5.6) and (5.9) with the corresponding eigenvectors yields

$$\begin{cases} \langle \mathcal{L}v_0, v_0^{\#}\rangle &= -i\lambda_0\langle \sigma_3 v_0, v_0^{\#}\rangle, \\ \langle v_0, \mathcal{L}^* v_0^{\#}\rangle &= i\overline{\lambda}_0\langle v_0, \sigma_3 v_0^{\#}\rangle, \end{cases}$$

hence

$$i(\lambda_0 + \overline{\lambda}_0)K(\lambda_0) = 0.$$

If $\lambda_0 \in \mathbb{C}\backslash\{i\mathbb{R}\}$, then $\lambda_0 + \overline{\lambda}_0 \neq 0$ and $K(\lambda_0) = 0$. □

We shall now compare the Krein quantity $K(\lambda_0)$ in (5.12) for simple eigenvalues of the $\mathcal{PT}$-symmetric spectral problem (5.6) with the corresponding definition of the Krein quantity in the Hamiltonian case $\gamma = 0$ and in the linear $\mathcal{PT}$-symmetric case $\Phi = 0$.

In the Hamiltonian case ($\gamma = 0$), the operator $\mathcal{L}$ in the spectral problem (5.6) is self-adjoint in $L^2(\mathbb{R})$, that is, $\mathcal{L} = \mathcal{L}^*$. The standard definition of Krein quantity [69, 92] is given by

$$\gamma = 0: \quad K(\lambda_0) = \langle \mathcal{L} v_0, v_0 \rangle = -i\lambda_0 \int_{\mathbb{R}} \left[|Y(x)|^2 - |Z(x)|^2 \right] dx. \tag{5.14}$$

If $\gamma = 0$ and $\lambda_0 \in i\mathbb{R}$, then the adjoint eigenvector $(Y^\#, Z^\#)$ satisfies the same equation as (Y, Z). Therefore, it is natural to choose the adjoint eigenvector in the form:

$$\gamma = 0: \quad Y^\#(x) = Y(x), \quad Z^\#(x) = Z(x), \quad x \in \mathbb{R}, \tag{5.15}$$

in which case the definition (5.12) yields the integral in the right-hand side of (5.14). Note that the signs of $K(\lambda_0)$ in (5.12) and (5.14) are the same if $\lambda_0 \in i\mathbb{R}_+$.

Remark 24. *Since the potential V is even in (5.2), the eigenvector $v_0 := (Y, Z)$ of the spectral problem (5.6) for a simple eigenvalue $\lambda_0 \in i\mathbb{R}\backslash\{0\}$ is either even or odd in the Hamiltonian case $\gamma = 0$ by the parity symmetry. It follows from the $\mathcal{PT}$-symmetry (5.10) that the $\mathcal{PT}$-normalized eigenvector v_0 is real if it is even and is purely imaginary if it is odd.*

Remark 25. *Since the adjoint eigenvector $v_0^\# := (Y^\#, Z^\#)$ satisfying the $\mathcal{PT}$-symmetry condition (5.11) is defined up to an arbitrary sign, the Krein quantity $K(\lambda_0)$ in (5.12) is defined up to the sign change. In the continuation of the NLSE (5.1) with respect to the parameter γ from the Hamiltonian case $\gamma = 0$, the sign of the Krein quantity $K(\lambda_0)$ in (5.12) can be chosen so that it matches the sign of $K(\lambda_0)$ in (5.14) for $\lambda_0 \in i\mathbb{R}_+$ and $\gamma = 0$. In other words, the choice (5.15) is always made for $\gamma = 0$ and the Krein quantity $K(\lambda_0)$ is extended continuously with respect to the parameter γ.*

In the linear $\mathcal{PT}$-symmetric case ($\Phi = 0$), the spectral problem (5.6) becomes diagonal. If $Z = 0$, then Y satisfies the scalar Schrödinger equation

$$\left(-\partial_x^2 + V(x) + i\gamma W(x) - \mu\right) Y(x) = -i\lambda Y(x). \tag{5.16}$$

The $\mathcal{PT}$-Krein signature for the simple eigenvalue $\lambda_0 \in i\mathbb{R}$ of the scalar Schrödinger equation (5.16) is defined in [105] as follows:

$$\Phi = 0, \quad Z = 0: \qquad K(\lambda_0) = \int_{\mathbb{R}} Y(x)\overline{Y(-x)} dx. \tag{5.17}$$

If $\lambda_0 \in i\mathbb{R}$, then the adjoint eigenfunction $Y^\#$ satisfies a complex-conjugate equation to the spectral problem (5.16), which becomes identical to (5.16) after the parity transformation. Therefore, it is natural to choose the adjoint eigenfunction $Y^\#$ in the form:

$$\Phi = 0, \quad Z = 0: \qquad Y^\#(x) = Y(-x), \quad x \in \mathbb{R},$$

after which the definition (5.12) with $Z = 0$ corresponds to the definition (5.17). If $Y = 0$, then Z satisfies the scalar Schrödinger equation

$$\left(-\partial_x^2 + V(x) - i\gamma W(x) - \mu\right) Z(x) = i\lambda Z(x). \tag{5.18}$$

The $\mathcal{PT}$-Krein signature for the simple eigenvalue $\lambda_0 \in i\mathbb{R}$ of the scalar Schrödinger equation (5.18) is defined by

$$\Phi = 0, \quad Y = 0: \qquad K(\lambda_0) = \int_{\mathbb{R}} Z(x)\overline{Z(-x)}dx, \tag{5.19}$$

which coincides with the definition (5.12) for $Y = 0$ if the adjoint eigenfunction $Z^{\#}$ is chosen in the form:

$$\Phi = 0, \quad Y = 0: \qquad Z^{\#}(x) = -Z(-x), \quad x \in \mathbb{R}. \tag{5.20}$$

Note that if the choice $Z^{\#}(x) = Z(-x)$ is made instead of (5.20), then the definition (5.12) with $Y = 0$ is negative with respect to the definition (5.19).

5.3 Necessary condition for instability bifurcation

Recall that the eigenvalue is called *semi-simple* if algebraic and geometric multiplicities coincide and *defective* if algebraic multiplicity exceeds geometric multiplicity. Here we consider the case when the nonzero eigenvalue $\lambda_0 \in i\mathbb{R}$ of the spectral problem (5.6) is defective with geometric multiplicity *one* and algebraic multiplicity *two*. This situation occurs in the parameter continuations of the NLSE (5.1) when two simple isolated eigenvalues $\lambda_1, \lambda_2 \in i\mathbb{R}\backslash\{0\}$ coalesce at the point $\lambda_0 \neq 0$ and split into the complex plane resulting in the *instability bifurcation*. We will use the parameter γ to control the coalescence of two simple eigenvalues $\lambda_1, \lambda_2 \in i\mathbb{R}$.

Our main result states that the instability bifurcation occurs from the defective eigenvalue $\lambda_0 \in i\mathbb{R}$ of algebraic multiplicity two only if the Krein signatures of $K(\lambda_1)$ and $K(\lambda_2)$ for the two simple isolated eigenvalues $\lambda_1, \lambda_2 \in i\mathbb{R}$ before coalescence are opposite to each other. Therefore, we obtain the necessary condition for the instability bifurcation in the $\mathcal{PT}$-symmetric spectral problem (5.6), which has been proven for the Hamiltonian spectral problems [69, 92].

Remark 26. *The necessary condition for instability bifurcation allows us to predict the transition from stability to instability when a pair of imaginary eigenvalues collide. Pairs with the same Krein signature do not bifurcate off the imaginary axis if they collide, whereas pairs with the opposite Krein signature may bifurcate off the imaginary axis under a technical non-degeneracy condition (5.27) below.*

First, we state why the perturbation theory can be applied to the spectral problem (5.6).

Lemma 13. *Under Assumptions 1, 2, and 3, the operator*

$$\mathcal{L} : D(L_0) \times D(L_0) \to L^2(\mathbb{R}) \times L^2(\mathbb{R})$$

in the spectral problem (5.6) is real-analytic with respect to $\gamma \in (-\gamma_*, \gamma_*)$. Consequently, if $\mathcal{L}(\gamma_0)$ with $\gamma_0 \in (-\gamma_*, \gamma_*)$ has a spectrum consisting of two separated parts, then the subspaces of $L^2(\mathbb{R}) \times L^2(\mathbb{R})$ corresponding to the separated parts are also real-analytic in γ.

Proof. Operator $\mathcal{L}$ depends on γ via the potential $i\gamma W$ and the bound state Φ, the latter is real-analytic for $\gamma \in (-\gamma_*, \gamma_*)$ by Assumption 3. The assertion of the lemma follows from Theorem 1.7 in Chapter VII on p.368 in [71]. □

By Lemma 13, simple isolated eigenvalues $\lambda_1, \lambda_2 \in i\mathbb{R}$ of the spectral problem (5.6) and their eigenvectors $v_1 := (Y_1, Z_1)$ and $v_2 := (Y_2, Z_2)$ are continued analytically in γ before the coalescence point. Similarly, the adjoint eigenvectors $v_1^\# := (Y_1^\#, Z_1^\#)$ and $v_2^\# := (Y_2^\#, Z_2^\#)$ of the adjoint spectral problem (5.9) for $\lambda_1, \lambda_2 \in i\mathbb{R}$ are continued analytically in γ. Therefore, the Krein quantities $K(\lambda_1)$ and $K(\lambda_2)$ are continued analytically in γ.

Let γ_0 denote the bifurcation point when the two eigenvalues coalesce: $\lambda_1 = \lambda_2 = \lambda_0 \in i\mathbb{R}\backslash\{0\}$. For this $\gamma_0 \in \mathbb{R}$, we can define a small parameter $\varepsilon \in \mathbb{R}$ such that $\gamma = \gamma_0 + \varepsilon$. If $\mathcal{L}$ is denoted by $\mathcal{L}(\gamma)$, then $\mathcal{L}(\gamma)$ can be represented by the Taylor expansion:

$$\mathcal{L}(\gamma) = \mathcal{L}(\gamma_0) + \varepsilon \mathcal{L}'(\gamma_0) + \varepsilon^2 \hat{\mathcal{L}}(\varepsilon), \tag{5.21}$$

where $\hat{\mathcal{L}}(\varepsilon)$ denotes the remainder terms,

$$\mathcal{L}'(\gamma_0) = \begin{bmatrix} iW - 2g\partial_\gamma |\Phi(\gamma_0)|^2 & -g\partial_\gamma \Phi^2(\gamma_0) \\ -g\partial_\gamma \overline{\Phi^2(\gamma_0)} & -iW - 2g\partial_\gamma |\Phi(\gamma_0)|^2 \end{bmatrix}, \tag{5.22}$$

and ∂_γ denotes a partial derivative with respect to the parameter γ. Since the remainder terms in $\hat{\mathcal{L}}(\varepsilon)$ come from the second derivative of Φ in γ near γ_0, then $\hat{\mathcal{L}}(\varepsilon) \in L^2(\mathbb{R}) \cap L^\infty(\mathbb{R})$ thanks to Assumption 3.

Instead of Assumption 4, we shall now use the following assumption.

Assumption (A4′). *For $\gamma = \gamma_0$, we assume that there exists a defective isolated eigenvalue $\lambda_0 \in i\mathbb{R}\backslash\{0\}$ of the spectral problems (5.6) and (5.9) with the eigenvector $v_0 := (Y_0, Z_0) \in D(L_0) \times D(L_0)$, the generalized eigenvector $v_g := (Y_g, Z_g) \in D(L_0) \times D(L_0)$ and the adjoint eigenvector $v_0^\# := (Y_0^\#, Z_0^\#) \in D(L_0) \times D(L_0)$, the adjoint generalized eigenvector $v_g^\# := (Y_g^\#, Z_g^\#) \in D(L_0) \times D(L_0)$, respectively.*

By setting $\lambda_0 = i\Omega_0$, we can write the linear equations for the eigenvectors and generalized eigenvectors in Assumption (A4′):

$$\begin{aligned} \mathcal{L}(\gamma_0) v_0 &= \Omega_0 \sigma_3 v_0, \\ \mathcal{L}(\gamma_0) v_g &= \Omega_0 \sigma_3 v_g + \sigma_3 v_0, \end{aligned} \tag{5.23}$$

$$\begin{aligned} \mathcal{L}^*(\gamma_0) v_0^\# &= \Omega_0 \sigma_3 v_0^\#, \\ \mathcal{L}^*(\gamma_0) v_g^\# &= \Omega_0 \sigma_3 v_g^\# + \sigma_3 v_0^\#. \end{aligned} \tag{5.24}$$

The solvability conditions for the inhomogeneous equations (5.23) and (5.24) yield the following elementary facts.

Lemma 14. *Under Assumption (A4′), we have*

$$K(\lambda_0) = \langle v_0, \sigma_3 v_0^{\#} \rangle = 0. \tag{5.25}$$

and

$$\langle v_g, \sigma_3 v_0^{\#} \rangle = \langle v_0, \sigma_3 v_g^{\#} \rangle \neq 0. \tag{5.26}$$

Proof. Since v_g exists by Assumption (A4′), the solvability condition for (5.23) implies (5.25), see similar computations in Lemma 12. Since the eigenvalue λ_0 is double, no second generalized eigenvector $\tilde{v}_g$ exists from solutions of the inhomogeneous equation

$$\mathcal{L}(\gamma_0)\tilde{v}_g = \Omega_0 \sigma_3 \tilde{v}_g + \sigma_3 v_g.$$

The nonsolvability condition for this equation implies $\langle v_g, \sigma_3 v_0^{\#} \rangle \neq 0$. Finally, equations (5.23) and (5.24) yield

$$\begin{aligned} \langle v_g, \sigma_3 v_0^{\#} \rangle &= \langle v_g, (\mathcal{L}^* - \Omega_0 \sigma_3) v_g^{\#} \rangle = \langle (\mathcal{L} - \Omega_0 \sigma_3) v_g, v_g^{\#} \rangle \\ &= \langle \sigma_3 v_0, v_g^{\#} \rangle = \langle v_0, \sigma_3 v_g^{\#} \rangle, \end{aligned}$$

which proves the symmetry in (5.26). □

Remark 27. *Since the generalized eigenvectors are given by solutions of the inhomogeneous linear equations (5.23) and (5.24) and the eigenvectors satisfy the $\mathcal{PT}$-symmetry (5.10) and (5.11), the generalized eigenvectors also satisfy the same $\mathcal{PT}$-symmetry (5.10) and (5.11).*

The following result gives the necessary condition that the defective eigenvalue λ_0 in Assumption (A4′) splits into the complex plane in a one-sided neighborhood of the bifurcation point γ_0.

Theorem 13. *Assume 1, 2, 3, (A4′), and the non-degeneracy condition*

$$\langle \mathcal{L}'(\gamma_0) v_0, v_0^{\#} \rangle \neq 0. \tag{5.27}$$

There exists $\varepsilon_0 > 0$ such that two simple eigenvalues λ_1, λ_2 of the spectral problem (5.6) exist near λ_0 for every $\varepsilon \in (-\varepsilon_0, \varepsilon_0) \backslash \{0\}$ with $\lambda_{1,2} \to \lambda_0$ as $\varepsilon \to 0$. On one side of $\varepsilon = 0$, the eigenvalues are $\lambda_1, \lambda_2 \in i\mathbb{R}$ and

$$\operatorname{sign}\left[K(\lambda_1)\right] = -\operatorname{sign}\left[K(\lambda_2)\right]. \tag{5.28}$$

On the other side of $\varepsilon = 0$, the eigenvalues are $\lambda_1, \lambda_2 \notin i\mathbb{R}$.

Proof. We are looking for an eigenvalue $\Omega(\varepsilon)$ of the perturbed spectral problem

$$\left(\mathcal{L}_0 + \varepsilon \widetilde{\mathcal{L}}(\varepsilon)\right) v(\varepsilon) = \Omega(\varepsilon) \sigma_3 v(\varepsilon), \tag{5.29}$$

such that $\Omega(\varepsilon) \to \Omega_0$ as $\varepsilon \to 0$. Here we denote operators from the decomposition (5.21) as $\mathcal{L}_0 = \mathcal{L}(\gamma_0)$ and $\widetilde{\mathcal{L}}(\varepsilon) = \mathcal{L}'(\gamma_0) + \varepsilon\hat{\mathcal{L}}(\varepsilon)$. Since Ω_0 is a defective eigenvalue of geometric multiplicity *one* and algebraic multiplicity *two*, we apply Puiseux expansions [82]:

$$\begin{cases} \Omega(\varepsilon) = \Omega_0 + \varepsilon^{1/2}\widetilde{\Omega}(\varepsilon), \\ v(\varepsilon) = v_0 + \varepsilon^{1/2}a(\varepsilon)v_g + \varepsilon\widetilde{v_1}(\varepsilon), \end{cases} \tag{5.30}$$

where v_0 and v_g are the eigenvector and the generalized eigenvector for the eigenvalue Ω_0, $a(\varepsilon)$ is the projection coefficient to be defined, and $\widetilde{\Omega}(\varepsilon)$ and $\widetilde{v_1}(\varepsilon)$ are the remainder terms. To define $\widetilde{v_1}(\varepsilon)$ uniquely, we add the orthogonality condition

$$\langle \widetilde{v_1}(\varepsilon), \sigma_3 v_0^{\#} \rangle = \langle \widetilde{v_1}(\varepsilon), \sigma_3 v_g^{\#} \rangle = 0. \tag{5.31}$$

Plugging (5.30) into (5.29) and dropping the dependence on ε for $\widetilde{\mathcal{L}}$, $\widetilde{v}_1$, a and $\widetilde{\Omega}$ gives us the nonhomogeneous equation

$$\left(\mathcal{L}_0 - \Omega_0\sigma_3 + \varepsilon\widetilde{\mathcal{L}} - \varepsilon^{1/2}\widetilde{\Omega}\sigma_3\right)\widetilde{v}_1 = h, \tag{5.32}$$

where

$$h = \varepsilon^{-1/2}(\widetilde{\Omega} - a)\sigma_3 v_0 - \widetilde{\mathcal{L}}v_0 + a\big(\widetilde{\Omega}\sigma_3 - \varepsilon^{1/2}\widetilde{\mathcal{L}}\big)v_g.$$

By Assumption (A4′), the limiting operator $\sigma_3(\mathcal{L}_0 - \Omega_0\sigma_3)$ has the two-dimensional generalized null space $X_0 = \text{span}\{v_0, v_g\} \subset L^2(\mathbb{R}) \times L^2(\mathbb{R})$. Since $\Omega_0 \notin \sigma_c(\sigma_3\mathcal{L}_0)$ is isolated from the rest of the spectrum of $\sigma_3\mathcal{L}_0$, the range of $\sigma_3(\mathcal{L}_0 - \Omega_0\sigma_3)$ is orthogonal with respect to generalized null space $Y_0 = \text{span}\{\sigma_3 v_0^{\#}, \sigma_3 v_g^{\#}\} \subset L^2(\mathbb{R}) \times L^2(\mathbb{R})$ of the adjoint operator $(\mathcal{L}_0^* - \Omega_0\sigma_3)\sigma_3$. As a result, $\sigma_3(\mathcal{L}_0 - \Omega_0\sigma_3)$ is invertible on an element of $Y_0^{\perp}$ and the inverse operator is uniquely defined and bounded in $Y_0^{\perp}$. In other words, there exist positive constants ε_0, Ω_0, and C_0 such that for all $|\varepsilon| \leq \varepsilon_0$, $|\widetilde{\Omega}| \leq \Omega_0$, and all $\sigma_3 f \in Y_0^{\perp}$, there exists a unique $(\mathcal{L}_0 - \Omega_0\sigma_3)^{-1}f \in D(L_0) \times D(L_0)$ satisfying the orthogonality conditions (5.31) and the bound

$$\|(\mathcal{L}_0 - \Omega_0\sigma_3)^{-1}f\|_{L^2} \leq C_0\|f\|_{L^2}. \tag{5.33}$$

In order to provide existence of a unique $(\mathcal{L}_0 - \Omega_0\sigma_3)^{-1}f$, we add the orthogonality constraints $\langle f, v_0^{\#} \rangle = \langle f, v_g^{\#} \rangle = 0$. By using (5.26) and (5.31), we obtain two equations from (5.32):

$$\varepsilon\langle \widetilde{\mathcal{L}}\widetilde{v}_1, v_0^{\#} \rangle + \langle \widetilde{\mathcal{L}}v_0, v_0^{\#} \rangle = \widetilde{\Omega}a\langle v_g, \sigma_3 v_0^{\#} \rangle - \varepsilon^{1/2}a\langle \widetilde{\mathcal{L}}v_g, v_0^{\#} \rangle, \tag{5.34}$$

and

$$\begin{aligned} \varepsilon\langle \widetilde{\mathcal{L}}\widetilde{v}_1, v_g^{\#} \rangle + \langle \widetilde{\mathcal{L}}v_0, v_g^{\#} \rangle = {} & \widetilde{\Omega}a\langle v_g, \sigma_3 v_g^{\#} \rangle - \varepsilon^{1/2}a\langle \widetilde{\mathcal{L}}v_g, v_g^{\#} \rangle \\ & + \varepsilon^{-1/2}(\widetilde{\Omega} - a)\langle v_0, \sigma_3 v_g^{\#} \rangle. \end{aligned} \tag{5.35}$$

Since $\widetilde{\mathcal{L}}$ and $\widetilde{\Omega}\sigma_3$ are relatively compact perturbations to $(\mathcal{L}_0 - \Omega_0\sigma_3)$, there exists a unique solution of the nonhomogeneous equation (5.32) under the constraints (5.34) and (5.35) satisfying the orthogonality conditions (5.31) and the resolvent estimate (5.33). In particular, there exist positive constants ε_0, Ω_0, A_0, and C_0 such that for all $|\varepsilon| \leq \varepsilon_0$, $|\widetilde{\Omega}| \leq \Omega_0$, and $|a| \leq A_0$, the solution $\widetilde{v}_1 \in D(L_0) \times D(L_0)$ of equation (5.32) satisfies the estimate

$$\|\widetilde{v}_1\|_{L^2} \leq C_0 \left(\varepsilon^{-1/2}|a - \widetilde{\Omega}| + 1\right). \tag{5.36}$$

Equation (5.35) yields

$$\varepsilon^{-1/2}(a - \widetilde{\Omega}) = \frac{1}{\langle v_0, \sigma_3 v_g^{\#}\rangle}\Big(\widetilde{\Omega}a\langle v_g, \sigma_3 v_g^{\#}\rangle - \varepsilon^{1/2}a\langle\widetilde{\mathcal{L}}v_g, v_g^{\#}\rangle - \langle\widetilde{\mathcal{L}}v_0, v_g^{\#}\rangle - \varepsilon\langle\widetilde{\mathcal{L}}\widetilde{v}_1, v_g^{\#}\rangle\Big),$$

where $\langle v_0, \sigma_3 v_g^{\#}\rangle \neq 0$ due to Lemma 14. Combining with the estimate (5.36), we obtain for some $C_1 > 0$

$$|a - \widetilde{\Omega}| \leq C_1\varepsilon^{1/2} \quad \text{and} \quad \|\tilde{v}_1\|_{L^2} \leq C_1. \tag{5.37}$$

Equation (5.34) yields

$$\widetilde{\Omega}a = \frac{1}{\langle v_g, \sigma_3 v_0^{\#}\rangle}\left(\langle\widetilde{\mathcal{L}}v_0, v_0^{\#}\rangle + \varepsilon^{1/2}a\langle\widetilde{\mathcal{L}}v_g, v_0^{\#}\rangle + \varepsilon\langle\widetilde{\mathcal{L}}\widetilde{v_1}, v_0^{\#}\rangle\right),$$

where $\langle v_g, \sigma_3 v_0^{\#}\rangle \neq 0$ due to Lemma 14. Thanks to (5.37), we obtain

$$|\widetilde{\Omega} - \Omega_g| \leq C_2\varepsilon^{1/2},$$

where $C_2 > 0$ is a constant, and Ω_g is a root of the quadratic equation

$$\Omega_g^2 = \frac{\langle\mathcal{L}'(\gamma_0)v_0, v_0^{\#}\rangle}{\langle v_g, \sigma_3 v_0^{\#}\rangle}, \tag{5.38}$$

with $\mathcal{L}'(\gamma_0)$ given by (5.22). Since $\mathcal{L}'(\gamma_0)v_0$, v_g, and $v_0^{\#}$ satisfy the $\mathcal{PT}$-symmetry conditions, both the nominator and the denominator of (5.38) are real-valued by the same computations as in the proof of Lemma 12. By the assumption (5.27), Ω_g^2 is nonzero, either positive or negative.

Let us assume that $\Omega_g^2 > 0$ without loss of generality and pick $\Omega_g > 0$. Then $\varepsilon^{1/2}\Omega_g \in \mathbb{R}$ if $\varepsilon > 0$ and we obtain the expansions for the two simple eigenvalues:

$$\begin{cases}\Omega_1(\varepsilon) = \Omega_0 + \varepsilon^{1/2}\Omega_g + \mathcal{O}(\varepsilon),\\ \Omega_2(\varepsilon) = \Omega_0 - \varepsilon^{1/2}\Omega_g + \mathcal{O}(\varepsilon)\end{cases}$$

and their corresponding eigenvectors:

$$\begin{cases} v_1(\varepsilon) = v_0 + \varepsilon^{1/2}\Omega_g v_g + \mathcal{O}(\varepsilon), \\ v_2(\varepsilon) = v_0 - \varepsilon^{1/2}\Omega_g v_g + \mathcal{O}(\varepsilon). \end{cases}$$

The same expansions hold for eigenvectors of the adjoint spectral problems corresponding to the same eigenvalues Ω_1, Ω_2:

$$\begin{cases} v_1^{\#}(\varepsilon) = v_0^{\#} + \varepsilon^{1/2}\Omega_g v_g^{\#} + \mathcal{O}(\varepsilon), \\ v_2^{\#}(\varepsilon) = v_0^{\#} - \varepsilon^{1/2}\Omega_g v_g^{\#} + \mathcal{O}(\varepsilon). \end{cases}$$

The leading order of Krein quantities for eigenvalues $\lambda_1 = i\Omega_1$ and $\lambda_2 = i\Omega_2$ is given by

$$\begin{cases} K(\lambda_1) &= \langle v_1, \sigma_3 v_1^{\#} \rangle = \varepsilon^{1/2}\Omega_g \langle v_g, \sigma_3 v_0^{\#} \rangle + \overline{\varepsilon^{1/2}\Omega_g} \langle v_0, \sigma_3 v_g^{\#} \rangle + \mathcal{O}(\varepsilon), \\ K(\lambda_2) &= \langle v_2, \sigma_3 v_2^{\#} \rangle = -\varepsilon^{1/2}\Omega_g \langle v_g, \sigma_3 v_0^{\#} \rangle - \overline{\varepsilon^{1/2}\Omega_g} \langle v_0, \sigma_3 v_g^{\#} \rangle + \mathcal{O}(\varepsilon), \end{cases}$$

which is simplified with the help of (5.26) to

$$\begin{cases} K(\lambda_1) = 2\varepsilon^{1/2}\Omega_g \langle v_g, \sigma_3 v_0^{\#} \rangle + \mathcal{O}(\varepsilon), \\ K(\lambda_2) = -2\varepsilon^{1/2}\Omega_g \langle v_g, \sigma_3 v_0^{\#} \rangle + \mathcal{O}(\varepsilon). \end{cases}$$

Since $\varepsilon^{1/2}\Omega_g \in \mathbb{R}$ and $\langle v_g, \sigma_3 v_0^{\#} \rangle \neq 0$, we obtain (5.28). If $\varepsilon < 0$, then $\varepsilon^{1/2}\Omega_g \in i\mathbb{R}$, so that $\lambda_1, \lambda_2 \notin i\mathbb{R}$. □

Remark 28. *If the non-degeneracy assumption (5.27) is not satisfied, then $\Omega_g = 0$ and the perturbation theory must be extended to the next order. In this case, the defective eigenvalue $\lambda_0 = i\Omega_0$ may split along $i\mathbb{R}$ both for $\varepsilon > 0$ and $\varepsilon < 0$.*

5.4 Numerical Approximations

We approximate nonlinear modes Φ of the stationary NLSE (5.3) and eigenvectors (Y, Z) of the spectral problem (5.6) with the Chebyshev interpolation method [137]. This method was recently applied to massive Dirac equations in [112]. Chebyshev polynomials are defined on the interval $[-1, 1]$. The stationary NLSE (5.3) is defined on the real line, therefore we make a coordinate transformation for the Chebyshev grid points $\{z_j = \cos(\frac{j\pi}{N})\}_{j=0}^{j=N}$:

$$x_j = L \operatorname{arctanh}(z_j), \quad j = 1, 2, \ldots, N-1, \tag{5.39}$$

where $x_0 = +\infty$ and $x_N = -\infty$. The scaling parameter L is chosen so that the grid points $\{x_j\}_{j=1}^{j=N-1}$ are concentrated in the region where the nonlinear mode Φ changes fast. We apply the chain rule for the second derivative:

$$\frac{d^2u}{dx^2} = \frac{d}{dx}\left(\frac{du}{dx}\right) = \frac{d}{dz}\left(\frac{du}{dz}\frac{dz}{dx}\right) = \frac{d^2u}{dz^2}\left(\frac{dz}{dx}\right)^2 + \frac{du}{dz}\frac{d^2z}{dx^2},$$

where

$$\frac{dz}{dx} = \frac{1}{L}\operatorname{sech}^2\left(\frac{x}{L}\right) = \frac{1}{L}(1-z^2)$$

and

$$\frac{d^2z}{dx^2} = -\frac{2}{L^2}\operatorname{sech}^2\left(\frac{x}{L}\right)\tanh\left(\frac{x}{L}\right) = -\frac{2}{L^2}z(1-z^2).$$

The first and second derivatives for ∂_z and ∂_z^2 are approximated by the Chebyshev differentiation matrices D_N and D_N^2, respectively (see p.53 in [137]).

The stationary NLSE (5.3) is written in the form:

$$F(\Phi) := (-\partial_x^2 + V + i\gamma W - \mu - g|\Phi|^2)\Phi = 0. \tag{5.40}$$

We fix μ, γ, g, V, W and use Newton's method to look for a solution Φ satisfying Assumption 3:

$$\begin{bmatrix} \Phi_{n+1} \\ \bar{\Phi}_{n+1} \end{bmatrix} = \begin{bmatrix} \Phi_n \\ \bar{\Phi}_n \end{bmatrix} - \mathcal{L}_n^{-1}\begin{bmatrix} F(\Phi_n) \\ \bar{F}(\Phi_n) \end{bmatrix}, \tag{5.41}$$

where $\mathcal{L}_n$ is the Jacobian operator to the nonlinear problem (5.40), which coincides with (5.5) computed at Φ_n. Since $\Phi(x_0) = \Phi(x_N) = 0$, the Jacobian operator $\mathcal{L}_n$ is represented by the $2(N-1)\times 2(N-1)$ matrix.

It follows by the gauge transformation that

$$\mathcal{L}\begin{bmatrix} i\Phi \\ -i\bar{\Phi} \end{bmatrix} = \begin{bmatrix} 0 \\ 0 \end{bmatrix}, \tag{5.42}$$

where $\mathcal{L}$ is computed at Φ. Therefore, $\mathcal{L}$ is a singular operator for every parameter choice of equation (5.40). However, if the eigenvector satisfies the symmetry $\bar{Z} = Y$ as in (5.42), then the eigenvector does not satisfy the $\mathcal{PT}$-symmetry:

$$\mathcal{PT}\begin{bmatrix} i\Phi \\ -i\bar{\Phi} \end{bmatrix} = \begin{bmatrix} -i\overline{\Phi(-x)} \\ i\Phi(-x) \end{bmatrix} = -\begin{bmatrix} i\Phi \\ -i\bar{\Phi} \end{bmatrix}.$$

Hence, $\mathcal{L}$ is invertible on the space of $\mathcal{PT}$-symmetric functions satisfying (5.4). In terms of the coefficients of Chebyshev polynomials, the restriction means that the even-numbered coefficients are purely real, whereas the odd-numbered coefficients are purely imaginary.

Choosing a first guess for the iterative procedure (5.41) depends on the choice of the potentials V and W. For the Scarf II potential

$$V(x) = -V_0\operatorname{sech}^2(x), \quad W(x) = \operatorname{sech}(x)\tanh(x), \tag{5.43}$$

where $V_0 \in \mathbb{R}$ is a parameter, one can use a scalar multiple of the $\operatorname{sech}(x)$ function for the first branch of solutions and a scalar multiple of the $\operatorname{sech}(x)\tanh(x)$ function for the second branch of

	$\|\Phi_{exact} - \Phi_{numerical}\|^2$
N = 50	1.5×10^{-6}
N = 100	2.4×10^{-13}
N = 500	2.2×10^{-13}

Table 5.1: The numerical error for the exact solution (5.45) versus N.

solutions [3] (See also Appendix B. For the confining potential

$$V(x) = x^2, \quad W(x) = xe^{-\frac{x^2}{2}}, \tag{5.44}$$

one can use the corresponding Gauss-Hermite functions of the linear system for each branch [145].

The spectral problem (5.6) uses the same operator $\mathcal{L}$ and can be discretized similarly. One looks for eigenvalues and eigenvectors of the discretized matrix by using the standard numerical methods for non-Hermitian matrices. For example, MATLAB® performs these computations by using the QZ algorithm.

Throughout the numerical results, we pick the value of a scaling parameter L to be $L = 10$. This choice ensures that Φ remains nonzero up to 16 decimals on the interior grid points $\{x_j\}_{j=1}^{j=N-1}$. The algorithm was tested on the exact solution derived in Appendix C for the Scarf II potential (5.43) with $V_0 = 1$ and $\mu = \gamma = -1$:

$$\Phi(x) = \sin\alpha \operatorname{sech}(x) \exp\left[\frac{i}{2}\cos\alpha \arctan(\sinh(x))\right], \tag{5.45}$$

where $\alpha = \arccos(2/3)$. Table 5.1 shows a good agreement between exact and numerical results.

Once we computed eigenvalues and eigenvectors for the spectral problem (5.6), we proceed to computations of the Krein quantity defined by (5.12). Several obstacles arise in the definition of the Krein quantity:

1. Eigenvectors of the Chebyshev discretization matrices are normalized with respect to z.
2. Eigenvectors are not necessarily $\mathcal{PT}$-symmetric.
3. The sign of the adjoint eigenvectors relative to the eigenvectors is undefined.

Here we explain how to deal with these difficulties.

1. The eigenvectors are normalized in the $L^2([-1,1])$ norm with respect to the variable z. In order to normalize them in the $L^2(\mathbb{R})$ norm with respect to the variable x, we perform the change of coordinates (5.39). In particular, we use integration with the composite trapezoid method on the grid points $\{x_j\}_{j=1}^{j=N-1}$ and neglect integrals for $(-\infty, x_{N-1})$ and $(x_1, +\infty)$.
2. In order to restore the $\mathcal{PT}$-symmetry condition (5.10), we multiply the component Y of the eigenvector (Y, Z) by $e^{i\theta}$ with $\theta \in [0, 2\pi]$ and require

$$e^{i\theta}Y(x) = e^{-i\theta}\overline{Y(-x)} \quad \Rightarrow \quad 2i\theta = \log\frac{\overline{Y(-x)}}{Y(x)},$$

where the point x is chosen so that $Y(x)$ and $Y(-x)$ are nonzero. For example, we compute θ for all interior grid points $\{x_j\}_{j=1}^{j=N-1}$ for which $Y(x_j) \neq 0$ and take the average. Both Y and Z in the same eigenvector are rotated with the same angle θ. Similarly, this step is performed for $Y^{\#}$ and $Z^{\#}$ according to the $\mathcal{PT}$-symmetry condition (5.11).

3. We fix the sign of the adjoint eigenvectors at the Hamiltonian case $\gamma = 0$ by using (5.15). Then we continue the eigenvectors and the adjoint eigenvectors for simple eigenvalues before coalescence points. Numerically, we take two steps in γ: $\gamma_1 < \gamma_2$, with $|\gamma_2 - \gamma_1| \ll 1$. Suppose that the sign of eigenvector for γ_1 has been chosen already. We take eigenvectors for γ_1 and γ_2 and compare them. If eigenvectors have been made $\mathcal{PT}$-symmetric and properly normalized, then the norm of their difference is either small (the eigenvectors are almost the same) or close to 2 (the eigenvectors are negatives of each other). We choose the sign of the eigenvector so that the norm of their difference is small.

With the refinements described above, we can now compute the Krein quantity $K(\lambda)$ defined by (5.12) using the same numerical method as the one used for computing the norms of eigenvectors.

In numerical computations, we have often encountered situations when eigenvalues nearly coalesce, but the standard MATLAB® numerical routines do not approximate well the coalescence of eigenvalues. In order to check if the eigenvectors are linearly dependent near the possible coalescence point, we compute the norm of the difference between the two eigenvectors and plot it with respect to the parameter γ. If the difference between the two eigenvectors vanishes as γ is increased towards the coalescence point, we say that the defective eigenvalue arises at the bifurcation point. If the difference remains finite, either we are dealing with the semi-simple eigenvalue at the coalescence point or the two simple eigenvalues pass each other without coalescence.

5.5 Numerical Examples

In the numerical examples, we set $N = 500$. This gives enough accuracy for computing eigenvalues, as it was shown in [112]. We will demonstrate numerical results in Figures 5.1,5.2,5.3 and 5.4. Each figure displays branches of the nonlinear modes Φ versus a parameter used in the numerical continuations (either μ or γ), where the blue solid line corresponds to stable modes and the red dashed line denotes unstable ones. The top and middle panels show the power curves of $\|\Phi\|^2$, a sample profile of the nonlinear mode Φ, and the spectrum of linearization before and after the instability bifurcation. The bottom panels show the imaginary part of eigenvalues λ and the Krein quantity of isolated eigenvalues. Green color corresponds to eigenvalues $\lambda \in i\mathbb{R}$ with the positive Krein signature, red – to those with the negative Krein signature, and black color is used for complex eigenvalues $\lambda \notin i\mathbb{R}$ and for the continuous spectrum.

Figure 5.1 (a)-(f) shows the instability bifurcation for the Scarf II potential (5.43) studied in [105] in the focusing case with $g = 1$. Here $V_0 = 2$, $\gamma = -2.21$, and the first branch of the nonlinear modes Φ is considered. As two eigenvalues with different Krein signatures coalesce, they bifurcate into a complex quadruplet, in agreement with Theorem 13. Note that there is a small region of stability for the nonlinear modes Φ of small amplitudes, as it was shown in [105].

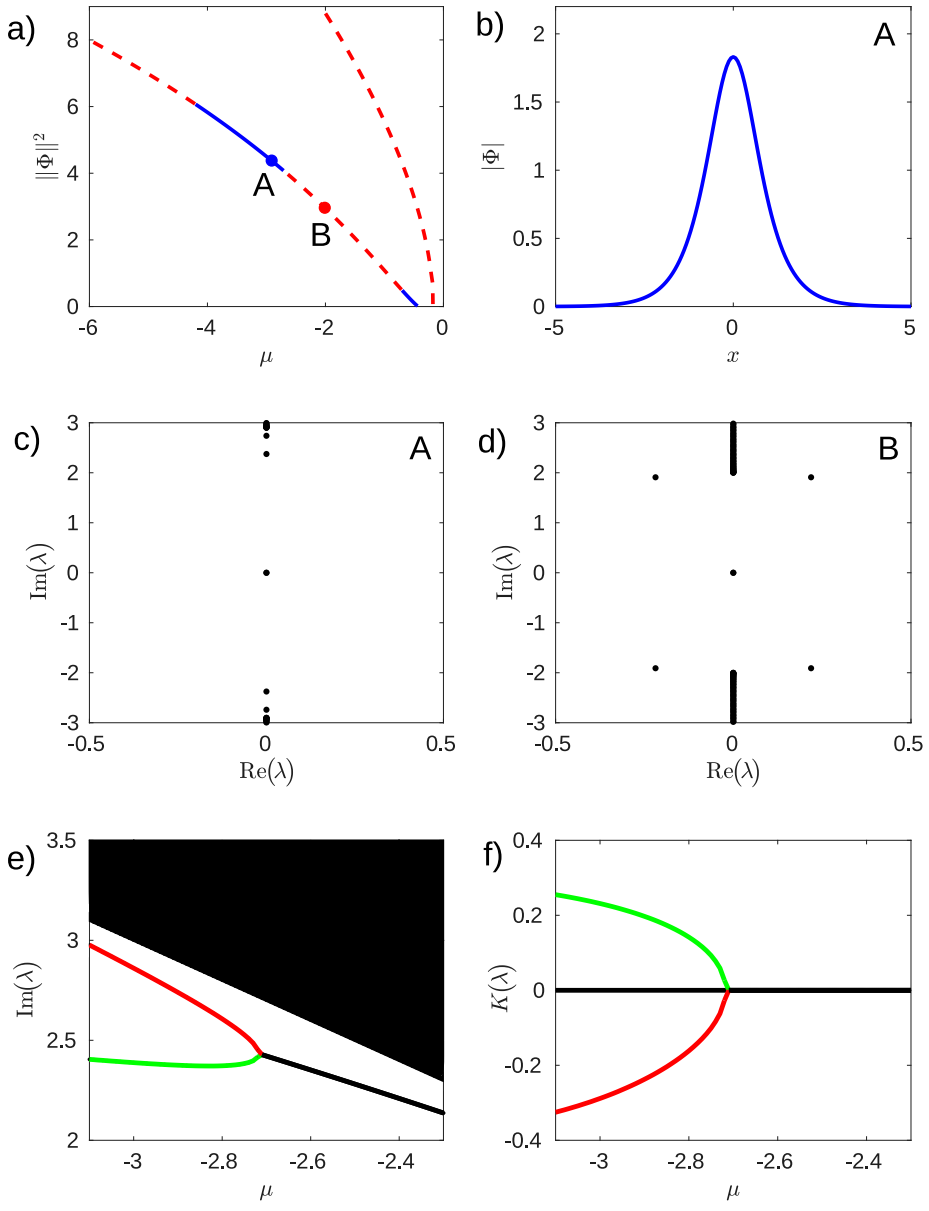

Figure 5.1: Scarf II potential (5.43) with $V_0 = 2$, $\gamma = -2.21$. (a) Power curves versus μ. (b) Amplitude profile for point A. (c) Spectrum of linearization for point A. (d) Same for point B. (e) $\mathrm{Im}(\lambda)$ for the spectrum of linearization versus μ. (f) Krein quantities for isolated eigenvalues versus μ.

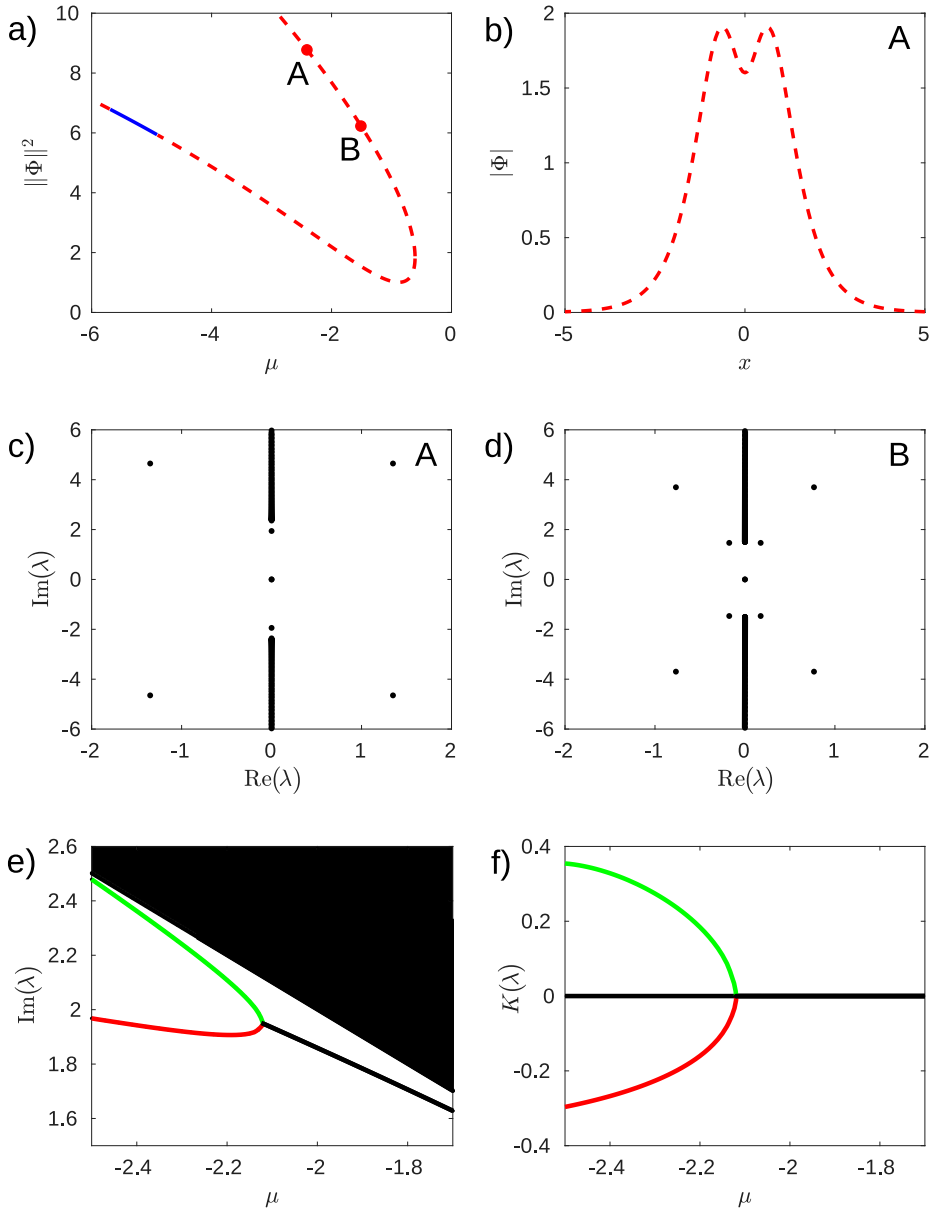

Figure 5.2: Scarf II potential (5.43) with $V_0 = 3$, $\gamma = -3.7$. (a) Power curves versus μ. (b) Amplitude profile for point A. (c) Spectrum of linearization for point A. (d) Same for point B. (e) $\mathrm{Im}(\lambda)$ for the spectrum of linearization versus μ. (f) Krein quantities for isolated eigenvalues versus μ.

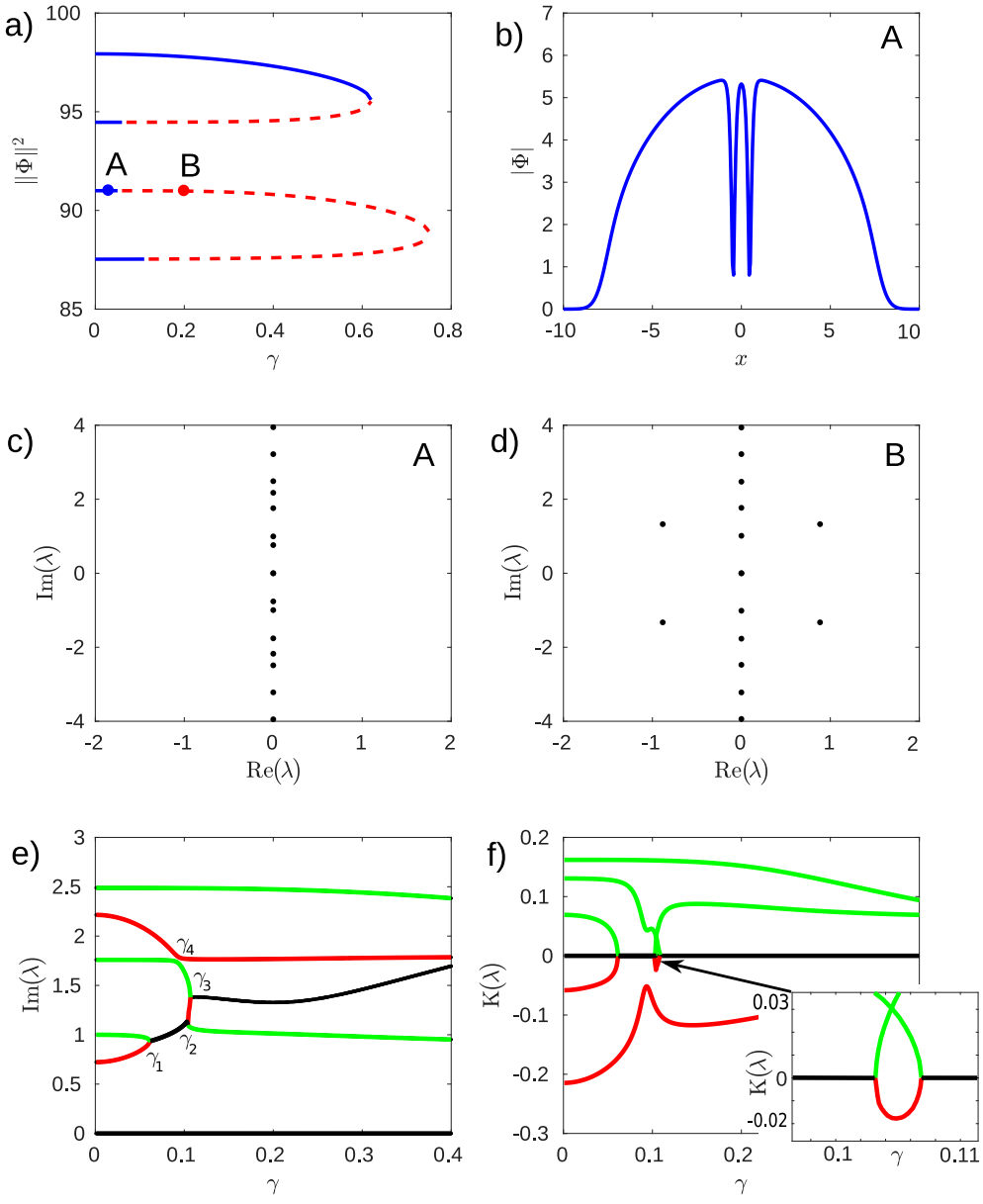

Figure 5.3: Confining potential (5.44), scaled as in (5.46). (a) Power curves versus γ. (b) Amplitude profile for point A. (c) Spectrum of linearization for point A. (d) Same for point B. (e) Im(λ) for the spectrum of linearization versus γ. (f) Krein quantities for isolated eigenvalues versus γ.

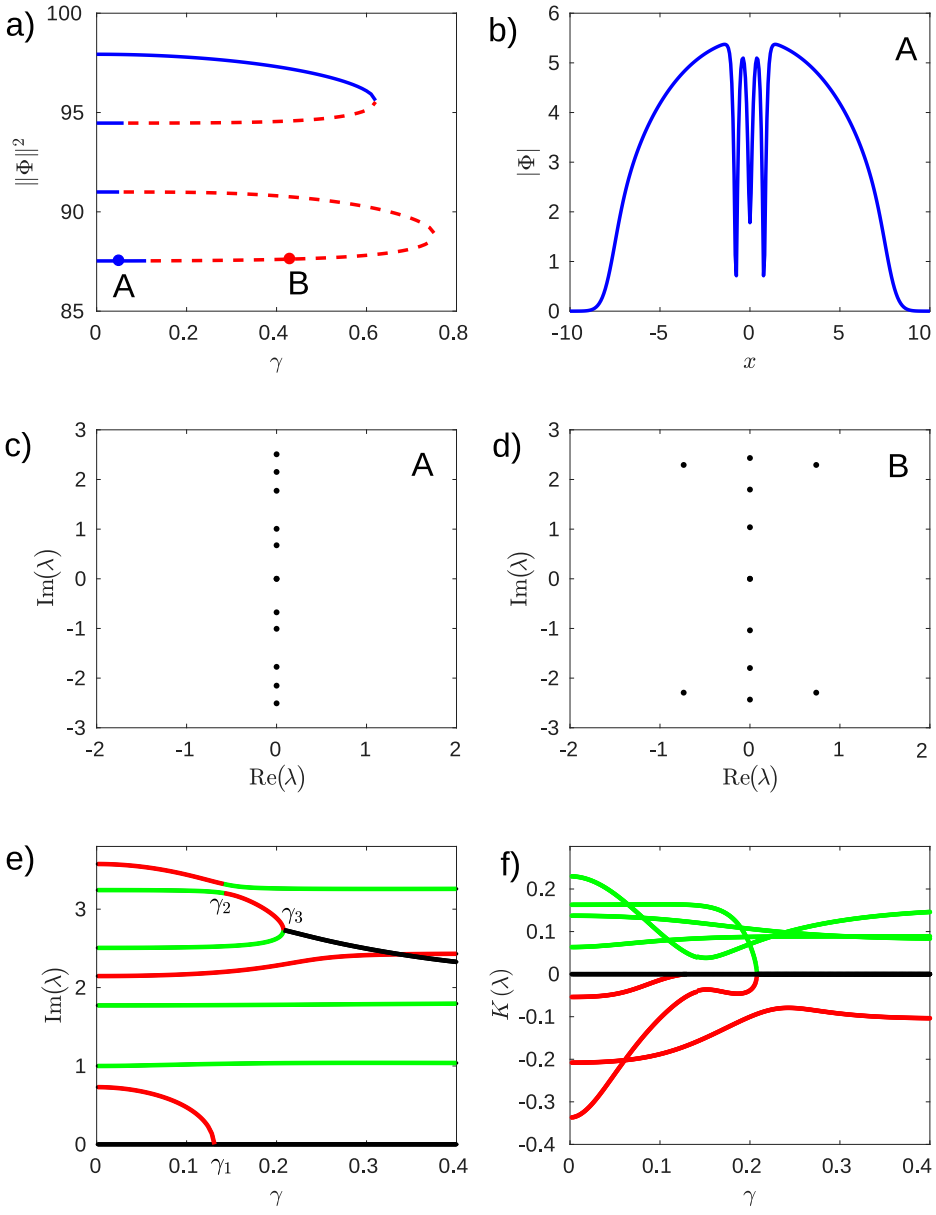

Figure 5.4: Confining potential (5.44), scaled as in (5.46). (a) Power curves versus γ. (b) Amplitude profile for point A. (c) Spectrum of linearization for point A. (d) Same for point B. (e) Im(λ) for the spectrum of linearization versus γ. (f) Krein quantities for isolated eigenvalues versus γ.

Figure 5.2 (a)-(f) shows the instability bifurcation for the Scarf II potential (5.43) studied in [17] in the focusing case with $g = 1$. Here $V_0 = 3$, $\gamma = -3.7$, and the second branch of the nonlinear modes Φ is considered. The second branch is unstable with at least one complex quadruplet for all values of parameter μ used. The imaginary part of this complex quadruplet is not visible in Figure 5.2 (e) as it coincides with the location of the continuous spectrum. In the presence of this complex quadruplet, we observe a coalescence of two simple eigenvalues $\lambda_1, \lambda_2 \in i\mathbb{R}$ and the instability bifurcation into another complex quadruplet. Numerical evidence confirms that the eigenvalues have the opposite Krein signatures prior to collision, allowing us to predict the instability bifurcation, in agreement with Theorem 13.

Figures 5.3,5.4 (a)-(f) show the confining potential (5.44) studied in [1], in the defocusing case with $g = -2$. Compared to (5.44), we use a scaled version of this potential to match the one in [1]:

$$V(x) = x^2, \quad W(x) = 2\Omega^{-3/2} x e^{-\frac{x^2}{2\Omega}}, \tag{5.46}$$

where $\Omega = 10^{-1}$ is a scaling parameter. There are four branches of the nonlinear modes Φ shown, out of which we highlight only the third and fourth branches. The first branch is stable, whereas the second branch becomes unstable because of a coalescence of a pair of eigenvalues $\pm\lambda \in i\mathbb{R}$ with the negative Krein signature at the origin [1]. The third and fourth branches are studied in Figures 5.3 and 5.4.

In Figure 5.3 we can see that there are three bifurcations occurring at $\gamma_1 \approx 0.07$, $\gamma_2 \approx 0.1031$ and $\gamma_3 \approx 0.1069$. For each bifurcation two eigenvalues with different Krein signatures collide and bifurcate off to the complex plane in accordance with Theorem 13. In addition, two simple eigenvalues with different Krein signatures nearly coalesce near $\gamma_4 \approx 0.1$. Figure 5.5 (a) shows the norm of the difference between the two eigenvectors and two adjoint eigenvectors for the two simple eigenvalues while γ is increased towards γ_4. As the difference does not vanish, we rule out this point as the bifurcation point for the defective eigenvalue. Consequently, the eigenvalues are continued past this point with preservation of their Krein signatures.

In Figure 5.4 we can see three bifurcations occurring at $\gamma_1 \approx 0.1303$, $\gamma_2 \approx 0.1427$, and $\gamma_3 \approx 0.2078$. At γ_1, an eigenvalue pair with negative Krein signature coalesce at zero and become a pair of real (unstable) eigenvalues. As γ is increased towards γ_2, two eigenvalues with opposite Krein signature move towards each other. Figure 5.5 (b) illustrates that the norm of the difference between the two eigenvectors and the two adjoint eigenvectors vanishes at the coalescence point. Therefore, we conclude that at γ_2 we have a defective eigenvalue which does not split into a complex quadruplet. According to Theorem 13, the defective eigenvalue does not split into complex unstable eigenvalues only if the non-degeneracy condition (5.27) is not satisfied. Similar safe passing of eigenvalues of opposite Krein signature through each other is observed in [105]. The behavior near γ_2 shows that having opposite Krein signatures prior to coalescence of two simple eigenvalues into a defective eigenvalue is a *necessary but not sufficient* condition for the instability bifurcation. At γ_3, two eigenvalues with opposite Krein signatures coalesce and bifurcate into a complex quadruplet according to Theorem 13.

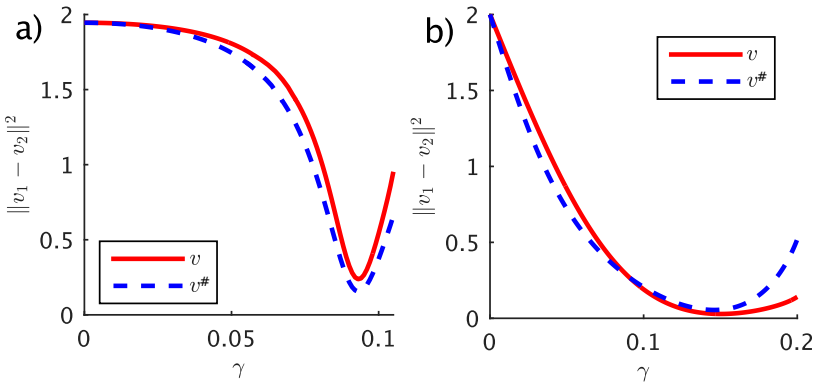

Figure 5.5: The norm of the difference between the two eigenvectors and the two adjoint eigenvectors prior to a possible coalescence point: (a) for Figure 5.3 (b) for Figure 5.4.

Chapter 6

Conclusion

In this thesis, we have presented several new contributions to stability analysis in $\mathcal{PT}$-symmetric systems both in discrete and continuous settings. Let us review the original results and provide some possible considerations for future work.

6.1 Summary of Main Results

Chapter 2 is dedicated to the study of existence and stability of breather type solutions in infinite-dimensional dNLS model (1.3). These are solutions of the form

$$u(t) = Ue^{-iEt}, \quad v(t) = Ve^{-iEt},$$

where the frequency parameter E is real, and the sequence $(U, V) \in l^2(\mathbb{Z})$ is time-independent. Existence and spectral stability of breathers can be characterized in the limit of small coupling constant ϵ, when breathers bifurcate from solutions of the dimer equation arising at a single site, say the central site at $n = 0$. This technique was introduced for the $\mathcal{PT}$-symmetric systems in [80, 115] and is applied to the system of amplitude equations (1.3) in Chapter 2.

Figure 6.1 represents branches of the time-periodic solutions of the central dimer at $\epsilon = 0$, where the amplitude of the central dimer $A = |U_0| = |V_0|$ is plotted versus the frequency parameter E. The left panel corresponds to the solution with $\Omega > \gamma > 0$, whereas the right panel corresponds to the solution with $\Omega < -\gamma < 0$. The constraint $|\gamma| < |\Omega|$ is used for stability of the zero equilibrium at $\epsilon = 0$ outside the central dimer. The values $\pm E_0$ with $E_0 := \sqrt{\Omega^2 - \gamma^2}$ correspond to bifurcation of the small-amplitude solutions. The small-amplitude solutions are connected with the large-amplitude solutions for $\Omega > \gamma > 0$, whereas the branches of small-amplitude and large-amplitude solutions are disconnected for $\Omega < -\gamma < 0$.

Every time-periodic solution supported at the central dimer for $\epsilon = 0$ is continued uniquely and smoothly with respect to the small coupling parameter ϵ by the implicit function arguments. The

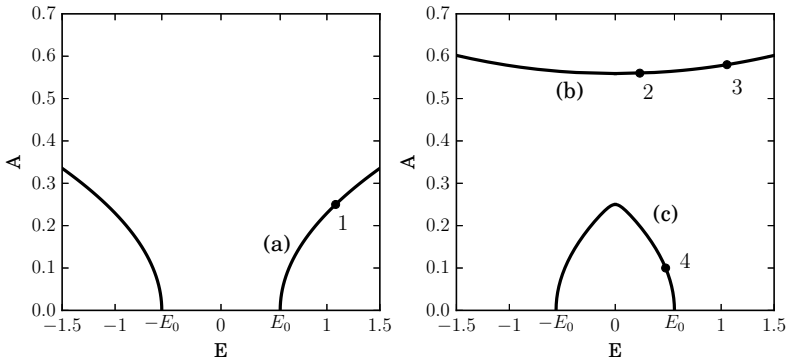

Figure 6.1: Time-periodic solutions of the $\mathcal{PT}$-symmetric dimer with $A = |U_0| = |V_0|$ versus frequency E for $\gamma = \frac{1}{2}$ and (a) $\Omega = \frac{3}{4} > \gamma$ or (b) $\Omega = -\frac{3}{4} < -\gamma$.

resulting breather is symmetric about the central site and $\mathcal{PT}$-symmetric so that

$$V_n = \bar{U}_n = \bar{U}_{-n} = V_{-n}, \quad n \in \mathbb{Z}. \tag{6.1}$$

Moreover, the breather profile decays fast at infinity.

Since breather solutions (U, V) are critical points of the extended energy function

$$H_E := H - EQ, \tag{6.2}$$

we study the nonlinear stability of breathers by the Lyapunov method if the second variation of H_E is sign-definite in $\ell^2(\mathbb{Z})$. The second variation of H_E is given by a quadratic form associated with the self-adjoint (Hessian) operator $\mathcal{H}_E'' : \ell^2(\mathbb{Z}) \to \ell^2(\mathbb{Z})$.

For the two solution branches with $\Omega < -\gamma < 0$ and $|E| < E_0$ (points 2 and 4 on Figure 6.1), it is shown in Chapter 2 that the infinite-dimensional part of the spectrum of $\mathcal{H}_E''$ in $\ell^2(\mathbb{Z})$ is negative definite and the rest of the spectrum includes a simple zero eigenvalue due to gauge symmetry and either three (in case of point 2) or one (in case of point 4) positive eigenvalues. As a result, the nonlinear orbital stability of the corresponding breathers is developed in Chapter 2 by using the standard energy methods [42, 68].

On the other hand, for the solution branches with $|E| > E_0$ (points 1 and 3 on Figure 6.1), it is shown in Chapter 2 that the spectrum of $\mathcal{H}_E''$ in $\ell^2(\mathbb{Z})$ includes infinite-dimensional positive and negative parts. Therefore, for $|E| > E_0$ both for $\Omega > \gamma > 0$ and $\Omega < -\gamma < 0$, (U, V) is an infinite-dimensional saddle point of the extended energy function H_E. This is very similar to the Hamiltonian systems of the Dirac type, where the zero equilibrium and standing waves are located in the gap between the positive and negative continuous spectrum.

Spectral stability of the solution branches with $\Omega > \gamma > 0$ and $|E| > E_0$ is proved for sufficiently small ϵ under the non-resonance condition, which is checked numerically. On the other hand, the solution branch with $\Omega < -\gamma < 0$ and $|E| > E_0$ is spectrally stable for sufficiently small ϵ almost everywhere except for the narrow interval in the parameter space, where the non-resonance condition

is not satisfied. Since in both cases, (U, V) is an infinite-dimensional saddle point of the extended energy function H_E, the standard energy methods [68] can not be applied to the proof of nonlinear stability of the solution branches with $|E| > E_0$.

The main contribution of Chapter 3 is a proof of long-time nonlinear stability of the infinite-dimensional saddle point (U, V) by using the asymptotic limit of small coupling parameter ϵ. The novel method which we develop there works for the solution branches with $\Omega > \gamma > 0$ (point 1 on Figure 6.1) but does not work for the solution branch with $\Omega < -\gamma < 0$ and $|E| > E_0$ (point 3 on Figure 6.1).

To remedy the difficulty with the energy method, we select the energy function in the form

$$\Lambda_E := H - E(u_0\bar{v}_0 + \bar{u}_0 v_0). \tag{6.3}$$

Note that Λ_E is different from the extended energy function H_E in (6.2), since Λ_E only includes the part of Q at the central site $n = 0$, where (U, V) is supported if $\epsilon = 0$. With the definition of Λ_E given by (6.3), we obtain a function with a positive second variation at (U, V), however, two new obstacles arise now:

- the first variation of Λ_E does not vanish at (U, V) if $\epsilon \neq 0$;
- the value of Λ_E is no longer constant in the time evolution of the dNLS equation (1.3).

The first difficulty is overcome with a local transformation of dependent variables. However, due to the second difficulty, instead of the nonlinear stability for all times, as in Lyapunov's stability theorem (see Section 1.5), we only establish a long-time nonlinear stability of the breather on a long but finite time interval. This long-time stability is usually referred as *metastability*.

We note that the energy functional similar to (6.3) is typically used in the normal form transformations as the leading-order Hamiltonian, where it can be adopted for the proof of asymptotic stability of breathers under some restrictive assumptions on the nonlinear functions [12]. Compared to this approach, we do not use dispersive decay estimates and hence have no control on the perturbations to extend the time interval for long-time stability of breathers to all times.

Chapter 4 does not contain original results. We review the Hamiltonian theory, including the necessary condition for instability bifurcation as a result of the splitting upon collision of two eigenvalues of opposite Krein signature. An instructive case example from the area of Bose–Einstein condensation provides a countable sequence of nonlinear states bifurcating from eigenstates of a quantum harmonic oscillator. The Krein signature is defined for the linearized NLS equation at each of these nonlinear states in the Hamiltonian case.

In Chapter 5 we introduce the Krein quantity for simple isolated eigenvalues in the linearization of the nonlinear modes in the $\mathcal{PT}$-symmetric NLS equation. We prove that the Krein quantity is zero for complex eigenvalues and nonzero for simple purely imaginary eigenvalues. When two simple eigenvalues coalesce on the imaginary axis in a defective eigenvalue, the Krein quantity vanishes and we prove under the non-degeneracy assumption that this bifurcation point produces complex unstable eigenvalues on one side of the bifurcation point. This result shows that the main feature of the instability bifurcation in Hamiltonian systems is extended to the $\mathcal{PT}$-symmetric NLS equation.

There are nevertheless limitations of this theory in the $\mathcal{PT}$-symmetric systems. First, the adjoint eigenvectors are no longer related to the eigenvectors of the spectral problem, which opens up a problem of normalizing the adjoint eigenvector relative to the eigenvector. We fix the sign of the adjoint eigenvector in the Hamiltonian limit and continue the sign off the Hamiltonian limit by using continuity of eigenvectors along the parameters of the model.

Second, if the bifurcation point corresponds to a semi-simple eigenvalue, then the bifurcation theory does not lead to the same conclusion as in the Hamiltonian case. The first-order perturbation theory results in the non-Hermitian matrices, hence it is not clear how to conclude on the splitting of the semi-simple eigenvalues on each side of the bifurcation point.

Finally, coalescence of the simple purely imaginary eigenvalues at the origin and the related instability bifurcations are observed frequently in the $\mathcal{PT}$-symmetric systems and they are not predicted from the Krein quantity. Therefore, we conclude that the stability theory of Hamiltonian systems cannot be fully extended to the $\mathcal{PT}$-symmetric NLS equation, only the necessary condition for the instability bifurcation can be, as is shown in Chapter 5.

6.2 Future Directions

This thesis leads to the following open questions and directions for further studies:

- It is known that in Hamiltonian systems negative Krein signature of an eigenvalue can lead to nonlinear instability even if the stationary state is linearly stable [78]. It is worthwhile to use our definition of $\mathcal{PT}$-Krein signature to verify whether the same phenomena is present in general $\mathcal{PT}$-symmetric systems.

- In the studies of the spectral stability problems, we have often encountered bifurcation at zero, i.e. when the smallest eigenvalue coalesces with its symmetric counterpart at $\lambda = 0$. The role of bifurcation at zero is not well understood. Classical bifurcation theory suggests that there might exist additional stationary states appearing after this bifurcation, i.e., a symmetry-breaking point occurs. Notice that unlike $\mathcal{PT}$-symmetry breaking point defined in a linear system, this symmetry-breaking bifurcation occurs in the nonlinear system and is of interest in its own.

- It is worthwhile to consider two-dimensional $\mathcal{PT}$-symmetric version of nonlinear Schrödinger equation arising in condensed matter theory [43, 73, 116]. Using a traditional simplification, one can replace the non-local interaction potential with a localized short-range interaction proportional to the delta function. This leads to the Gross–Pitaevskii equation, more precisely to nonlinear Schrödinger equation with cubic nonlinearity and with a spatially dependent trap potential stationary in a frame rotating with a certain frequency about the vertical axis. The equation in question, like many other nonlinear Schrödinger equations, supports the existence of localized-in-space solutions of different kinds. In particular, one could look for vortex-type solutions and investigate their stability properties in the case of complex-valued $\mathcal{PT}$-symmetric potential.

- In the Hamiltonian version of the Gross–Pitaevskii equation (with real-valued potential) there has been a great progress in numerical algorithms utilizing the so-called Evans function [83]. Evans function enables one to find spectra more efficiently and precisely. It will be worthwhile to adapt Evans function to $\mathcal{PT}$-symmetric systems and equip the algorithm with the ability to compute $\mathcal{PT}$-Krein signature.

Overall, there are a number of other challenging problems in the topic of $\mathcal{PT}$-symmetry. One can study formation of $\mathcal{PT}$-symmetric rogue waves in inhomogeneous and non-Hermitian optical systems, or the connection between modulational instability and formation of $\mathcal{PT}$-symmetric lattice solitons, to name a few [39].

Appendix A

Perturbation theory near Hamiltonian case

In this Appendix we attempt to build a connection between eigenvectors and adjoint eigenvectors of the stability problem (5.6) near the Hamiltonian case $\gamma = 0$. We show that there is no simple relationship between eigenvectors of original and adjoint operators. This is the reason why we have to compute both eigenvectors in Krein signature definition for $\mathcal{PT}$-symmetric systems.

A.1 Series in γ

Recall the eigenvalue problem (5.6) describing the spectrum of linearization about a stationary state Φ:

$$\begin{bmatrix} L & -\Phi^2 \\ -\overline{\Phi^2} & L^* \end{bmatrix} \begin{bmatrix} Y \\ Z \end{bmatrix} = i\lambda\sigma_3 \begin{bmatrix} Y \\ Z \end{bmatrix}, \tag{A.1}$$

where $L = -\partial_x^2 + V(x) + i\gamma W(x) - \mu - 2|\Phi(x)|^2$, and $W(x), \Phi(x)$ decay to zero at $x \to \pm\infty$. Moreover, $V(-x) = V(x), W(-x) = -W(x)$ are real-valued functions, and $\mu \in \mathbb{R}$. Recall that $\Phi(x)$ is $\mathcal{PT}$-symmetric: $\Phi(x) = \overline{\Phi(-x)}$ and satisfies the equation

$$\mu\Phi = (-\partial_x^2 + V(x) + i\gamma W(x) - |\Phi|^2)\Phi. \tag{A.2}$$

Let $\gamma = 0$ in eigenvalue problem (A.1). Then it can be rewritten as:

$$\begin{bmatrix} L_0 & -\Phi_0^2 \\ -\overline{\Phi_0^2} & L_0 \end{bmatrix} \begin{bmatrix} Y_0 \\ Z_0 \end{bmatrix} = i\lambda_0\sigma_3 \begin{bmatrix} Y_0 \\ Z_0 \end{bmatrix}, \tag{A.3}$$

where we have used the fact that operator $L_0 = -\partial_x^2 + V - \mu - 2|\Phi_0|^2$ is self-adjoint. We will denote operator in (A.3) as $\mathcal{L}_0$. For $\lambda_0 \in i\mathbb{R}$ problem (A.3) is self-adjoint. If λ_0 is also simple, then the

eigenvector for the adjoint operator can be chosen so that

$$\begin{bmatrix} Y_0^* \\ Z_0^* \end{bmatrix} = \begin{bmatrix} Y_0 \\ Z_0 \end{bmatrix}. \tag{A.4}$$

Recall that Φ_0 satisfies the following equation:

$$\mu\Phi_0 = (-\partial_x^2 + V(x) - |\Phi_0|^2)\Phi_0. \tag{A.5}$$

Notice that coefficients in this equation are all real, therefore $\Phi_0(x) \in \mathbb{R}$. Since $\Phi_0(x)$ is also $\mathcal{PT}$-symmetric, it follows that it is an *even* function.

Putting $\lambda_0 = i\Omega_0, \Omega_0 \in \mathbb{R}$ simple, we set $\gamma \neq 0, \gamma \in \mathbb{R}$ and employ perturbation theory. First of all, we write series in γ for all terms that depend on γ. Notice that Φ, although not visibly, depends on γ. We write series up to $O(\gamma^3)$:

$$\begin{aligned} i\lambda(\gamma) &= -\Omega_0 - i\gamma\Omega_1 - \gamma^2\Omega_2 + O(\gamma^3), \\ \Phi(\gamma) &= \Phi_0 + i\gamma\Phi_1 + \gamma^2\Phi_2 + O(\gamma^3), \\ \begin{bmatrix} Y(x;\gamma) \\ Z(x;\gamma) \end{bmatrix} &= \begin{bmatrix} Y_0 \\ Z_0 \end{bmatrix} + i\gamma \begin{bmatrix} Y_1 \\ Z_1 \end{bmatrix} + \gamma^2 \begin{bmatrix} Y_2 \\ Z_2 \end{bmatrix} + O(\gamma^3), \\ \begin{bmatrix} Y^*(x;\gamma) \\ Z^*(x;\gamma) \end{bmatrix} &= \begin{bmatrix} Y_0 \\ Z_0 \end{bmatrix} + i\gamma \begin{bmatrix} Y_1^* \\ Z_1^* \end{bmatrix} + \gamma^2 \begin{bmatrix} Y_2^* \\ Z_2^* \end{bmatrix} + O(\gamma^3). \end{aligned}$$

Let us write $O(\gamma)$ terms for (A.2):

$$\mu\Phi_1 = (-\partial_x^2 + V(x) - |\Phi_0|^2)\Phi_1 + W\Phi_0 - \Phi_0^2(\overline{\Phi_1} + \Phi_1). \tag{A.6}$$

As we can see, this equation has real-valued coefficients and thus $\Phi_1(x)$ is real-valued. Symmetries of coefficients in the equation also imply that $\Phi_1(x)$ is an odd function: $\Phi_1(-x) = -\Phi_1(x)$. For $O(\gamma^2)$ terms, (A.2) gives

$$\mu\Phi_2 = (-\partial_x^2 + V(x) - |\Phi_0|^2)\Phi_2 - W\Phi_1 - \Phi_0\Phi_1^2 - \Phi_0^2(\Phi_2 + \overline{\Phi_2}). \tag{A.7}$$

From here we have $\Phi_2(x) \in \mathbb{R}$, and $\Phi_2(x)$ is even: $\Phi_2(x) = \Phi_2(-x)$.

A.2 $O(\gamma)$ balance equations

Let us rewrite eigenvalue problem (A.1) for $\gamma \neq 0$, keeping only $O(\gamma)$ terms:

$$(\mathcal{L}_0 + \Omega_0\sigma_3) \begin{bmatrix} Y_1 \\ Z_1 \end{bmatrix} = (-W(x) + 2\sigma_1\Phi_0\Phi_1 - \Omega_1)\,\sigma_3 \begin{bmatrix} Y_0 \\ Z_0 \end{bmatrix}, \tag{A.8}$$

and the adjoint problem becomes

$$(\mathcal{L}_0 + \Omega_0\sigma_3)\begin{bmatrix} Y_1^* \\ Z_1^* \end{bmatrix} = (W(x) + 2\sigma_1\Phi_0\Phi_1 - \Omega_1)\,\sigma_3\begin{bmatrix} Y_0 \\ Z_0 \end{bmatrix}. \tag{A.9}$$

According to the Fredholm theory, (A.8) and (A.9) have solutions only when the right-hand side is orthogonal to the kernel of corresponding adjoint operator, in our case consisting of a single eigenvector $[Y_0, Z_0]^T$. Let us split the right-hand side into several terms and consider them separately:

- $W(x)\sigma_3[Y_0, Z_0]^T$:

$$\left\langle W(x)\sigma_3\begin{bmatrix} Y_0 \\ Z_0 \end{bmatrix}, \begin{bmatrix} Y_0 \\ Z_0 \end{bmatrix}\right\rangle = \int_{\mathbb{R}} W(x)(Y_0^2 - Z_0^2)dx = 0, \tag{A.10}$$

  as an integral of odd function over the real line is equal to zero.

- $\sigma_1\Phi_0\Phi_1\sigma_3[Y_0, Z_0]^T$:

$$\left\langle \sigma_1\Phi_0\Phi_1\sigma_3\begin{bmatrix} Y_0 \\ Z_0 \end{bmatrix}, \begin{bmatrix} Y_0 \\ Z_0 \end{bmatrix}\right\rangle = \int_{\mathbb{R}} \Phi_0\Phi_1(Y_0Z_0 - Z_0Y_0) = 0. \tag{A.11}$$

- $\Omega_1\sigma_3[Y_0, Z_0]^T$:

$$\left\langle \Omega_1\sigma_3\begin{bmatrix} Y_0 \\ Z_0 \end{bmatrix}, \begin{bmatrix} Y_0 \\ Z_0 \end{bmatrix}\right\rangle = \Omega_1\int_{\mathbb{R}} (Y_0^2 - Z_0^2)dx, \tag{A.12}$$

  where the integral is nonzero. This follows from nonexistence condition for the generalized eigenvector $[Y_g, Z_g]^T$, as eigenvalue $\lambda_0 = i\Omega_0$ is assumed to be simple. Therefore we must choose $\Omega_1 = 0$.

Moreover, if $[Y_1, Z_1]^T$ is orthogonal to $[Y_0, Z_0]^T$, then the solution of (A.8) is unique. Same holds for the adjoint counterpart. By adding and subtracting (A.8) with (A.9), we can relate eigenvectors in a unique way.

Note that both (A.8) and (A.9) have real-valued coefficients, which also have odd symmetry, therefore $[Y_1, Z_1]^T$ and $[Y_1^*, Z_1^*]^T$ are both real-valued functions and possess odd symmetry property.

A.3 $O(\gamma^2)$ balance equations

Collecting only $O(\gamma^2)$ terms in (A.1) for $\gamma \neq 0$, we get

$$\begin{aligned}(\mathcal{L}_0 + \Omega_0\sigma_3)\begin{bmatrix} Y_2 \\ Z_2 \end{bmatrix} = &(W(x) - 2\sigma_1\Phi_0\Phi_1)\,\sigma_3\begin{bmatrix} Y_1 \\ Z_1 \end{bmatrix} \\ &+ \left(\begin{bmatrix} 2\Phi_1^2 + 4\Phi_0\Phi_2 & -\Phi_1^2 + 2\Phi_0\Phi_2 \\ -\Phi_1^2 + 2\Phi_0\Phi_2 & 2\Phi_1^2 + 4\Phi_0\Phi_2 \end{bmatrix} - \Omega_2\sigma_3\right)\begin{bmatrix} Y_0 \\ Z_0 \end{bmatrix}.\end{aligned} \tag{A.13}$$

For the adjoint problem we have:

$$(\mathcal{L}_0+\Omega_0\sigma_3)\begin{bmatrix} Y_2^* \\ Z_2^* \end{bmatrix} = (-W(x)-2\sigma_1\Phi_0\Phi_1)\,\sigma_3\begin{bmatrix} Y_1^* \\ Z_1^* \end{bmatrix} + \left(\begin{bmatrix} 2\Phi_1^2+4\Phi_0\Phi_2 & -\Phi_1^2+2\Phi_0\Phi_2 \\ -\Phi_1^2+2\Phi_0\Phi_2 & 2\Phi_1^2+4\Phi_0\Phi_2 \end{bmatrix} - \Omega_2\sigma_3\right)\begin{bmatrix} Y_0 \\ Z_0 \end{bmatrix}. \tag{A.14}$$

In both equations (A.13), (A.14), coefficients are given by real-valued even functions, therefore $[Y_2, Z_2]^T, [Y_2^*, Z_2^*]^T$ are real-valued and even, as well.

We could employ Fredholm theory again, but this time the projections on the kernel of the adjoint operator would have to be incorporated in the coefficient Ω_2, which will be nonzero, in general. If both $[Y_2, Z_2]^T$ and $[Y_2^*, Z_2^*]^T$ exist and are orthogonal to $[Y_0, Z_0]^T$, they are unique and so is their relationship (add or subtract (A.13) and (A.14)).

To find a relationship between $[Y, Z]^T$ and $[Y^*, Z^*]^T$ we could use the obtained equations to split each eigenvector as $[Y, Z]^T = [Y^+, Z^+]^T + [Y^-, Z^-]^T$, and adjoint eigenvector as $[Y^*, Z^*]^T = [Y^+, Z^+]^T - [Y^-, Z^-]^T$. Let us consider this separation for the first order in γ:

$$\begin{bmatrix} Y_1 \\ Z_1 \end{bmatrix} = \begin{bmatrix} Y_1^+ \\ Z_1^+ \end{bmatrix} - \begin{bmatrix} Y_1^- \\ Z_1^- \end{bmatrix}, \tag{A.15}$$
$$\begin{bmatrix} Y_1^+ \\ Z_1^+ \end{bmatrix} = (2\sigma_1\Phi_0\Phi_1-\Omega_1)\sigma_3\begin{bmatrix} Y_0 \\ Z_0 \end{bmatrix},$$
$$\begin{bmatrix} Y_1^- \\ Z_1^- \end{bmatrix} = W(x)\sigma_3\begin{bmatrix} Y_0 \\ Z_0 \end{bmatrix}.$$

For the next order in γ we get

$$\begin{bmatrix} Y_2 \\ Z_2 \end{bmatrix} = \begin{bmatrix} Y_2^+ \\ Z_2^+ \end{bmatrix} - \begin{bmatrix} Y_2^- \\ Z_2^- \end{bmatrix},$$
$$\begin{bmatrix} Y_2^+ \\ Z_2^+ \end{bmatrix} = (-2\sigma_1\Phi_0\Phi_1)\sigma_3\begin{bmatrix} Y_1 \\ Z_1 \end{bmatrix} + \left(\begin{bmatrix} 2\Phi_1^2+4\Phi_0\Phi_2 & -\Phi_1^2+2\Phi_0\Phi_2 \\ -\Phi_1^2+2\Phi_0\Phi_2 & 2\Phi_1^2+4\Phi_0\Phi_2 \end{bmatrix} - \Omega_2\sigma_3\right)\begin{bmatrix} Y_0 \\ Z_0 \end{bmatrix},$$
$$\begin{bmatrix} Y_2^- \\ Z_2^- \end{bmatrix} = W(x)\sigma_3\begin{bmatrix} Y_1 \\ Z_1 \end{bmatrix}.$$

Unfortunately, here $[Y_2^+, Z_2^+]^T$ depends on both $[Y_1^+, Z_1^+]^T$ and $[Y_1^-, Z_1^-]^T$ through (A.15). Therefore the solution cannot be separated into $[Y^+, Z^+]^T$ and $[Y^-, Z^-]^T$ parts independent of each other, and there is no simple relationship between eigenvectors and adjoint eigenvectors for $\gamma \neq 0$.

Appendix B

Spectrum of the linear problem for Scarf II potential

In this Appendix we are going to derive analytic formulas for eigenvalues and eigenfunctions of the stationary problem for linear Schrödinger equation with Scarf II type potential (1.12). Our goal is to correct the mistake of [3], where the author missed one of the solutions to the eigenvalue problem.

Consider a linear Schrödinger equation:

$$i\partial_t\psi + \partial_x^2\psi - U(x)\psi = 0,$$

with Scarf II potential

$$U(x) = V_1 \operatorname{sech}^2(x) + iV_2 \operatorname{sech}(x)\tanh(x),$$

where V_1, V_2 are real constants. We will be looking for stationary modes in the form $\psi(x,t) = \Phi(x)e^{iEt}$, where $E \in \mathbb{R}$, $\Phi(x)$ decays to zero at infinity, and solves

$$\Phi_{xx} + (-E + V_1 \operatorname{sech}^2(x) + iV_2 \operatorname{sech}(x)\tanh(x))\Phi = 0. \tag{B.1}$$

This equation can also be viewed as an eigenvalue problem for E with eigenfunctions Φ. In that case the mode Φ is stable when E is real, and unstable otherwise, due to symmetry of eigenvalues in $\mathcal{PT}$-symmetric systems. Using a change of coordinates $z = \frac{1}{2}(1 - i\sinh(x))$ and a substitution $\Phi = z^{-p}(1-z)^{-q}w(z)$, we can rewrite linear stationary problem (B.1) as

$$z(1-z)w''(z) + \left(-2p + \frac{1}{2} - (-2p-2q+1)z\right)w'(z) - \left((p+q)^2 - E\right)w(z) = 0, \tag{B.2}$$

where p, q are given by:

$$p_{1,2} = -\frac{1}{4} \pm \frac{1}{2}\sqrt{\frac{1}{4} + V_1 + V_2}, \quad q_{1,2} = -\frac{1}{4} \pm \frac{1}{2}\sqrt{\frac{1}{4} + V_1 - V_2}. \tag{B.3}$$

Recall Gauss hypergeometric equation [58]:

$$z(1-z)\frac{d^2u}{dz^2} + (\gamma - (\alpha+\beta+1)z)\frac{du}{dz} - \alpha\beta u = 0, \tag{B.4}$$

where $\alpha, \beta, \gamma \in \mathbb{C}$ are constants. Comparing (B.4) with (B.2), one can find α, β, γ:

$$\begin{cases} \alpha = \frac{1}{2} \mp \frac{1}{2}\sqrt{\frac{1}{4} + V_1 + V_2} \mp \frac{1}{2}\sqrt{\frac{1}{4} + V_1 - V_2} \pm \sqrt{E}, \\ \beta = \frac{1}{2} \mp \frac{1}{2}\sqrt{\frac{1}{4} + V_1 + V_2} \mp \frac{1}{2}\sqrt{\frac{1}{4} + V_1 - V_2} \mp \sqrt{E}, \\ \gamma = 1 \mp \sqrt{\frac{1}{4} + V_1 + V_2}. \end{cases} \tag{B.5}$$

The solution of (B.4) is given by hypergeometric series [58]:

$$\begin{aligned} u &= F(\alpha, \beta, \gamma, z) \\ &= 1 + \frac{\alpha \cdot \beta}{\gamma \cdot 1} z + \frac{\alpha(\alpha+1)\beta(\beta+1)}{\gamma(\gamma+1)\cdot 1 \cdot 2} z^2 + \frac{\alpha(\alpha+1)(\alpha+2)\beta(\beta+1)(\beta+2)}{\gamma(\gamma+1)(\gamma+2)\cdot 1 \cdot 2 \cdot 3} z^3 + \dots \end{aligned}$$

Notice that when α or β is a negative integer, series are truncated and contain finitely many terms. More precisely, α and β have to satisfy one of the quantization conditions:

$$\alpha = -n \text{ or } \beta = -n, \text{ where } n = 0, 1, 2, \dots \tag{B.6}$$

The final solution of (B.1) is given by

$$\Phi(x) = \left(\frac{1 - i\sinh(x)}{2}\right)^{-p} \left(\frac{1 + i\sinh(x)}{2}\right)^{-q} F\left(\alpha, \beta, \gamma, \frac{1 - i\sinh(x)}{2}\right), \tag{B.7}$$

where by quantization condition F is a polynomial of degree n. In order for the eigenfunction $\Phi(x)$ to satisfy the boundary condition at $\pm\infty$, the following inequality must hold:

$$0 \le n < \mathrm{Re}(p+q),$$

or, using (B.3),

$$0 \le n < \mathrm{Re}\left(-\frac{1}{2} \pm \frac{1}{2}\sqrt{\frac{1}{4} + V_1 + V_2} \pm \frac{1}{2}\sqrt{\frac{1}{4} + V_1 - V_2}\right), \tag{B.8}$$

where the upper bound has to be positive. Therefore minus-minus sign combination cannot be chosen for both $\pm$ in (B.8). Note that the expression in brackets is real when $|V_2| < V_1 + \frac{1}{4}$.

Using either one of quantization conditions (B.6) and definitions of α, β in (B.5), we derive a formula for n and discuss all possible cases:

$$n = -\frac{1}{2} \pm \frac{1}{2}\sqrt{\frac{1}{4} + V_1 + V_2} \pm \frac{1}{2}\sqrt{\frac{1}{4} + V_1 - V_2} \pm \sqrt{E}. \tag{B.9}$$

In order for inequality (B.8) to be satisfied, the minus sign for $\sqrt{E}$ must be selected. Out of 8 possible combinations, there are only 3 left:

$$n^{(1)} = -\frac{1}{2} + \frac{1}{2}\sqrt{\frac{1}{4} + V_1 + V_2} + \frac{1}{2}\sqrt{\frac{1}{4} + V_1 - V_2} - \sqrt{E},$$
$$n^{(2)} = -\frac{1}{2} + \frac{1}{2}\sqrt{\frac{1}{4} + V_1 + V_2} - \frac{1}{2}\sqrt{\frac{1}{4} + V_1 - V_2} - \sqrt{E},$$
$$n^{(3)} = -\frac{1}{2} - \frac{1}{2}\sqrt{\frac{1}{4} + V_1 + V_2} + \frac{1}{2}\sqrt{\frac{1}{4} + V_1 - V_2} - \sqrt{E}.$$

The case $n^{(1)}$ was studied in detail in [3], where it was shown that the corresponding eigenvalue $E^{(1)}$ becomes complex for $|V_2| > V_1 + \frac{1}{4}$. Unfortunately, in [3] branches $n^{(2)}$ and $n^{(3)}$ were omitted, and author did not discuss why eigenvalue bifurcates off to the complex plane. We know from bifurcation theory that generally such bifurcation happens when two simple discrete eigenvalues coalesce on the real axis, or a simple discrete eigenvalue collides with continuous spectrum, in our case located on the real axis $[0, +\infty)$. Using expressions for $n^{(j)}$ above, we can write three branches of eigenvalues explicitly:

$$E_n^{(1)} = \left(-n - \frac{1}{2} + \frac{1}{2}\sqrt{\frac{1}{4} + V_1 + V_2} + \frac{1}{2}\sqrt{\frac{1}{4} + V_1 - V_2}\right)^2,$$
$$E_n^{(2)} = \left(-n - \frac{1}{2} + \frac{1}{2}\sqrt{\frac{1}{4} + V_1 + V_2} - \frac{1}{2}\sqrt{\frac{1}{4} + V_1 - V_2}\right)^2,$$
$$E_n^{(3)} = \left(-n - \frac{1}{2} - \frac{1}{2}\sqrt{\frac{1}{4} + V_1 + V_2} + \frac{1}{2}\sqrt{\frac{1}{4} + V_1 + V_2}\right)^2.$$

Notice that for $V_2 = V_1 + \frac{1}{4}$, eigenvalues corresponding to first and second branches coalesce and bifurcate off to the complex plane for $V_2 > V_1 + \frac{1}{4}$. Also, for $V_2 = -V_1 - \frac{1}{4}$, first and third branches coalesce and bifurcate into the complex plane for $V_2 < -V_1 - \frac{1}{4}$.

For example, for $V_1 = 1, V_2 = 1.2$, the upper bound for n for first and second branches is positive and nonzero, therefore $n = 0$ gives $E_0^{(1)} \approx 0.1556, E_0^{(2)} \approx 0.0292$, and for $V_2 = 1.25$ these two are equal: $E_0^{(1)} = E_0^{(2)} \approx 0.0844$. For $V_2 > 1.25$ both become complex. See also Figure B.1.

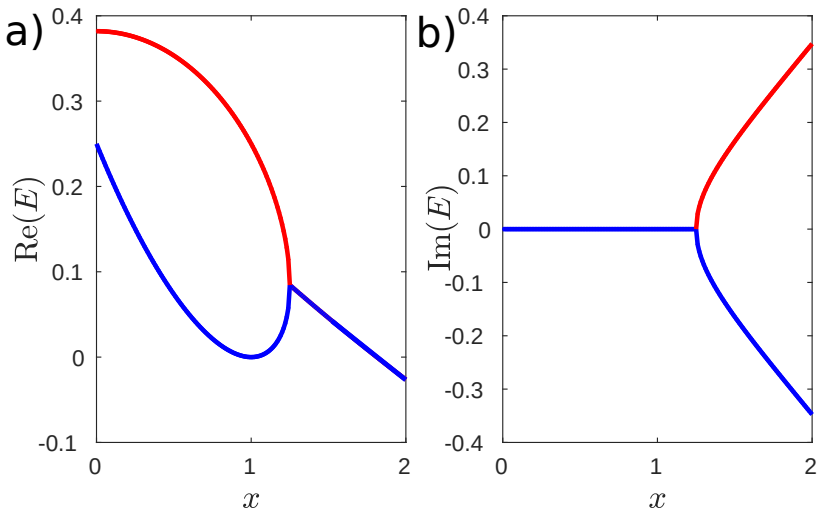

Figure B.1: First two eigenvalues for spectral problem (B.1) with $n = 0$. Red color corresponds to $E_0^{(1)}$, whereas blue corresponds to $E_0^{(2)}$. a) Real parts b) Imaginary parts.

Appendix C

Wadati potentials: exact solutions

In this Appendix we derive a formula for exact solutions for $\mathcal{PT}$-symmetric stationary NLS (1.11) with Wadati-type potentials, for which Scarf II potential (1.12) is a special case. The technique used here was presented in [17], where authors described the way to construct potentials for which exact solutions are available. Notice that the exact solutions are obtained for the full nonlinear equation, unlike the Appendix B. The exact solutions obtained via this method were used for verification of numerical algorithms presented in Chapter 5.

C.1 Derivation

Let us write the problem (A.2) for the nonlinear mode Φ:

$$\Phi_{xx} + (U^2 - iU_x)\Phi + 2\Phi|\Phi|^2 = \mu\Phi,$$

where $\Phi(x) = \overline{\Phi(-x)}$ is $\mathcal{PT}$-symmetric, $\mu \in \mathbb{R}$ is a real eigenvalue parameter, and $U(x) = U(-x)$ is a real valued function. Let us rewrite this equation as a system of equations:

$$\begin{cases} \frac{d\Phi}{dx} = iU\Phi - \Psi, \\ \frac{d\Psi}{dx} = \mu\Phi - iU\Phi + 2|\Phi|^2\Phi, \end{cases} \tag{C.1}$$

where $\Psi = -d\Phi/dx + iU\Phi$. Take

$$\Phi = ae^{i\theta}, \quad \Psi = be^{i\chi}, \tag{C.2}$$

where $a(x), b(x), \theta(x), \chi(x)$ are real-valued functions of x. Substituting these into system (C.1), one can get:

$$\begin{cases} a_x = -b\cos\nu, \\ b_x = a(2a^2 + \mu)\cos\nu, \\ a(U - \theta_x) = b\sin\nu, \\ b(\chi_x + U) = -a(2a^2 + \mu)\sin\nu, \end{cases} \tag{C.3}$$

where $\nu(x) = \chi(x) - \theta(x)$. System (C.3) has a conserved quantity:

$$a^2(\mu + a^2) + b^2 = 0. \tag{C.4}$$

From here we can see that μ must be chosen negative: $\mu = -\kappa^2$, $\kappa \in \mathbb{R}$.

Using (C.4) and first equation in (C.3), we get:

$$\int_0^x \frac{dy}{a\sqrt{\kappa^2 - a^2}} = -\int_0^x \cos\nu(y)dy + C,$$

and choosing seed function $\cos\nu(y)$, we take $D(x)$ to be

$$D(x) = \kappa \int_0^x \cos\nu(y)dy + C,$$

where constant of integration C can be chosen to be zero without loss of generality. Then we rewrite the equation for a:

$$a = \kappa\,\mathrm{sech}(D(x)),$$

and for b

$$b = a\sqrt{\kappa^2 - a^2} = \kappa^2\,\mathrm{sech}(D(x))\tanh(D(x)).$$

Adding and subtracting two last equations in (C.3), one can get:

$$U = -\frac{\nu_x}{2} + \frac{a}{2b}(2\kappa^2 - 3a^2)\sin\nu \tag{C.5}$$

and

$$\theta = -\frac{\nu}{2} - \int \frac{a^3}{2b}\sin\nu dx. \tag{C.6}$$

The main idea of [17] can be summarized as follows: *given a seed function* $\cos\nu(x)$*, find potential* U *and exact solution* $\Phi(x)$*, namely find* $a(x)$ *and* $\theta(x)$. We would also like to find an exact solution in a simple form.

One can rewrite equation (C.5) as

$$U = \frac{(\cos\nu(x))'}{2\sin\nu(x)} - \frac{\kappa\sin\nu(x)}{2\tanh(D(x))} + \frac{3}{2}\kappa\sin\nu(x)\tanh(D(x))$$

or, using the definition of $D(x)$, as

$$U = \frac{(\cos\nu(x))'}{2\sin\nu(x)} - \frac{\kappa\sin\nu(x)}{2\tanh\left(\kappa\int\cos\nu(x)dx\right)} + \frac{3}{2}\kappa\sin\nu(x)\tanh\left(\kappa\int\cos\nu(x)dx\right).$$

From here we can see that to construct a potential (and a corresponding exact solution), one needs a smart choice of a seed function $\cos\nu(x)$. As we see, it is not trivial to find a seed function $\cos\nu(x)$ such that $U(x)$ will be independent of κ. Otherwise the solutions obtained by this method will only be valid for fixed μ.

C.2 An example

Let us select the seed function as

$$\cos\nu = \frac{\sinh(\kappa x)}{\sqrt{1-\kappa\sin^2\alpha+\sinh^2(\kappa x)}}, \tag{C.7}$$

where $\alpha \in (0, \frac{\pi}{2})$ is a parameter. Then

$$\begin{aligned} D(x) &= \operatorname{arctanh}\sqrt{1-\kappa\sin^2\alpha\,\operatorname{sech}^2(\kappa x)}, \\ a &= \kappa^{3/2}\sin\alpha\,\operatorname{sech}(\kappa x), \qquad (C.8)\\ b &= \kappa^{5/2}\sin\alpha\,\operatorname{sech}(\kappa x)\sqrt{1-\kappa\sin^2\alpha\,\operatorname{sech}^2(\kappa x)}. \qquad (C.9)\end{aligned}$$

In order to find U, we need to find ν_x and $\sin\nu$, as well:

$$\begin{aligned} \nu_x &= \frac{-\kappa\cosh(\kappa x)(1-\kappa\sin^2\alpha)}{,}(\cosh^2(\kappa x)-\kappa\sin^2\alpha)\sqrt{1-\kappa\sin^2\alpha}, \\ \sin\nu &= \sqrt{\frac{1-\kappa\sin^2\alpha}{\cosh^2(\kappa x)-\kappa\sin^2\alpha}}. \end{aligned}$$

Let us write equation for U:

$$\begin{aligned} U &= \frac{\kappa\cosh(\kappa x)\sqrt{1-\kappa\sin^2\alpha}}{2(\cosh^2(\kappa x)-\kappa\sin^2\alpha)} + \frac{\cosh(\kappa x)\sqrt{1-\kappa\sin^2\alpha}}{2\kappa(\cosh^2(\kappa x)-\kappa\sin^2\alpha)}(2\kappa^2-3\kappa^3\sin^2\alpha\,\operatorname{sech}^2(\kappa x)) \\ &= \frac{3}{2}\kappa\,\operatorname{sech}(\kappa x)\sqrt{1-\kappa\sin^2\alpha}, \end{aligned}$$

where for $\kappa = 1$ we obtain Scarf II potential (1.12) with $V_0 = -\frac{9}{4}\cos^2\alpha$, and $V_1 = -\frac{3}{2}\cos\alpha$. The associated exact solution $\Phi = ae^{i\theta}$ follows from (C.6), (C.8) and (C.9):

$$\Phi(x) = \sin\alpha\,\operatorname{sech}(x)\exp\left[\frac{i}{2}\cos\alpha\arctan(\sinh(x))\right]. \tag{C.10}$$

Bibliography

[1] V. Achilleos, P.G. Kevrekidis, D.J. Frantzeskakis, and R. Carretero-González, *Dark solitons and vortices in PT-symmetric nonlinear media: From spontaneous symmetry breaking to nonlinear PT phase transitions*, Phys. Rev. A **86**, 013808 (7 pp) (2012).

[2] R. Adams, and J. Fournier, *Sobolev spaces* (Academic Press, New York, 2003).

[3] Z. Ahmed, *Real and complex discrete eigenvalues in an exactly solvable one-dimensional complex PT-invariant potential*, Phys. Lett. A **282**, 343–348 (2001).

[4] N. Akhmediev, and A. Ankiewicz, *Dissipative Solitons in the Complex Ginzburg-Landau and Swift-Hohenberg Equations* in *Dissipative Solitons*, Lecture Notes in Physics **661**, 1–17 (Springer, New York, 2005).

[5] N.V. Alexeeva, I.V. Barashenkov, and Yu.S. Kivshar, *Solitons in $\mathcal{PT}$-symmetric ladders of optical waveguides*, New J. Phys. **19**, 113032 (30 pp) (2017).

[6] N.V. Alexeeva, I.V. Barashenkov, K. Rayanov, and S. Flach, *Actively coupled optical waveguides*, Phys. Rev. A **89**, 013848 (5 pp) (2014).

[7] N.V. Alexeeva, I.V. Barashenkov, A.A. Sukhorukov, and Yu.S. Kivshar, *Optical solitons in $\mathcal{PT}$-symmetric nonlinear couplers with gain and loss*, Phys. Rev. A **85**, 063837 (13 pp) (2012).

[8] V.I. Arnold, *Mathematical Methods of Classical Mechanics*, (Springer–Verlag, Berlin, 1978).

[9] B. Bagchi and C. Quesne, *Non-Hermitian Hamiltonians with real and complex eigenvalue in a Lie-algebraic framework*, Phys. Lett. A **300**, 18–26 (2002).

[10] B. Bagchi and C. Quesne, *sl(2, C) as a complex Lie algebra and the associated non-Hermitian Hamiltonians with real eigenvalues*, Phys. Lett. A **273**, 285–292 (2000).

[11] B. Bagchi, R. Roychoudhury, *A new PT-symmetric complex Hamiltonian with a real spectrum*, J. Phys. A: Math. Gen. **33**, L1–L3 (2000).

[12] D. Bambusi, *Asymptotic stability of breathers in some Hamiltonian networks of weakly coupled oscillators*, Comm. Math. Phys. **324**, 515–547 (2013).

[13] I.V. Barashenkov, *Hamiltonian formulation of the standard PT-symmetric nonlinear Schrödinger dimer*, Phys. Rev. A **90**, 045802 (4 pp) (2014).

[14] I.V. Barashenkov, L. Baker, and N.V. Alexeeva, *PT-symmetry breaking in a necklace of coupled optical waveguides*, Phys. Rev. A **87**, 033819 (5 pp) (2013).

[15] I.V. Barashenkov and M. Gianfreda, *An exactly solvable PT-symmetric dimer from a Hamiltonian system of nonlinear oscillators with gain and loss*, J. Phys. A: Math. Theor. **47**, 282001 (18 pp) (2014).

[16] I.V. Barashenkov, D.E. Pelinovsky, and P. Dubard, *Dimer with gain and loss: Integrability and $\mathcal{PT}$-symmetry restoration*, J. Phys. A: Math. Theor. **48**, 325201 (28 pp) (2015).

[17] I.V. Barashenkov, D.A. Zezyulin, and V.V. Konotop, *Exactly solvable Wadati potentials in the PT-symmetric Gross-Pitaevskii equation* in *Non-Hermitian Hamiltonians in Quantum Physics*, Springer Proceedings in Physics **184**, 143–155 (Cham, Switzerland, 2016).

[18] C.M. Bender, Making Sense of Non-Hermitian Hamiltonians, Rep. Prog. Phys. **70**, 947–1018 (2007).

[19] C.M. Bender, B. Berntson, D. Parker and E. Samuel, *Observation of PT phase transition in a simple mechanical system*, Am. J. Phys. **81**, 173–179 (2013).

[20] C.M. Bender, M.V. Berry, and A. Mandilara, *Generalized PT symmetry and real spectra*, J. Phys. A: Math. Gen. **35**, L467–L471 (2002).

[21] C.M. Bender, S. Boettcher, *Real Spectra in Non-Hermitian Hamiltonians Having $\mathcal{PT}$ Symmetry*, Phys. Rev. Lett. **80**, 5243–5246 (1998).

[22] C.M. Bender, S. Boettcher, P.N. Meisinger, *PT-symmetric quantum mechanics*, J. Math. Phys. **40**, 2201–2229 (1999).

[23] O. Bendix, R. Fleischmann, T. Kottos, and B. Shapiro, *Exponentially fragile PT symmetry in lattices with localized eigenmodes*, Phys. Rev. Lett. **103**, 030402 (4 pp) (2009).

[24] S. Bittner, B. Dietz, U. Günther, H.L. Harney, M. Miski-Oglu, A. Richter and F. Schäfer, *PT Symmetry and Spontaneous Symmetry Breaking in a Microwave Billiard*, Phys. Rev. Lett. **108**, 024101 (5 pp) (2012).

[25] I.I. Blekhman, *Synchronization in science and technology* (ASME Press, New York, 1988).

[26] J. Boussinesq, *Theorie des ondes et des remous qui se propagent le long d'un canal rectangulaire horizontal, en communiquant an liquide contenu dans ce canal de vitesses sensiblement pareilles de la surface anfond, Liouvilles*, J. Math. **17**, 55–108 (1872).

[27] O. Braun and Y. Kivshar, *The Frenkel-Kontorova model: concepts, methods, and applications* (Springer, Berlin, Heidelberg, 2013).

[28] Th. Busch and J.R. Anglin, *Motion of Dark Solitons in Trapped Bose-Einstein Condensates*, Phys. Rev. Lett. **84**, 2298–2301 (2000).

[29] E. Caliceti, F. Cannata, and S. Graffi, *Perturbation theory of $\mathcal{PT}$ symmetric Hamiltonians*, Phys. Rev. A: Math. Gen. **39**, 10019–10027 (2006).

[30] E. Caliceti, S. Graffi, and J. Sjöstrand, *Spectra of PT-symmetric operators and perturbation theory*, J. Phys. A: Math. Gen. **38**, 185–193 (2005).

[31] R. Carretero-González, D.J. Frantzeskakis, and P.G. Kevrekidis, *Nonlinear waves in Bose–Einstein condensates: physical relevance and mathematical techniques*, Nonlinearity **21**, R139–R202 (2008).

[32] H. Cartarius and G. Wunner, *Model of a PT-symmetric Bose-Einstein condensate in a δ-function double-well potential*, Phys. Rev. A **86**, 013612 (5 pp) (2012).

[33] A. Chernyavsky, P.G. Kevrekidis, and D.E. Pelinovsky, *Krein signature in Hamiltonian and PT-symmetric systems* in *Parity-time Symmetry and Its Applications*, Springer Tracts in Modern Physics, Volume in press (Springer, New York, 2018).

[34] A. Chernyavsky and D.E. Pelinovsky, *Breathers in Hamiltonian $\mathcal{PT}$-symmetric chains of coupled pendula under a resonant periodic force*, Symmetry **8**, 59 (26 pp) (2016).

[35] A. Chernyavsky and D.E. Pelinovsky, *Krein signature for instability of $\mathcal{PT}$-symmetric states*, Physica D **371**, 48–59 (2018).

[36] A. Chernyavsky and D.E. Pelinovsky, *Long-time stability of breathers in Hamiltonian PT-symmetric lattices*, J. Phys. A: Math. Theor. **49**, 475201 (20 pp) (2016).

[37] D.N. Christodoulides, F. Lederer, and Y. Silberberg, *Discretizing light behaviour in linear and nonlinear waveguide lattices*, Nature **424**, 817–823 (2003).

[38] M. Chugunova and D. Pelinovsky, *Count of eigenvalues in the generalized eigenvalue problem*, J. Math. Phys. **51**, 052901 (19 pp) (2010).

[39] J.T. Cole, K.G. Makris, Z.H. Musslimani, D.N. Christodoulides, and S. Rotter, *Modulational instability in a PT-symmetric vector nonlinear Schrödinger system*, Physica D **336**, 53–61 (2016).

[40] M.P. Coles, D.E. Pelinovsky, and P.G. Kevrekidis, *Excited states in the large density limit: a variational approach*, Nonlinearity **23**, 1753–1770 (2010).

[41] M.G. Crandall and P.H. Rabinowitz, *Bifurcation from Simple Eigenvalues*, J. Funct. Anal. **8**, 321–340 (1971).

[42] S. Cuccagna, *Orbitally but not asymptotically stable ground states for the discrete NLS*, Discr. Cont. Dynam. Syst. **26**, 105–134 (2010).

[43] F. Dalfovo, S. Giorgini, L.P. Pitaevskii, and S. Stringari, *Theory of Bose–Einstein condensation in trapped gases*, Rev. Mod. Phys. **71**, 463–512 (1999).

[44] J. D'Ambroise, P.G. Kevrekidis, and S. Lepri, *Asymmetric wave propagation through nonlinear PT-symmetric oligomers*, J. Phys. A **45**, 444012 (16 pp) (2012).

[45] D. Dast, D. Haag, and H. Cartarius, *Eigenvalue structure of a Bose-Einstein condensate in a PT-symmetric double well*, J. Phys. A **46**, 375301 (19 pp) (2013).

[46] E. Destyl, S.P. Nuiro, D.E. Pelinovsky, P. Poullet, *Coupled pendula chains under parametric $\mathcal{PT}$-symmetric driving force*, Phys. Lett. A **381**, 3884–3892 (2017).

[47] R. Duggan, M.A. Miri and A. Alù, *Scattering properties of parity-time symmetric nanoparticle dimers*, in *2017 IEEE International Symposium on Antennas and Propagation USNC/URSI National Radio Science Meeting*, 1067–1068 (2017).

[48] N.K. Efrimidis, S. Sears, D.N. Christodoulides, J.W. Fleischer, and M. Segev, *Discrete solitons in photorefractive optically induced photonic lattices*, Phys. Rev. E **66**, 046602 (5 pp) (2002).

[49] H.S. Eisenberg, Y. Silberberg, R. Morandotti, A.R. Boyd, and J.S. Aitchison, *Discrete Spatial Optical Solitons in Waveguide Arrays*, Phys. Rev. Lett. **81**, 3383–3386 (1998).

[50] L. Evans, *Partial Differential Equations*, Graduate Studies in Mathematics (AMS, Providence, 1998).

[51] D.L. Feder, M.S. Pindzola, L.A. Collins, B.I. Schneider, and C.W. Clark, *Dark-soliton states of Bose-Einstein condensates in anisotropic traps*, Phys. Rev. A **62**, 053606 (11 pp) (2000).

[52] L. Feng, Z.J. Wong, R. Ma, Y. Wang, and X. Zhang, *Single-mode laser by parity-time symmetry breaking*, Science **346**, 972–975 (2014).

[53] L. Feng, Y.-L. Xu, W.G. Fegadolli, M.-H. Lu, J.E.B. Oliveira, V.R. Almeida, Y.-F. Chen, and A. Scherer, *Experimental demonstration of a unidirectional reflectionless parity-time metamaterial at optical frequencies*, Nat. Matter **12**, 108–113 (2013).

[54] A.T. Filippov, *The Versatile Soliton* (Birkhäuser, Boston, 2010).

[55] J.W. Fleischer, M. Segev, N.K. Efremidis, and D.N. Christodoulides, *Observation of two-dimensional discrete solitons in optically induced nonlinear photonic lattices*, Nature **422**, 147–150 (2003).

[56] Th. Gallay and D.E. Pelinovsky, Orbital stability in the cubic defocusing NLS equation. Part I: Cnoidal periodic waves, Journal of Differential Equations **258**, 3607–3638 (2015).

[57] H. Goldstein, *Classical Mechanics* (Addison-Wesley, New York, 1980).

[58] I.S. Gradsteyn, I.M. Ryzhik, *Table of integrals, series, and products* (Academic Press, San Diego, 2014).

[59] M. Grillakis, J. Shatah, and W. Strauss, *Stability theory of solitary waves in the presence of symmetry, I*, J. Funct. Anal. **74**, 160–197 (1987).

[60] M. Grillakis, J. Shatah, and W. Strauss, *Stability theory of solitary waves in the presence of symmetry, II*, J. Funct. Anal. **94**, 308–348 (1990).

[61] M. Haragus, and G. Iooss, *Local Bifurcations, Center Manifolds, and Normal Forms in Infinite-Dimensional Dynamical Systems* (Springer, New York, 2011).

[62] B. Heffler, *Spectral Theory and its Applications*, Cambridge Studies in Advanced Mathematics **139** (Cambridge University Press, New York, 2013).

[63] P.D. Hislop and I.M. Sigal, *Introduction to Spectral Theory: With Applications to Schrödinger Operators*, Applied Mathematical Sciences **113** (Springer, New York, 1995).

[64] H. Hodaei, M.-A. Miri, M. Heinrich, D.N. Christodoulides, and M. Khajavikhan, *Parity-time–symmetric microring lasers*, Science **346**, 975–978 (2014).

[65] S. Hu, X. Ma, D. Lu, Z.Yang, Y. Zheng, and W. Hu, *Solitons supported by complex $\mathcal{PT}$-symmetric Gaussian potentials*, Phys. Rev. A **84**, 043818 (6 pp) (2011).

[66] C. Huygens, *The pendulum clock or geometrical demonstrations concerning the motion of pendula as applied to clocks*, Iowa State University Press Series in the History of Technology and Science (Iowa State University Press, Ames, IA, 1986).

[67] C.P. Jisha, L. Devassy, A. Alberucci, and V.C. Kuriakose, *Influence of the imaginary component of the photonic potential on the properties of solitons in $\mathcal{PT}$-symmetric systems*, Phys. Rev. A **90**, 043855 (9 pp) (2014).

[68] T. Kapitula, P.G. Kevrekidis, and B. Sanstede, *Counting eigenvalues via the Krein signature in infinite-dimensional Hamiltonian systems*, Physica D **195**, 263–282 (2004).

[69] T. Kapitula and K. Promislow, *Spectral and dynamical stability of nonlinear waves*, Applied Mathematical Sciences **185** (Springer, Berlin, 2013).

[70] T. Kapitula and K. Promislow, *Stability indices for constrained self-adjoint operators*, Proc. Amer. Math. Soc. **140**, 865–880 (2012).

[71] T. Kato, *Perturbation theory for linear operators* (Springer–Verlag, Berlin, 1995).

[72] P.G. Kevrekidis, *The Discrete Nonlinear Schrödinger Equation: Mathematical Analysis, Numerical Computations and Physical Perspectives*, Springer Tracts in Modern Physics **232** (Springer–Verlag, Berlin, Heidelberg, 2009).

[73] P.G. Kevrekidis, R. Carretero-González, and D.J. Frantzeskakis, *Emergent Nonlinear Phenomena in Bose–Einstein Condensates* (Springer–Verlag, Berlin, Heidelberg, 2008).

[74] P.G. Kevrekidis, R. Carretero-González, and D.J. Frantzeskakis, *Stability of single and multiple matter-wave dark solitons in collisionally inhomogeneous Bose-Einstein condensates*, Int. J. Mod. Phys. B **31**, 1742013 (12 pp) (2017).

[75] P.G. Kevrekidis, J. Cuevas-Maraver, A. Saxena, F. Cooper, and A. Khare, *Interplay between parity-time symmetry, supersymmetry, and nonlinearity: An analytically tractable case example*, Phys. Rev. E **92**, 042901 (7 pp) (2015).

[76] P.G. Kevrekidis, D.J. Frantzeskakis, and R. Carretero-González, *The Defocusing Nonlinear Schrödinger Equation: From Dark Solitons to Vortices and Vortex Rings* (SIAM, Philadelphia, 2015).

[77] P.G. Kevrekidis and D.E. Pelinovsky, *Distribution of eigenfrequencies for oscillations of the ground state in the Thomas-Fermi limit*, Phys. Rev. A **81**, 023627 (5 pp) (2010).

[78] P.G. Kevrekidis, D.E. Pelinovsky, and A. Saxena, *When Linear Stability Does Not Exclude Nonlinear Instability*, Phys. Rev. Lett. **114**, 214101 (5 pp) (2015).

[79] P.G. Kevrekidis, D.E. Pelinovsky, and D.Y. Tyugin, *Nonlinear dynamics in $\mathcal{PT}$-symmetric lattices*, J. Phys. A: Math. Theor. **46**, 365201 (17 pp) (2013).

[80] P.G. Kevrekidis, D.E. Pelinovsky and D.Y. Tyugin, *Nonlinear stationary states in PT-symmetric lattices*, SIAM Journal of Applied Dynamical Systems **12**, 1210–1236 (2013).

[81] Y.S. Kivshar, and G.P. Agrawal, *Optical Solitons: From Fibers to Photonic Crystals* (Academic Press, San Diego, 2003).

[82] K. Knopp, *Theory of functions, part II* (Dover, New York, 1947).

[83] R. Kollár and P. Miller, *Graphical Krein Signature Theory and Evans–Krein Functions*, SIAM Rev. **56**, 73–123 (2014).

[84] V.V. Konotop, J. Yang, and D.A. Zezyulin, *Nonlinear waves in $\mathcal{PT}$-symmetric systems*, Rev. Mod. Phys. **88**, 035002 (59 pp) (2016).

[85] T.A. Kontorova and Y.I. Frenkel, *The model of dislocation in solid body*, Zh. Eksp. Teor. Fiz. **8**, 1340–1348 (1938).

[86] M. Kulishov, J.M. Laniel, N. Belanger, J. Azana, and D.V. Plant, *Nonreciprocal waveguide Bragg gratings*, Opt. Express **13**, 3068–3078 (2005).

[87] J.P. LaSalle and S. Lefschetz, *Stability by Lyapunov's Second Method with Applications* (Academic Press, New York, 1961).

[88] T.D. Lee, G.C. Wick, *Negative metric and the unitarity of the S-matrix*, Nucl. Phys. B **9**, 209–243 (1969).

[89] K. Li and P.G. Kevrekidis, *PT-symmetric oligomers: Analytical solutions, linear stability, and nonlinear dynamics*, Phys. Rev. E **83**, 066608 (7 pp) (2011).

[90] K. Li, P.G. Kevrekidis, B.A. Malomed, and U. Gunther, *Nonlinear PT-symmetric plaquettes*, J. Phys. A **45**, 444021 (23 pp) (2012).

[91] Z. Lin, H. Ramezani, T. Eichelkraut, T. Kottos, H. Cao, and D.N. Christodoulides, *Unidirectional invisibility induced by PT-symmetric periodic structures*, Phys. Rev. Lett. **106**, 213901 (4 pp) (2011).

[92] R.S. MacKay, *Stability of equilibria of Hamiltonian systems* in *Nonlinear phenomena and chaos (Malvern, 1985)* 254–270, Malvern Physics Series (Hilger, Bristol, 1986).

[93] K.G. Makris, R. El-Ganainy, D.N. Christodoulides, and Z.H. Musslimani, *Beam Dynamics in $\mathcal{PT}$ Symmetric Optical Lattices*, Phys. Rev. Lett. **100**, 103904 (4 pp) (2008).

[94] J. Marion, *Classical Dynamics of Particles and Systems* (Academic Press, New York, 1970).

[95] A.J. Martinez, M.I. Molina, S.K. Turitsyn, and Y.S. Kivshar, *Nonlinear multicore waveguiding structures with balanced gain and loss*, Phys. Rev. A **91**, 023822 (8 pp) (2015).

[96] C. Mejia-Cortes, and M.I. Molina, *Interplay of disorder and PT symmetry in one-dimensional optical lattices*, Phys. Rev. A **91**, 033815 (8 pp) (2015).

[97] K.R. Meyer, G.R. Hall, D. Offin, *Introduction to Hamiltonian Dynamical Systems and the N-Body Problem*, Applied Mathematical Sciences **90** (Springer, New York, 2009).

[98] A.E. Miroshnichenko, B.A. Malomed, and Y.S. Kivshar, *Nonlinearly PT-symmetric systems: Spontaneous symmetry breaking and transmission resonances*, Phys. Rev. A **84**, 012123 (2 pp) (2011).

[99] Y.A.R.I. Mohamed, M.A. Rahman and R. Seethapathy, *Robust line-voltage sensorless control and synchronization of LCL-filtered distributed generation inverters for high power quality grid connection*, Power Electronics, IEEE Transactions **27**, 87–98 (2012).

[100] N. Moiseyev, S. Friedland, *Association of resonance states with the incomplete spectrum of finite complex-scaled Hamiltonian matrices*, Phys. Rev. A **22**, 618–624 (1980).

[101] A. Mostafazadeh, *Pseudo-Hermiticity versus $\mathcal{PT}$ symmetry: The necessary condition for the reality of the spectrum of a non-Hermitian Hamiltonian*, J. Math. Phys. **43**, 205–214 (2002).

[102] A. Mostafazadeh, *Pseudo-Hermiticity versus $\mathcal{PT}$ symmetry. II. A complete characterization of non-Hermitian Hamiltonians with a real spectrum*, J. Math. Phys. **43**, 2814–2816 (2002).

[103] Z.H. Musslimani, K.G. Makris, R. El-Ganainy, and D.N. Christodoulides, *Optical Solitons in $\mathcal{PT}$ Periodic Potentials*, Phys. Rev. Lett. **100**, 030402 (4 pp) (2008).

[104] H. Nijmeijer, A. Rodriguez-Angeles, *Synchronization of mechanical systems* (World Scientific, Singapore, 2003).

[105] S. Nixon and J. Yang, *Nonlinear wave dynamics near phase transition in PT-symmetric localized potentials*, Physica D **331**, 48–57 (2016).

[106] D. Pelinovsky, *Asymptotic properties of excited states in the Thomas-Fermi limit*, Nonlinear Analysis **73**, 2631–2643 (2010).

[107] D.E. Pelinovsky, *Inertia law for spectral stability of solitary waves in coupled nonlinear Schrödinger equations*, Proc. Roy. Soc. A **461**, 783–812 (2005).

[108] D.E. Pelinovsky, *Localization in Periodic Potentials: From Schrödinger Operators to the Gross–Pitaevskii Equation*, LMS Lecture Note Series **390** (Cambridge University Press, Cambridge, 2011).

[109] D.E. Pelinovsky, D. Frantzeskakis, and P.G. Kevrekidis, *Oscillations of dark solitons in trapped Bose-Einstein condensates*, Phys. Rev. E **72**, 016615 (12 pp) (2005).

[110] D. Pelinovsky, T. Penati and S. Paleari, *Approximation of small-amplitude weakly coupled oscillators with discrete nonlinear Schrödinger equations*, Rev. Math. Phys **28**, 1650015 (25 pp) (2016).

[111] D. Pelinovsky and A. Sakovich, *Internal modes of discrete solitons near the anti-continuum limit of the dNLS equation*, Physica D **240**, 265–281 (2011).

[112] D. Pelinovsky and Y. Shimabukuro, *Transverse instability of line solitary waves in massive Dirac equations*, J. Nonlin. Sci. **26**, 365–403 (2016).

[113] D.E. Pelinovsky and J. Yang, *Instabilities of Multihump Vector Solitons in Coupled Nonlinear Schrödinger Equations*, Stud. Appl. Math. **115**, 109–137 (2005).

[114] D.E. Pelinovsky, D.A. Zezyulin, and V.V. Konotop, *Global existence of solutions to coupled $\mathcal{PT}$-symmetric nonlinear Schrödinger equations*, Int. J. Theor. Phys. **54**, 3920–3931 (2015).

[115] D.E. Pelinovsky, D.A. Zezyulin, and V.V. Konotop, *Nonlinear modes in a generalized PT-symmetric discrete nonlinear Schrödinger equation*, J. Phys. A: Math. Theor. **47**, 085204 (20 pp) (2014).

[116] C.J. Pethick and H. Smith, *Bose–Einstein Condensation in Dilute Gases* (Cambridge University Press, Cambridge, 2008).

[117] J. Pickton and H. Susanto, *Integrability of $\mathcal{PT}$-symmetric dimers*, Phys. Rev. A **88**, 063840 (8 pp) (2013).

[118] A. Pikovsky, M. Rosenblum, and J. Kurths, *Synchronization: a universal concept in nonlinear sciences*, Cambridge Nonlinear Science Series **12** (Cambridge University Press, Cambridge, 2003).

[119] L. Pitaevskii and S. Stringari, *Bose–Einstein Condensation*, International Series of Monographs on Physics **116** (Oxford University Press, New York, 2003).

[120] H. Ramezani, T. Kottos, R. El Ganainy, and D.N. Christodoulides, *Unidirectional nonlinear PT symmetric optical structures*, Phys. Rev. A **82**, 043803 (6 pp) (2010).

[121] M. Reed and B. Simon, *Methods of modern mathematical physics*, Vol. **4**: *Analysis of Operators* (Academic Press, New York, 1978).

[122] N.N. Rosanov, *Spatial Hysteresis and Optical Patterns*, Springer Series in Synergetics (Springer, New York, 2002).

[123] J. Rubinstein, P. Sternberg and Q. Ma, *Bifurcation diagram and pattern formation of phase slip centers in superconducting wires driven with electric currents*, Phys. Rev. Lett. **99**, 167003 (4 pp) (2007).

[124] A. Ruschhaupt, F. Delgado, and J.G. Muga, *Physical Realization of $\mathcal{PT}$-symmetric potential scattering in a planar slab waveguide*, J. Phys. A: Math Gen. **38**, L171–L176 (2005).

[125] C.E. Rüter, K.G. Makris, R. El-Ganainy, D.N. Christodoulides, M. Segev and D. Kip, *Observation of parity–time symmetry in optics*, Nat. Phys. **6**, 192-195 (2010).

[126] F.L. Scarf, *New Soluble Energy Band Problem*, Phys. Rev. **112**, 1137–1140 (1958).

[127] J. Schindler, A. Li, M.C. Zheng, F.M. Ellis, T. Kottos, *Experimental study of active LRC circuits with PT symmetries*, Phys. Rev. A **84**, 040101 (5 pp) (2011).

[128] J. Schindler, Z. Lin, J.M. Lee, H. Ramezani, F.M. Ellis, and T. Kottos, *$\mathcal{PT}$-symmetric electronics*, J. Phys. A: Math. Theor. **45**, 444029 (15 pp) (2012).

[129] Z. Shi, X. Jiang, X. Zhu, and H. Li, *Bright spatial solitons in defocusing Kerr media with $\mathcal{PT}$-symmetric potentials*, Phys. Rev. A **84**, 053855 (4 pp) (2011).

[130] D.V. Skryabin, *Instabilities of vortices in a binary mixture of trapped Bose-Einstein condensates: Role of collective excitations with positive and negative energies*, Phys. Rev. A **63**, 013602 (10 pp) (2000).

[131] M. Stanislavova and A. Stefanov, *On the stability of standing waves for $\mathcal{PT}$ symmetric Schrödinger and Klein-Gordon equations in higher space dimensions*, Proc. AMS **145**, 5273–5285 (2017).

[132] S. Stringari, *Collective Excitations of a Trapped Bose-Condensed Gas*, Phys. Rev. Lett. **77**, 2360–2363 (1996).

[133] S.V. Suchkov, A.A. Sukhorukov, J. Huang, S.V. Dmitriev, C. Lee, Yu.S. Kivshar, *Nonlinear switching and solitons in PT-symmetric photonic systems*, Laser Photonics Rev. **10**, 177–213 (2016).

[134] C. Sulem and P.-L. Sulem, *The Nonlinear Schrödinger Equation: Self-Focusing and Wave Collapse*, Applied Mathematical Sciences **139** (Springer–Verlag, New York, 1999).

[135] H. Susanto, Q.E. Hoq, and P.G. Kevrekidis, *Stability of discrete solitons in the presence of parametric driving*, Phys. Rev. E **74**, 067601 (4 pp) (2006).

[136] M. Syafwan, H. Susanto, and S. M. Cox, *Discrete solitons in electromechanical resonators*, Phys. Rev. E **81**, 026207 (14 pp) (2010).

[137] L.N. Trefethen, *Spectral Methods in MATLAB* (SIAM, Philadelphia, 2000).

[138] K. Weierstrass, *Mathematische werke*, vol. **1** (Johnson Reprint, New York, 1967).

[139] E. Wigner, *Group Theory and Its Application to Quantum Mechanics of Atomic Spectra* (Academic Press, New York, 1959).

[140] J. Wu and Xiangbo Yang, *Ultrastrong extraordinary transmission and reflection in PT-symmetric Thue-Morse optical waveguide networks*, Opt. Express **25**, 27724–27735 (2017)

[141] J.K. Yang, *Necessity of PT symmetry for soliton families in one-dimensional complex potentials*, Phys. Lett. A **378**, 367–373 (2014).

[142] E. Zeidler, *Applied Functional Analysis: Main Principles and Their Applications*, Applied Mathematical Sciences **109** (Springer–Verlag, New York, 1995).

[143] D.A. Zezyulin, G.L. Alfimov, V.V. Konotop, and V.M. Pérez-García, *Stability of excited states of a Bose-Einstein condensate in an anharmonic trap*, Phys. Rev. A **78**, 013606 (12 pp) (2008).

[144] D.A. Zezyulin and V.V. Konotop, *Nonlinear modes in finite-dimensional PT-symmetric systems*, Phys. Rev. Lett. **108**, 213906 (5 pp) (2012).

[145] D.A. Zezyulin and V.V. Konotop, *Nonlinear modes in the harmonic $\mathcal{PT}$-symmetric potential*, Phys. Rev. A **85**, 043840 (6 pp) (2012).

[146] B.G. Zhu, R. Lu, and S. Chen, *Interplay between Fano resonance and PT symmetry in non-Hermitian discrete systems*, Phys. Rev. A **91**, 042131 (6 pp) (2015).